Republic of Iraq
Ministry of Higher Education
and Scientific Research
University of Babylon
College of Science
Physics Department

Skin Cancer Cells Therapy Using Visible Light Spectrum with Some Nanoparticles

A Thesis
Submitted to the Department of Physics, College of Science, University of Babylon in Partial Fulfillment of the Requirements for the Degree of Doctor in Philosophy of Science in Physics

By

Duaa Jafer Dheaa Jaber Fayad

B.Sc., Physics, University of Kufa (2015)
M.Sc., Physics, University of Kufa (2018)

Supervised by

Asst.Prof.Dr. Samira Adnan Mahdi

2023 A.D. **1445 A.H.**

{ يَرْفَعِ اللهُ الَّذِينَ آَمَنُوا مِنكُمْ والَّذينَ أُوتُوا الْعِلْمَ

دَرَجَاتٍ وَاللهُ بِمَا تَعْمَلُونَ خَبِير }

صدق الله العلي العظيم

سُورَة المجادلة ايه 11

Dedication

This Thesis is dedicated to

My parents …..

The shortest way to win the satisfaction of Allah

My husband ……

For his patience with me in all circumstances

My brothers…..

The source of my strength

My son and my daughter ……....

My life's hope and those who are going to remember me after the death.

Duaa

Acknowledgement

First and foremost, praise and thanks to God, the Almighty, for His showers of blessings throughout my research work to complete the research successfully.

I would like to express my deep and sincere gratitude to my supervisor , Asst. Prof. Dr. Samira Adnan Mahdi, supervisor and Head of the Department of Physics, College of Sciences, University of Babylon, for giving me the opportunity to do research and providing invaluable guidance throughout this research. She taught me the methodology for conducting the research and presenting the findings as clearly as possible. It was a great privilege and honor to work and study under her guidance. I am extremely grateful for what she has offered me.

I am extremely grateful to my parents for their love, prayers, care, and sacrifices for educating and preparing me for my future. I am very thankful for my husband's understanding, prayers, and continuing support to complete this research work.

I would like to say thanks to my friends and research colleagues for their constant encouragement. I express my special thanks to Dr. Hammed Al Mullah , Head of the Rowafid Alelom Center for Cell Culture Techniques, for his genuine support throughout this research work.

I express my special thanks to Prof. Dr. Ali Hassan Nasser Fayyad, official of the Special Degrees Division at the Ministry of Higher Education, for his genuine support throughout my study.

Finally, my thanks go to all people who have supported me in completing the research work, either directly or indirectly.

God bless you all. **Duaa**

ɕ—— Certification of the Supervisor ——ɔ

I Certify that this thesis en titled (**Skin Cancer Cells Therapy Using Visible Light Spectrum with Some Nanoparticles)** was prepared by (**Duaa Jafer Dheaa Jaber**) under my supervision at Department of Physics, College of Science, University of Babylon, as a partial fulfillment for the requirements for the Degree of Doctor of Philosophy in Physics.

Signature:

Name: **Dr. Samira Adnan Mahdi**

Title: Assistant Professor

Address: Department of Physics, College of Sciences, University of Babylon

Date: / /

ɕ—— Certification of the Head of the Department ——ɔ

In view of the available recommendations, I forward this thesis for debate by the examination committee.

Signature:

Name: **Dr. Samira Adnan Mahdi**

Title: Assistant Professor

Address: Head of Department of Physics, College of Sciences, University of Babylon

Date: / /

Summary

In this work, cells were seeded on sterile 96-well plates in 200 µL of medium with cover during irradiation. Cell culture is the process of removing cells from living tissues and growing them in a laboratory setting until they are ready to be tested using photodynamic therapy and nanoparticles. Skin cell plates (A431 cell line) grown in culture medium supplemented with 10% fetal bovine serum (FBS) were irradiated with blue light by a light-emitting diode, laser, and xenon lamp at wavelengths of 420–480 nm and treated with titanium dioxide-decorated silver nanoparticles (TiO_2/Ag) and single-walled carbon nanotube-OH (SWCNT-OH) after adding several concentrations of the nanomaterial (400, 200, 100, 50, 25 and 12.5) µg/ml and (200, 100, 50, 25, 12.5 and 6.25) µg/ml, respectively. X-ray diffraction examinations were utilized in order to conduct analysis on the crystallinity as well as the structural properties of the nanosized particles. shows the XRD pattern of the TiO_2/Ag-produced films. The XRD pattern showed peaks at $2\theta = 25.4°$ corresponding to planes (101) and the characteristic peaks at 24.2° and 25.6° were generated by reflections from hexagonal carbon atom layers and nanotube stacking layers (SWCNT-OH) that correspond to planes (002). The samples had rather tiny crystallite sizes for NPs, ranging from 5 to 25 nm. Various irradiance doses and time exposures have been considered. The blue light-emitting diode (LED) at wavelengths 420–480 nm and irradiances of 400 mW/cm^2 has active results. Exposure of skin cancer cells to blue LED induced a rapid and large reduction in viability, followed by the death of nearly half the cells. The newest and safest treatment is LED therapy. The treatment of radioactively irradiated cells with LED causes an increase in cell death. Blue-light exposure might open up new possibilities for treating superficial skin cancers in people.

Aminolevulinic acid (5-ALA) is a secure photosensitizer that can be used to create a useful photodynamic therapy (PDT) treatment for skin cancer. that the PDT-treated cell line showed the highest percentage of viability of cells, close to 73%, after 240 seconds of radiation exposure with a photosensitizer 5-ALA concentration of 250 µg/ml, which was considered the ideal concentration in this study.

Blue light-emitting diode results showed a considerable decrease at 240 seconds after 24 hours of incubation time in the viability percent; the titanium dioxide-decorated silver nanoparticles (TiO_2/Ag) and single-walled carbon nanotube-OH (SWCNT-OH) results showed a considerable decrease in the viability percent for all concentrations; the most effective concentration was 400 µg/ml; and the combination results showed a significant decrease in cell viability percent ($p \leq 0.001$) as compared with the control group.

The titanium dioxide-decorated silver nanoparticles with a concentration of 400 µg/ml produced the greatest results (19.131%) as compared with the control group (100%) when combined with a light exposure period of 240 seconds. It was observed that the viability of cells was very low, and this indicates the destruction of cancer cells due to the small size of the nanomaterial that can penetrate into the cell and spread into the cytoplasm of the cell. The Methyl Thiazolyl Tetrzolium (MTT) assay test was used to determine the viability of the cells in all the experiments, and the intensity of the color was measured by a plate reader.

Contents

Symbols and Abbreviations

Symbols	Description
μ_a	Absorption Coefficients
AK	Actinic keratosis
5-ALA	Aminolevulinic Acid
BCC	Basal Cell Carcinoma
BD	Bowen Disease
CO_2	Carbon Dioxide
CNT	Carbon Nanotube
Cm	Centimeter
DMEM	Complete Media (10 % FBS, 1 % P/S)
℃	Degree Celsius
DDW	Deionized Distilled Water
DNA	Deoxyribo-Nucleic Acid
DMSO	Dimethylsulfoxide
FBS	Fetal Bovine Serum
H	Hours
HPV	Human Papillomavirus
A431	Human Skin Cancer Cell Line Culture
ISCC	invasive Squamous Cell Carcinoma
IEC	Ion-Exchange Chromatography
J/cm^2	Joules per Centimetre Squared
KCs	keratinocyte Carcinomas
KA	Keratoacanthoma
LCs	Langerhans cells
LED	Light Emitting Diode
MAL	Methyl aminolevulinate
MTT	Methyl Thiazolyl Tetrazolium
µg/ml	Microgram per Milliliter
µm	Micrometer
Mw	Mill watt
Min	Minutes
Nm	Nanometer
NPs	Nanoparticles
NMSC	Non-melanoma Skin Cancer
P/S	Penicillin/streptomycin

%	Percent
PBS	Phosphate Buffer Saline
PDT	Photodynamic Therapy
PS(s)	Photosensitizer(s)
PEG	Polyethylene glycol
PpIX	Protoporphyrin IX
$-O_2$	Radical Superoxide
ROS	Reactive Oxygen Species
RET	Resonance Energy Transfer
RT	Room Temperature
SWCNT-OH	Single Walled Carbon Nanotube-OH
$^1O_2$	Singlet Oxygen
SCC	Squamous Cell Carcinoma
TiO_2/Ag	Titanium Decorated Silver Nanoparticle
$^3O_2$	Triplet Oxygen
P53	Tumor protein
P53	Tumor protein
UVA	Ultra-violet Radiations
Λ	Wavelength
XRD	X-Ray Diffraction

List of Figures

List of Tables

Chapter One

General Introduction

and Literature Review

1-1 General Introduction

The term "cancer" in this nowadays refers to a disease that ultimately results in death. The financial, psychological, and physical toll that cancer exacts on families is something that affects every family in the world. Cancer develops as a tumor at a particular location and spreads throughout the body as a collection of altered cells in an unregulated growth situation [1]. The primary reason for death from cancer is metastasis. Cancer is also known as a malignant tumor, neoplasm, lymphoma, and other names [1,2].

According to research published by the World Health Organization (WHO), cancer was the second leading cause of death worldwide in 2018, accounting for 9.6 million deaths, or one in every six. According to Bray et al. [3], some infections, including the human papillomavirus (HPV), Epstein-Barr virus, and hepatitis B and C viruses, are known to cause cancer. In addition to hereditary issues, inactivity, poor diet, exposure to UV radiation, smoking, drinking, and using tobacco-containing products are also risk factors for cancer.

The physical, chemical, and biological factors that contribute to the development of cancer are explained in Figure 1.1.

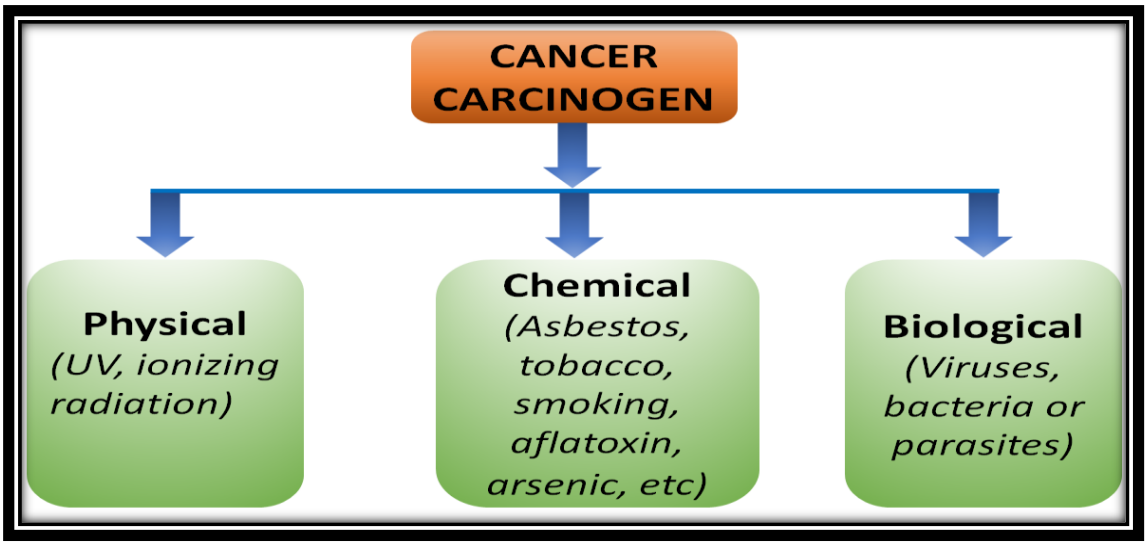

Figure (1-1): Three different types of cancer carcinogen-physical, chemical and biological cause [4].

Cancer is a condition in which live cells develop and multiply beyond the control of the body due to alterations in deoxyribonucleic acid (DNA). Some kinds of cancer may lead to the creation of tumor masses [5]. Cancers that originate in the skin are referred to as "skin cancers," and they arise when cells divide abnormally or mutate. Melanoma, squamous-cell carcinoma, and basal-cell carcinoma are the three subtypes of skin cancer. Squamous-cell carcinoma, often known as SCC, is the most aggressive form of skin cancer. Melanoma, on the other hand, is a more severe form of skin cancer that often manifests itself as a mole.

Non-melanoma skin cancers can include squamous cell and basal cell tumors. Overexposure to ultraviolet light is the root cause of almost all occurrences of skin cancer [6]. In most cases, excessive sun exposure will result in overexposure to UV radiation [7].

The human skin acts as an exterior barrier against the effects of the surrounding environment, and the skin's ability to function properly is essential to the health of the body as a whole. Skin that is still whole has

mechanisms that control how skin cells grow and change, which helps it keep its homeostasis stable. UV light is known by us for sure that [8] , sunlight can be gotten into and through skin, and this has an effect on how our skin works. This influence may be either useful or detrimental. On the other hand, there is a paucity of information about the impacts of the various wavelengths that are present in solar irradiation. Even though people don't know much about phototherapy, it has grown in popularity over the past few years.

In phototherapy, psoriasis, acne, keratosis, and skin cancer are hyperproliferative skin disorders that are treated using a wide range of wavelengths (380–440 nm). These wavelengths frequently include a significant proportion of ultraviolet light, which has been linked to the formation of cancer via DNA damage and subsequent mutations [9]. As a consequence of this, it is an unsafe method for treating skin illnesses since it is linked to an increased likelihood of tumor development. As a consequence of this, it is of the utmost importance to identify specific wavelengths and energy densities that have an effect on biological processes while minimizing any negative side effects. Research in this area has evolved because of the use of coherent light sources (low-power laser treatment) and non-coherent light sources (light-emitting diodes, or LEDs) with extremely tiny bandwidths. This has made it possible to attribute biological effects to specific wavelengths.

The biological relevance of these devices cannot be denied, notwithstanding the controversy surrounding the impact that they have on the processes that inside cells. Most of the time, radiation therapy, chemotherapy, biological therapies, and surgery are used to treat skin cancer [10,11]. Oncologists' primary method of treatment is early surgery. But because the procedure is so invasive, it often leads to big changes in

how a person looks, which can cause a lot of emotional stress [12]. Also, some long-term side effects of chemotherapy have been reported, such as chemo resistance, fibrosis, necrosis, and the growth of new tumors [13].

On the other hand, the inflammation that radiotherapy causes can result in skin issues like exudation, dermatitis, peeling, and ulcers. Because of this, it is very important to find possible alternative treatments for cSCC. Cisplatinum (cisdiamminedichloroplatinum (II)) is a powerful chemotherapeutic agent used to treat a wide range of tumor types, including testicular [14,15], ovarian [16, 17], cervical [18, 19], head and neck [20, 21], and lung cancer [22,23,24]. Photobiomodulation (PBM), or low-level light treatment, is one of the most important ways to heal [25]. Studies done in the lab and on living animals have shown that blue light kills cancer cells [26] and stops tumors from growing in mice [27]. Also, it has been shown that blue LED light causes apoptotic cell death, which has recently gotten the attention of researchers and doctors looking for ways to treat cancer [28]. On the other hand, it has been shown that when light therapy is used with chemical drugs, it works very well [29,30]. This is a big benefit because it makes it possible to lower the dose of a single drug while maintaining the treatment's effectiveness [31].

1-2 Mechanisms of Radiation Damage to DNA

Within the cell, radiation interacts with molecules at random. Although deoxyribonucleic acid (DNA) is the primary target for cell death, cellular and nuclear membrane damage is also a factor. Healthy cells that have been irradiated but have not been rendered fatal may be able to repair DNA damage. Ionizing radiation causes DNA damage, which is generated either directly by ionization within the DNA molecule or indirectly by the action of chemical radicals formed as a result of local ionizations in cell

water [32]. Free radicals play a role in indirect DNA damage. A pair of ions is created when photon radiation (electrons and positrons from pair formation) interacts with water (H_2O). will combine with H_2O to form H_2O − and the positron will combine with H_2O to form H_2O + . These H_2O + and H_2O − are called ion radicals (not free radicals). Ion radicals are very unstable and rapidly dissociate: H_2O + becomes H+ and OH• , and H_2O − becomes H• and OH− , OH• and H• are free radicals figure (1-2) [32]:

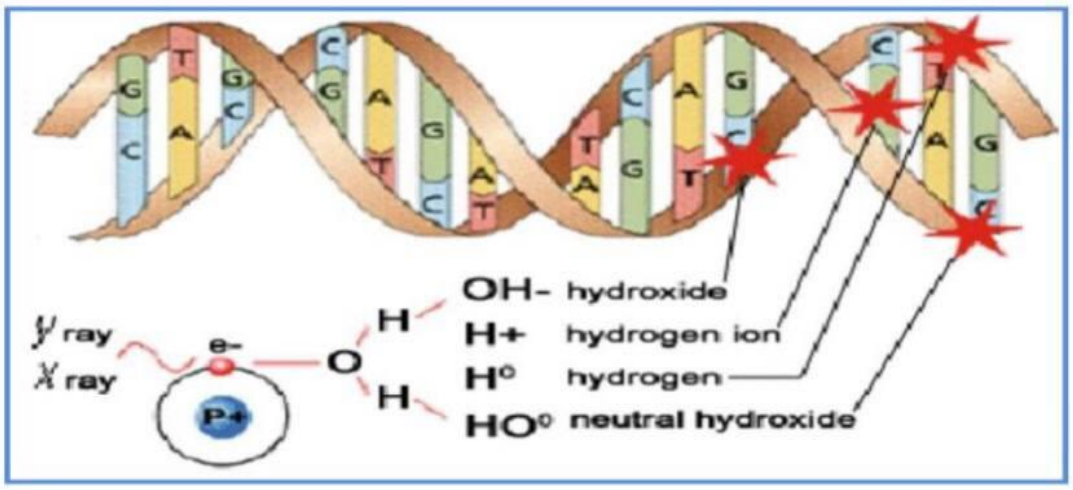

Figure(1-2): Mechanisms of Radiation Damage to DNA [32].

1-3 Differences Between Cancerous and Normal Cells

Characteristics of Cancerous and Normal Cells Serious DNA damage that has accumulated over time makes cancer cells significantly different from the cell types from which they originated. The most obvious distinction is the fast and ongoing proliferation. Normal cells need to be stimulated by signals like growth factors, extracellular matrix, and cell-to-cell contacts in order to expand. Without these signals, however, cancer cells can continue to divide. Production of growth factors, which stimulate cancer cells to multiply on their own, enables this [33].

Additionally, malignant cells frequently have acquired immortality; they continue to be capable of reproducing even after a certain number of doublings. Each time the chromosome duplicates, the length of the repeating sequences found in the DNA's telomeres, also known as chromosomal ends, shortens. The damaged cell expires when this protecting end is totally depleted [34]. Cancer cells keep their telomeres indefinitely by up-regulating the telomerase enzyme, which adds those DNA repeat sequences.

1-4 Principles of Fluorescence Resonance Energy Transfer

The process of resonance energy transfer (RET) can take place when a donor fluorophore in an electronically excited state transfers its excitation energy to a nearby chromophore, the acceptor. In principle, if the fluorescence emission spectrum of the donor molecule overlaps the absorption spectrum of the acceptor molecule, and the two are within a minimal spatial radius, the donor can directly transfer its excitation energy to the acceptor through long-range dipole-dipole intermolecular coupling [35]. A theory proposed by Theodor Förster in the late 1940s initially described the molecular interactions involved in resonance energy transfer, and Förster also developed a formal equation defining the relationship between the transfer rate, interchromophore distance, and spectral properties of the involved chromophores [36]. Resonance energy transfer is a non-radiative quantum mechanical process that does not require a collision or generate heat. When energy is transferred, the fluorescence of the donor molecule is quenched by the acceptor molecule, and if the acceptor is a fluorochrome, enhanced or sensitized fluorescence emission is detected [37]. Exciting a specimen containing both donor and acceptor molecules with light of maximum and detecting light released at

wavelengths centered on the acceptor's emission maximum will reveal the phenomena. [38]

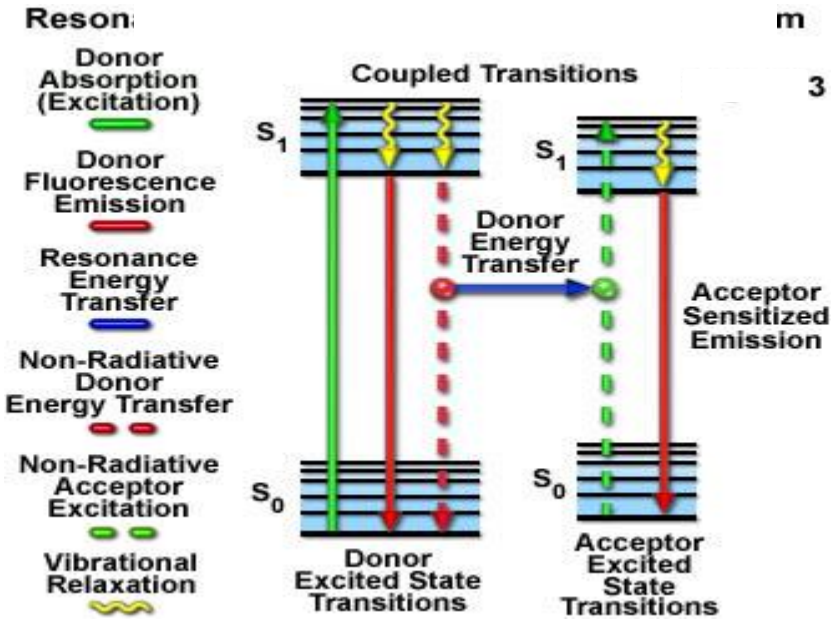

Figure (1-3): Resonance energy transfers jablonski diagram [38].

Presented in Figure (1-3) is a Jablonski diagram illustrating the coupled transitions involved between the donor emission and acceptor absorbance in fluorescence resonance energy transfer. Absorption and emission transitions are represented by straight vertical arrows (green and red, respectively), while vibrational relaxation is indicated by wavy yellow arrows [39]. The coupled transitions are drawn with dashed lines that suggest their correct placement in the Jablonski diagram should they have arisen from photon-mediated electronic transitions. In the presence of a suitable acceptor, the donor fluorophore can transfer excited state energy directly to the acceptor without emitting a photon. The resulting sensitized fluorescence emission has characteristics similar to the emission spectrum of the acceptor [40]. In summary, the rate of energy transfer depends upon the extent of spectral overlap between the donor

emission and acceptor absorption spectra, the quantum yield of the donor, the relative orientation of the donor and acceptor transition dipole moments, and the distance separating the donor and acceptor molecules [41].

1-5 Nanomaterials

The concept of nanotechnology was first given by renowned physicist Richard Feynman in 1959 and earned Nobel Prize. The term was also popularized by the invention of scanning tunneling microscope and fullerene. Nanotechnology involves designing and producing objects at nanoscale size (~1 to 100 nm). One nanometer is one billionth (10–9) of a metre. Nanomaterials are one of the main products of nanotechnology as nanoparticles, nanotubes, nanorods, etc. It is also explained as nanoparticles have a high surface to volume ratio. Nanoparticles can display properties significantly different from the bulk material because at this level quantum effects may be significant. Simply we can say the mechanical, electrical, optical, electronic, catalytic, magnetic, etc. properties of solids are significantly altered with great reduction in particle size [42].

1-5-1 Classification of Nanomaterials

The classification of nanomaterials is based on the number of dimensions as shown in Figure 1-4. According to Siegel, nanostructured materials are classified as: zerodimensional (0D), one-dimensional (1D), two-dimensional (2D) and threedimensional (3D) nanomaterials.

(i) Zero-dimensional nanomaterials: Here, all dimensions (x, y, z) are at nanoscale, i.e., no dimensions are greater than 100 nm. It includes nanospheres and nanoclusters.

(ii) One-dimensional nanomaterials: Here, two dimensions (x, y) are at nanoscale and the other is outside the nanoscale. This leads to needle shaped nanomaterials. It includes nanofibres, nanotubes, nanorods, and nanowires.

(iii) Two-dimensional nanomaterials: Here, one dimension (x) is at nanoscale and the other two are outside the nanoscale. The 2D nanomaterials exhibit platelike shapes. It includes nanofilms, nanolayers and nanocoatings with nanometre thickness.

(iv) Three-dimensional nanomaterials: These are the nanomaterials that are not confined to the nanoscale in any dimension. These materials have three arbitrary dimensions above 100 nm. The bulk (3D) nanomaterials are composed of a multiple arrangement of nanosize crystals in different orientations. It includes dispersions of nanoparticles, bundles of nanowires and nanotubes as well as multinanolayers (polycrystals) in which the 0D, 1D and 2D structural elements are in close contact with each other and form interfaces [42].

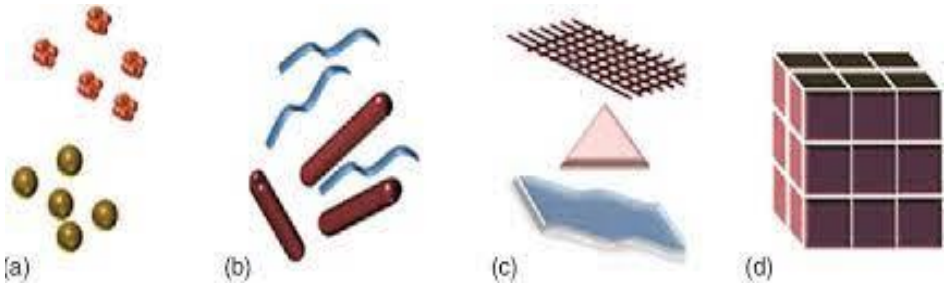

Figure (1-4): Classification of Nanomaterials (a) 0D spheres andclusters; (b) 1D nanofibers, nanowires, and nanorods; (c) 2D nanofilms, nanoplates, and networks; (d) 3D nanomaterials [42].

1-5-2 Properties of Nanomaterials

Nanomaterials have the structural features in between of those of atoms and the bulk materials. While most microstructured materials have

similar properties to the corresponding bulk materials, the properties of materials with nanometer dimensions are significantly different from those of atoms and bulks materials. This is mainly due to the nanometer size of the materials which render them: (i) large fraction of surface atoms; (ii) high surface energy; (iii) spatial confinement; (iv) reduced imperfections, which do not exist in the corresponding bulk materials.

Due to their small dimensions, nanomaterials have extremely large surface area to volume ratio, which makes a large to be the surface or interfacial atoms, resulting in more "surface" dependent material properties. Especially when the sizes of nanomaterials are comparable to length, the entire material will be affected by the surface properties of nanomaterials. This in turn may enhance or modify the properties of the bulk materials. For example, metallic nanoparticles can be used as very active catalysts. Chemical sensors from nanoparticles and nanowires enhanced the sensitivity and sensor selectivity.

The nanometer feature sizes of nanomaterials also have spatial confinement effect on the materials, which bring the quantum effects. The energy band structure and charge carrier density in the materials can be modified quite differently from their bulk and in turn will modify the electronic and optical properties of the materials. For example, lasers and light emitting diodes (LED) from both of the quantum dots and quantum wires are very promising in the future optoelections.

High density information storage using quantum dot devices is also a fast developing area. Reduced imperfections are also an important factor in determination of the properties of the nanomaterials. Nanosturctures and

Nanomaterials favors of a self-purification process in that the impurities and intrinsic material defects will move to near the surface upon thermal annealing. This increased materials perfection affects the properties of nanomaterials. For example, the chemical stability for certain nanomaterials may be enhanced, the mechanical properties of nanomaterials will be better than the bulk materials. The superior mechanical properties of carbon nanotubes are well known. Due to their nanometer size, nanomaterials are already known to have many novel properties. Many novel applications of the nanomaterials rose from these novel properties have also been proposed [43].

1-6 Current Cancer Therapies

There are now two therapy options for cancer patients: systemic and local treatments, which are described in Figure 1.5 Surgery and radiation therapy are examples of local treatments that target only the tumor and spare other body regions. Chemotherapy, immunotherapy, and gene therapy are all types of systematic treatment that use drugs that can be either orally or directly injected into the circulation to kill cancer cells throughout the body [44,45].

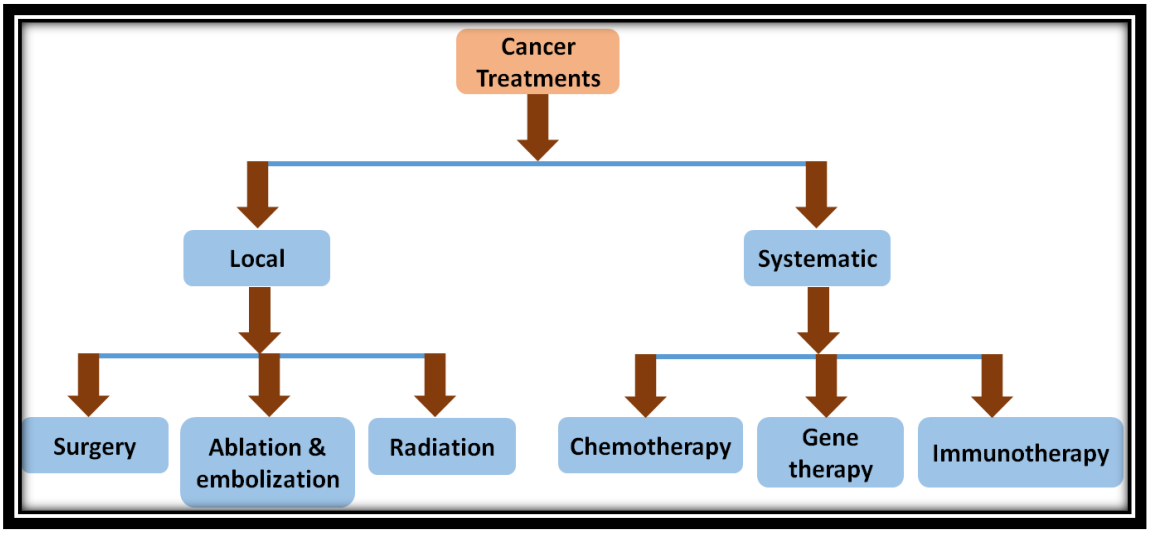

Figure (1-5): Schematic diagram of cancer treatments [45].

1-7 History of Phototherapy

Photodynamic therapy, often known as PDT, is a treatment that selectively attacks cancer cells while leaving the surrounding healthy cells unharmed [46,47] PDT, or photodynamic therapy, is an experimental treatment that was first developed in the early 20th century. It involves combining a photosensitizing medication, light, and oxygen in order to destroy cancer cells.

In the beginning, photodynamic therapy (PDT) was used to treat cancers of the bladder, bronchus, oesophagus, and skin. PDT offers the potential effectiveness of tumor clearance in comparison to traditional surgery, in addition to excellent cosmesis, patient acceptability, and a short amount of time needed for recovery. Many nations, including China, India, and Egypt, embraced sunshine as a treatment method for many illnesses in ancient.

People were treated for skin conditions after sun therapy, also known as heliotherapy, from the 15th through the middle of the 19th century. After the advent of modern medicine, individuals began to disregard sun protection [48]. Ancient Chinese medicine used distinct colors to represent each condition, with sunlight being used for males and moonlight being used for women [49]. Indian way of treatment based on to apply the plant extract or oil (seed oil or ayurvedic oil)on the affected area and exposure to sunlight. Modern phototherapy was looming in the field of biomedical to treat different diseases. PDT is the method of treatment known as photodynamic therapy, the incorporation of photosensitive substances (PS) into cancer cells is followed by the emission of light from a light source, which activates PS molecules, which, in turn, leads to the production of singlet oxygen and the death of the cells. Nanoparticles, each of which has

a thermal property after being subjected to a light source, are inserted as part of the PTT-photo thermal treatment procedure. This finally leads to the creation of heat energy, which is responsible for the death of the cell [50]. As a consequence of this, phototherapy attracted a large number of research specialists who created a wide variety of treatment methods to treat a wide variety of illnesses. According to Asgari et al. [51], the primary category of phototherapy is known as photobiomodulation (PBM).

This kind of phototherapy entails exposing cells to a low-intensity light source that has a very particular wavelength in order to either stimulate or enhance the cells. During photodynamic therapy, also known as PDT, the PS molecule is in its ground state when it is stimulated by a light source and goes into its excited state, at which point it spins one electron to reach the triplet state. Via type I and type II interactions, the triplet state interacts with the oxygen molecules surrounding it to create ROS [52], and photo thermal treatment (PTT).

The PS or nanoparticles are activated by the light source and release thermal energy to kill cells in the body [53]. The mechanism of action of the phototherapy is shown in Figure 1-6.

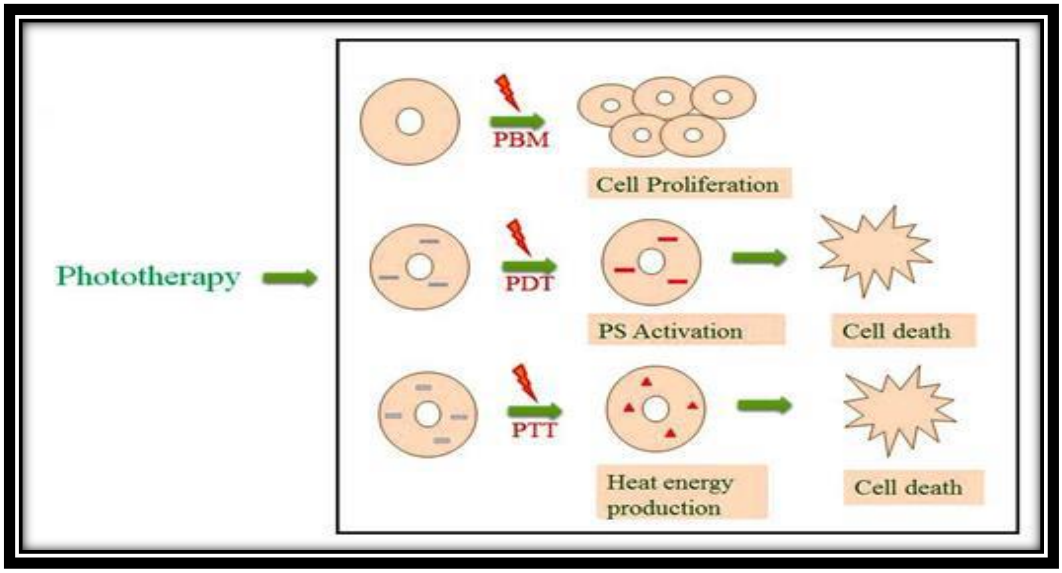

Figure (1-6): Mechanism action of phototherapy. Photosensitizers, PBM- Photo biomodulation mechanism of light source on cells leads to cell proliferation [4].

1-8 Role of Photosensitizers in PDT

Photosensitizers are organic or chemically generated compounds with a high sensitivity to light. These materials are often used in PDT because, at certain wavelengths, PS molecules become excited, or activated, and electron transfers cause ROS, which is bad for cells [54]. In order to avoid oversensitivity to sunlight, the highest by absorption wavelength varies between 600 and 800 nm, while the lowest absorption wavelength is between 400 and 600 nm [55,56]. PS molecules are now being used to treat cancer. They are usually created from tetrapyrrole compounds, and because of their protoporphyrin prosthetic group, which may easily enter cells, they resemble hemoglobin [57].

1-9 Laser Ablation and Photodynamic Therapy (PDT)

Laser ablation and photodynamic therapy (PDT), which both use light, are becoming more popular non-surgical treatments for skin cancers that are not caused by melanoma. Laser is an acronym for "light amplification by stimulated emission of radiation," which is what the whole phrase really says.

In spite of the fact that Einstein laid out the theoretical foundation for lasers in 1917, it wasn't until 1959 that Maiman developed the very first ruby laser that really worked. In the decades that followed, many different kinds of lasers were made that could be used in ways that affected almost every organ system.

In addition, noncoherent light sources and PDT with laser assistance have been developed as treatments for NMSC [58].

1-10 Light Sources in PDT

Now there is a wide range of coherent and noncoherent light sources that may be used, including dye lasers pumped by argon or metal vapor lasers and frequency-doubled Nd:YAG lasers. Nonlaser sources, including tungsten filament, xenon arc, metal halide, and fluorescent lamps, are also useful for PDT. New light source developments include light-emitting diode and femtosecond lasers [59] Limitations of current light sources include depth of penetration and diameter of spot size. Guidelines for the optimal disease-specific irradiance, wavelength, and total dose characteristics for different light sources have yet to be established [60].

1-11 Statistics Report of Skin Cancer in Iraq

Non-melanoma skin cancer is the most common type of cancer. It is more likely to happen to people with lighter skin tones and who spend a lot of time in the sun, which are the two biggest risk factors. Skin cancer among Iraqis has reportedly increased, according to many sources. Between 2000 and 2019, looked at the growth of skin cancer in Iraq. In addition to the age-specific incidence rates that were calculated using data from the Iraq Cancer Registry (ICR) from 2000 to 2019, the global standard population was used to calculate age-standardized incidence rates (ASIRs) for skin cancer. From 2000 to 2019, there were 4.144 skin cancer cases per 100,000 people in Iraq. It had an impact on people of all ages and sexes.

With an average annual percentage changes (AAPC) of +2.069%, male age-standardized rates (ASIRs) significantly increased between 2000 and 2019. With an AAPC of +2.206%, the incidence among women rose significantly. Seniors (age 70 and older) had the highest rates of skin cancer, with an AAPC of +2.481 for men and 3.86 for women. The research indicates that skin cancer is spreading across Iraq. Findings could help Iraqi officials get ready for skin cancer treatment, prevention, and early detection [61].

Table (1-1): The percentage for most frequent histology of Skin Cancer in Iraq, both gender, (2000-2019) in Iraq [61].

Histology	%
Basal cell carcinoma	36.827
Squamous cell carcinoma	34.449
Melanoma	5.912
Kaposi's sarcoma	2.046
Dermatofibrosarcoma	1.955
Adenocarcinoma	1.861
Others	16.950

1-12 Advantage of Photodynamic Therapy

When comparing PDT to other treatment modalities, there are clear advantages that allow the patient to live a better life according to Brown et al. [62]

1- It is not as invasive as radiotherapy and surgery

2- It can be specific and partially targeted towards diseased cells;

3- Treatment can be repeated as needed, unlike radiotherapy;

4- There is little or no scarring associated with post-treatment recovery

5- long term admittance to hospital is not required as most PDT treatments are done on an outpatient clinic

6- It is convenient for the patient.

1-13 Literature Review

This section highlights the previous research on the photodynamic therapy and the nanoparticles and its implementation as a treatment for skin cancer.

Lopez, R. F. V., et al. (2004) this study shows that the photodynamic therapy of skin cancer: controlled drug delivery of 5-ALA and its esters was done. Photodynamic therapy (PDT) is a tool that dermatologists use to treat some cancerous and precancerous skin conditions. The most common compounds used for this are 5-aminolevulinic acid (5-ALA) and its simple derivatives [63].

Makoto K. et al. (2005) evaluated the efficacy of photodynamic therapy (PDT) on murine thymic lymphoma cells (EL-4) cultured in vitro using flash wave (FW) and continuous wave (CW) light at 70 mW/cm^2. FW light pulse width and irradiation frequency were 1–32 Hz and less than 1 millisecond, respectively. ALA-PpIX served as a photosensitizer. demonstrated that EL-4's survival rate under FW light was lower than under CW light and decreased progressively with decreasing irradiation frequency and cell singlet oxygen generation [64].

Liebmann J. et al. (2010) studied irradiating human keratinocytes and skin-derived endothelial cells using light-emitting-diode devices of different wavelengths, allowed the researchers to investigate the effects of the treatment on the physiology of the cells. Irradiation with blue light at wavelengths of (412–426 nm) was shown to exhibit harmful effects at high intensities, but exposure to light with wavelengths between 632 and 940 nanometers had no impact [65].

Atif M. et al. (2010) in their study,the effects of photodynamic treatment (PDT) using 5-ALA as a photosensitizer were investigated in a research

published in 2010. Human muscle cancer cells served as the experimental model for this investigation. examine the photosensitizer uptake, cytotoxicity, phototoxicity, and cellular viability of the RD cells, all of which were determined by the use of a neutral-red spectrophotometric test. According to the results of the experiment, 76% of the cells were killed when the medication dosage was set at 250 g/ml and the light dose was set at 80 J/cm^2 [66].

Salman M. et el. (2015) study by Salman et al. mice with tumors were treated with cisplatin, riboflavin, and a combination of the two. Compared to the control group, the groups that were given cisplatin and riboflavin had a lower level of antioxidant enzymes, functional markers, and a higher level of lipid peroxidation. But these parameters tended to get closer to normal in the group that got both treatments. Findings show that combining cisplatin with riboflavin under photo illumination makes it more effective at killing cancer cells and lessens the side effects caused by cisplatin [67].

Jukapli N. M. et el. (2016) This research studied the history, basics, and cutting-edge usage of titanium nanoparticles (TiO_2) in photocatalytic chemistry to disinfect and kill cancer cells. TiO_2's photocatalytic properties—surface, light sensitivity, crystallinity, and toxicity—are examined. Considering target species including bacteria, viruses, fungi, and cancer cells. Hybridization of TiO2 with metal, metal oxide, and carbon nano materials increased its stability, selectivity, and photodynamic reactivity [68].

Abdel-Fattah, W. I. et al. (2018) reported on the anti-cancer effects of silver nanoparticles (Ag NPs), there has been a lot of research. This is because Ag NPs have better physical, chemical, and biological properties

than other nanoparticles. This paper wants to take a critical look at how AgNPs are made using different methods, how they are used to treat cancer, and what challenges they might face in the future. The silver nanoparticles proved unique anticancer activity against different types of cancer cells. The several syntheses approaches significantly affect the cytotoxic activity of the achieved Ag nanoparticles. Future challenges on AgNPs synthesis and their release into the environment other than scaling up production, assess several potential avenues for future works are to promote a safer and more efficient utilization of these nanoparticles. [69].

Magnon C. et al. (2018) published a study in 2018 that characterized the response of human dermal fibroblast subpopulations to visible and near-infrared (NIR) light. The purpose of this study was to determine the optical treatment parameters that have the greatest potential to address deficiencies in aging skin and chronic wounds that do not heal [70].

Nie, C. et el. (2020) Ag/TiO_2 NPs were created utilizing a simple sol-gel approach by synthesizing Ag NPs in two steps and coating them with TiO2. Ag/TiO_2 NPs display astoundingly high photothermal conversion efficiencies and biocompatibility in vivo and in vitro because of the oxide. In B16-F10 cells and C57BL/6J mice, the photothermal cytotoxicity of Ag/TiO_2 NPs was investigated for cytotoxicity and therapeutic effectiveness [71].

Ghaleb et al. (2020) used a green laser, Viscum album extract, or a combination of the two on colorectal cell plates (HCT-116 cell line) grown in culture media with 10% fetal bovine serum (FBS). The cells were kept in the incubator for 24, 48, and 72 hours. All investigations employed the crystal violet test to evaluate cell viability, and plate readers recorded color intensity. The green laser results showed a significant

decrease ($P \leq 0.001$) in cell viability percent after 48 and 72 hours of incubation; the viscum album extract showed a significant decrease ($P \leq 0.001$) for all concentrations, and the most effective concentration was 1000 μ g/ml, and the combination results showed a significant decrease ($p \leq 0.001$) for all concentrations compared to the control group [72].

Magni G. et al. (2020) examined the effects of blue LED light (410–430 nm, 0.69 W/cm2) on human fibroblasts from keloids and perilesional tissues in 2020. different light doses 3.43–6.87–13.7–20.6–30.9–41.2 J/cm^2 . Biochemical tests and particular stains assessed cell metabolism, proliferation, and viability. Micro-Raman spectroscopy was used in order to investigate the direct effects of blue LED light on the enzyme cytochrome C (Cyt C) [73].

Chen et al. (2020) say that melanoma is a type of cancer that spreads quickly. Recent studies have shown that blue light stops melanoma cells from growing. So, the goal of this study was to find out how B16F10 melanoma cells react to PBM at different irradiances and doses, as well as to learn more about how PBM works at the molecular level.

The results showed that B16F10 melanoma cells responded differently to PBM with different irradiance and dose, and that high irradiance was better than low irradiance at a constant total dose (0.04, 0.07, 0.15, 0.22, 0.30, 0.37, 0.45, 0.56, or 1.12 J/cm^2), probably because high irradiance can make more ROS, which can mess up the way mitochondria work [74].

Tartaglione et al. (2021) studied the combination of light and cisplatinum may be useful in treating skin cancer. The effects of several light radiations as well as cisplatinum were explored on A431 cutaneous squamous cell carcinoma (cSCC) and HaCaT non-tumorigenic cell lines. Before being treated with cisplatinum, both cell lines were exposed to

blue and red light sources for a period of three days. According to the findings, the use of blue light in conjunction with cisplatin might be a potentially effective therapy for cSCC [75].

Lee, Y. J. et el. (2022) Attempts were made to optimize the recovery of 5-ALA by analyzing the effects of hydrogen chloride, sodium acetate, and ammonia. As a result, a recovery of 92% was achieved in 1 M ammonia at a pH of 9.5. It was shown that the pure 5-ALA was able to kill 74% of the A549 human lung cancer cell line and 83% of the A375 melanoma skin cancer cell line. This research was the first to illustrate how broadly applicable 5-ALA is, and it did so rather convincingly [76].

Mousa A. Alghuthaymi et. al. (2023) They investigated the antibacterial and anticancer activities of silver nanoparticles in the A431 cell line. The PTAgNPs demonstrated a dose-dependent activity in E. coli and S. aureus, suggesting the bactericidal nature of AgNPs. The PTAgNPs exhibited dose-dependent toxicity in the A431 cell line, with an IC50 of 54.56 µg/mL arresting cell growth at the S phase, as revealed by flow cytometry analysis. The COMET assay revealed 39.9% and 18.15 severities of DNA damage and tail length in the treated cell line, respectively. Fluorescence staining studies indicate that PT Ag NPs cause reactive oxygen species (ROS) and trigger apoptosis. This research demonstrates that synthesized silver Nanoparticles have a significant effect on inhibiting the growth of melanoma cells and other forms of skin cancer. The results show that these particles can cause apoptosis, or cell death, in malignant tumors. cells. This suggests that they could be used to treat skin cancers without harming normal tissues [77].

1-14 Aims of the Work

In this study, squamous-cell carcinoma has been used for the first time in Iraq and the objective of this in vitro research are as follow:

1. Investigation the effect of treating the adopted cells by a blue light (420-480)nm that was either blue laser, light emitting diode or Xenon lamp.

2. Obtaining the best technology for treating skin cancer using electromagnetic rays in the visible light range with nanoparticles as well as photosensitizers.

Chapter Two

Theoretical Part

2-1 Introduction

This chapter gives a theoretical review including all the relations, scientific explanations, and the equations which are used in this thesis.

2-2 Skin Cancer

Skin cancer is a main common form of cancer, with non-melanoma types (NMSC), basal cell carcinoma (BCC) and squamous cell carcinoma (SCC), being the most frequent types [78, 79]. Although death from NMSC is rare, treatment of NMSC results in a considerable burden on the health-care system [80,81].The majority of kinds of superficial BCC are thought to have evolved from hair follicles, whereas the remaining 10% are thought to have originated from interfollicular epidermal basal stem cells (Figure 2-1) [82]. Other variations include pigmented BCCs, destructive and aggressive ulcerative forms, and [83,84]. The keratinocytes of the spinous layer of the epidermis are the source of SCC (Figure 2-1). Despite having a lesser incidence than BCC, SCC is more aggressive and has a significant capability for metastasis, which accounts for the majority of NMSC-related mortality. Additionally, it may be seen in places that are exposed to photos, including the head, neck, and extremities [85, 86,87]. The premalignant lesion actinic keratosis (AK) is the primary cause of SCC in the majority of instances. In the absence of treatment, Bowen Disease (BD) or SCC in situ may sometimes progress into an invasive SCC (iSCC). In contrast to BD, iSCC has atypical keratinocytes that may metastasis and are found in the dermis or somewhere deeper than the basement membrane. However, SCC is more prevalent among malignant tumors in transplant recipients, who exhibit more lesions and aggressive behavior than the normal population [88].

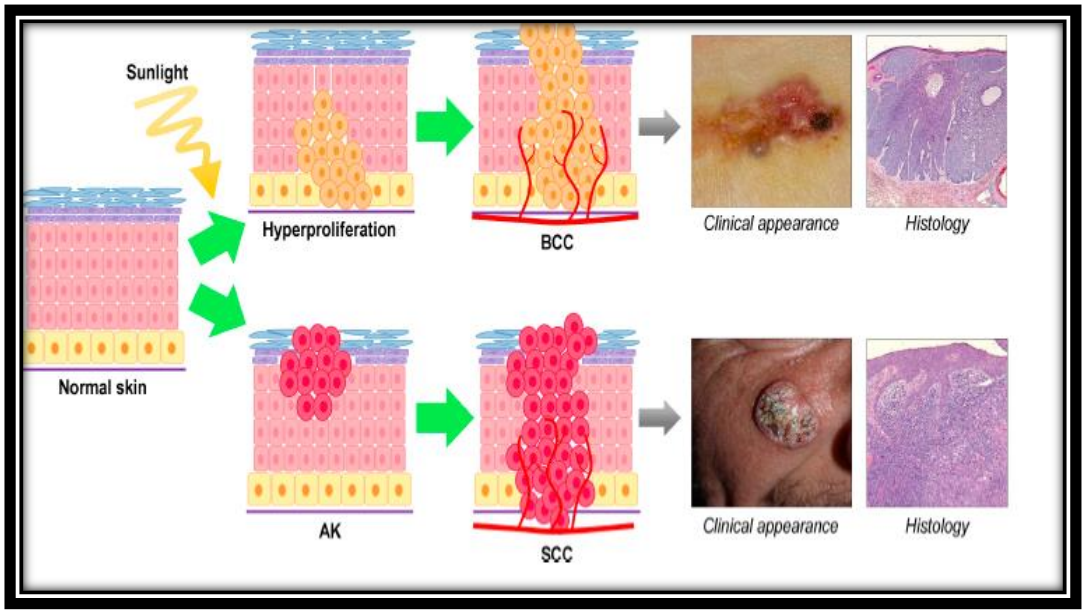

Figure (2-1): Formation process, clinical and histological appearance of basal cell carcinoma and squamous cell carcinoma [89].

AK is a skin ailment that mostly affects those with fair skin who are exposed to the sun a lot. Since its occurrence is strongly connected with cumulative UV exposure, exposed skin, such as the face, forearms, upper back, and legs, often exhibits it. The basis for the clonal expansion of genetically changed neoplastic cells is a "cancerization field" that surrounds AK and is often many in nature . SCC and AK essentially represent the same disease process, although being in different stages of development [90,91]. It is estimated that BD or SCC will manifest in 5% to 10% of AK cases [92].

2-3 Normal Skin and the Mechanisms of Cancerogenesis

Normal skin has four layers: the epidermis, the papillary layer, the reticulum dermis, and the subcutaneous fat. The epidermis is made up of four sub layers that all do different things. The stratum cornea, for example, acts as a shield and covers the other layers. Melanocytes in the

base layer also help protect the skin from UV rays. Langerhans cells (LCs) are important for getting the defense system going, while Merkel cells are in charge of light touch. The dermis is made up of fibroblasts, specialized cells, glands, blood vessels, and nerves, all of which play different roles in how the skin works [93].There are many things that can cause non-melanoma skin cancer (NMSC) and Merkel cell carcinoma (MCC) to happen, such as being exposed to UVR, which is also a risk factor for both melanoma and MCC [94-96].

UVR can damage DNA and lead to somatic changes, inflammation, oxidative stress, and immune cells that don't work right. These things are turning points in the way skin cancers start to grow. UVA and UVB, on the other hand, cause different skin changes. UVA causes greater damage and indirectly damages DNA by making free radicals, while UVB causes redness and directly damages DNA. Many studies have shown that UVR is mostly absorbed by epidermal keratinocytes and suppresses the immune system through the dimerization of cyclobutane pyrimidine, changes in Tumor protein (p53) and other tumor suppressor genes, and directly causing inflammation and death of keratinocytes [97,98].

2-4 Photodynamic Therapy PDT

For certain forms of cancer, including gastrointestinal, skin, head and neck, and gynecological malignancies, as well as non-malignant conditions, such as age-related macular degeneration (AMD) and psoriasis, as well as pre-malignant conditions, such as actinic keratosis condition. PDT makes use of a light source that has a few distinguishing characteristics. As a direct consequence of this, it is not possible to employ a single light source for all PDT applications. To begin, the kind of disease including the tissue type, location of the tumor, and size of the

tumor is what determines the type of light that should be used. Second, the PS's spectral qualities, such as its absorption spectrum, should be consistent with the light source's spectral properties. The intensity and volume of the light that will be emitted are both important characteristics of the source that should not be overlooked. It is possible to employ both coherent and non-coherent light sources for photodynamic therapy (PDT), some examples of which are fluorescent lamps, halogen lamps, metal halide lamps, xenon arc lamps, and phosphor-coated sodium lamps. According to Gibson and Kernohan (1993) [99],

The types of lasers that fall under the category of coherent light sources include argon and argon-pumped lasers, solid-state lasers, metal vapor-pumped dye lasers, and optical parametric oscillators lasers. Non-coherent light sources are preferable to lasers for treating superficial lesions (such as those that are found on the skin or in the oral cavity) due to the fact that they are less costly and may be found in a greater variety of locations. In addition, as a result of their extensive emission range, they are versatile enough to be used for a number of different PSs [100].

On the other hand, lasers are the piece of equipment that are used in the therapeutic applications of PDT the most often. They provide a light output that is monochromatic, coherent, and very powerful. As a consequence of this, they are able to cut down the amount of time necessary for the PDT application. Additionally, optical fibers and these may be utilized in combination with one another. This combination has showed potential for detecting cancers that are deeply rooted in the body (Brancaleon and Moseley, 2002) [100] Recent studies have concentrated on developing better light sources for photodynamic therapy (PDT). PDT that makes use of LEDs is one example of such a technique. Utilizing a source that is LED in PDT provides a variety of advantageous aspects.

For example, the area that is irradiated is far larger, and it is less expensive and more straightforward to produce LED sources.[101,102] the searcher When compared to the usage of daylight (DL), the PS effectiveness may be increased significantly with the careful selection of a narrow emission range. According to Cantisani et al. [103], PDT makes it possible to use natural light as a source of illumination. Because it is well knowledge that sunshine cannot penetrate deeply into tissues, and because its emission spectrum contains a considerable proportion of blue light, this therapy is useful for treating surface conditions such as non-melanoma skin cancer and actinic keratosis. [104,105]

Research has shown that this therapy is useful for treating superficial conditions, such as non-melanoma skin cancer and actinic keratosis. both the time and the location of the irradiation may be chosen by the individual. However, according to Stolik et al. [106], the light is unable to go deeper than a few millimeters into the tissue (Figure 2-2).

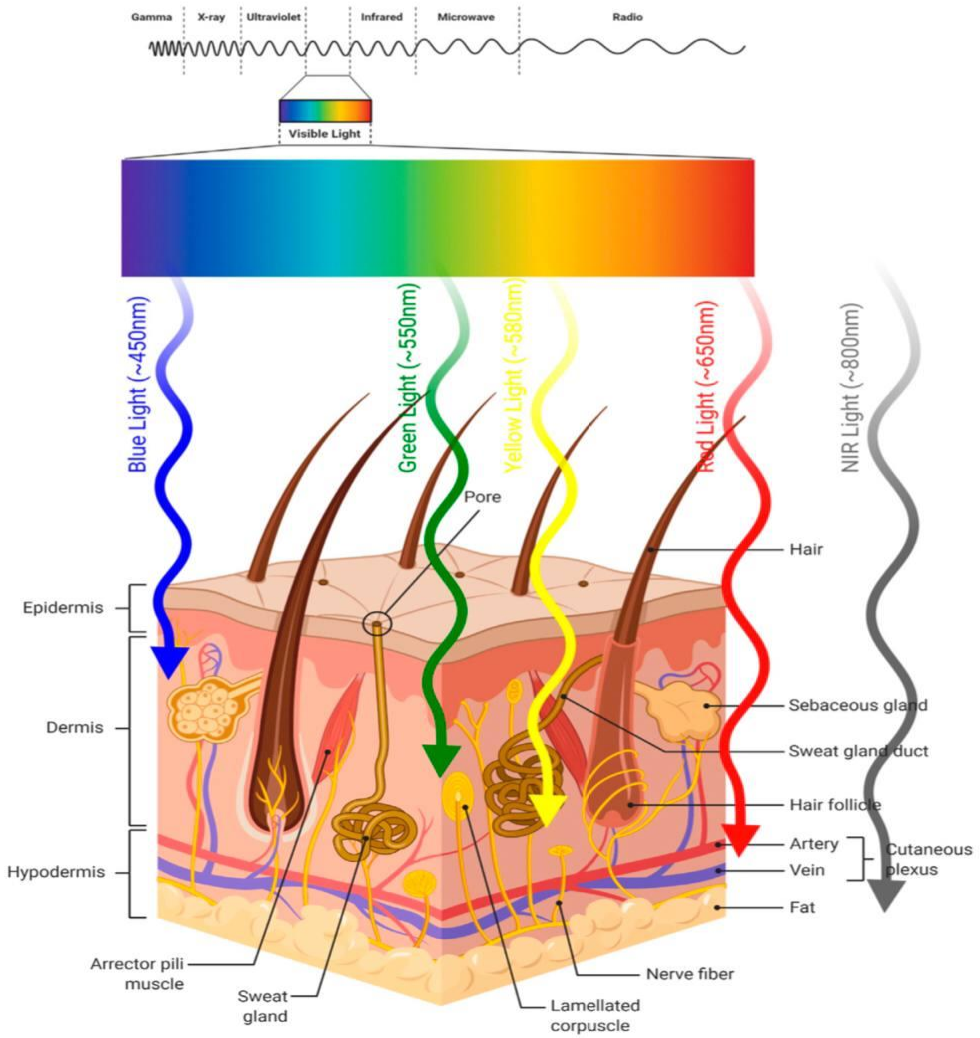

Figure (2-2): Light Penetration into Skin. Approximate penetration depths of light into skin according to its wavelength are illustrated [107].

Light penetration is influenced by the tissue's optical characteristics as well as the light's wavelength. Both across tissues and even within a tissue, there is variability. Nuclei, membranes, and other inhomogeneity sites result in light scattering, reflecting, transmitting, or absorption [108-110]. This restricts the therapeutic potential of the procedure to just superficial cancers. (Figure 2-3)

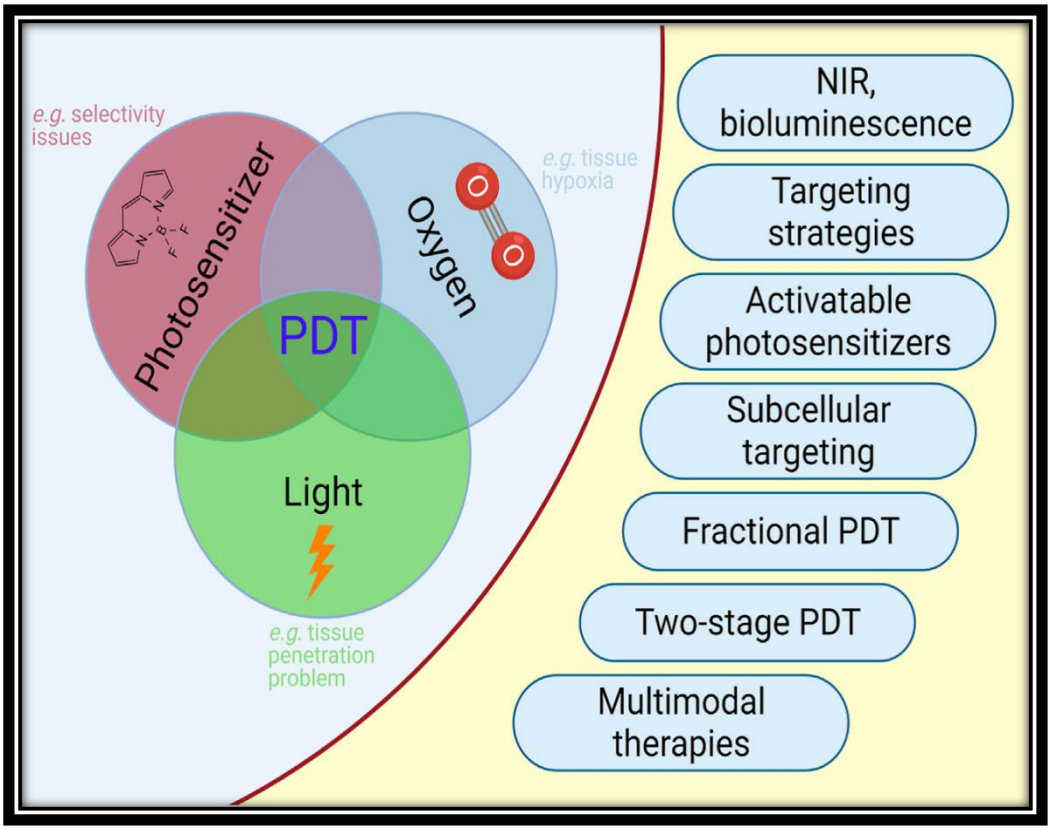

Figure (2-3): PDT in Cancer. Selected limitations and approaches to improve outcome of PDT in cancer are illustrated [107].

2-5-1 Major Components of PDT

The photosensitizer, which can be administered topically or systemically and accumulates in target tumor cells or tissues, light of a certain wavelength that activates the photosensitizer, and molecular oxygen make up the three components of PDT, each of which is safe on its own. Each of these elements is required for PDT to function [111,112]. Together, they could cause harm to the tissue that is being targeted.

2-5-2 Action Mechanism of PDT

After localization to target cells, the photosensitizer transforms from its ground singlet state to a short-lived excited singlet state (i.e., higher

energy level) upon absorption of photons by irradiation with light of the appropriate wavelength. The excited photosensitizer can either return to its ground state through photon emission (fluorescence), which can be used for photodynamic diagnosis by fluorescence imaging [113], or transform into a relatively long-lived excited triplet state via intersystem crossing [111].

The excited triplet state photosensitizer stimulates Type I and Type II photochemical reactions. The Type I reaction involves electron transfer between the triplet state photosensitizer and the cellular substrate, which forms free radicals or radical ions. These radicals interact with molecular oxygen to produce hydroxyl radicals, superoxide anions, and hydrogen peroxide. The Type II reaction involves direct energy transfer between the triplet and molecular oxygen, producing singlet oxygen. Most photosensitization reactions are thought to be Type II reactions, but the two reactions can occur simultaneously. The ratio of Type I and Type II reactions depends on the biochemical properties of the photosensitizer and the cellular substrates and the binding affinity of the sensitizer for the substrate. The primary photochemical product of PDT is singlet oxygen, which is the lowest excited electronic state of oxygen. Singlet oxygen is highly reactive and responsible for the most PDT lesions [111]. In biological systems, singlet oxygen has a very short lifetime (3μs) and a short radius of action ($2\text{-}4\times10^{-6}$ m^2/s). Therefore, the primary targets of photodamage are molecules and cells that are proximal to the area of ROS production after irradiation Therefore, PDT can selectively destroy tumors accessible to light with low systemic toxicity.

The ROS produced by PDT initiate a cascade of biochemical events that can induce three types of cell death mechanisms: apoptosis, necrosis, and

autophagy [111]. Apoptosis and necrosis are the major cell death mechanisms in the cytotoxic responses to PDT. The kinetics of apoptosis and necrosis are largely dependent on the nature of the photosensitizer, PDT dose, and cell type. A number of in vitro and in vivo studies have reported that the highly reactive photoproducts can kill cancer cells directly through apoptosis and necrosis. Recently, it has been reported that PDT can also activate autophagy as a death mechanism or a cytoprotective mechanism [111], and autophagy may occur concurrently with PDT-induced apoptosis. The precise understanding of the interconnection between apoptosis, necrosis, and autophagy may be useful in development of novel therapeutic strategies.

2-5-3 Photosensitizer

Photosensitizers are agents that absorb light of a specific wavelength and transform it into useful energy . In PDT, the creation of cytotoxic molecules occurs when photosensitizers are combined with light and molecular oxygen to cause cell death. Many natural and synthetic dyes have been put to the test as photosensitizers in PDT investigations during the past 20 years, both in vitro and in vivo [114-116] The efficiency of PDT has increased thanks to the creation of photosensitizers with strong anticancer properties. According to [117,118], the first-generation photosensitizer Photofrin is approved for the treatment of bladder, breast, lung, esophageal, gastric, cervical, and ovarian cancers.

A photosensitizing compound, light of an adequate wavelength and oxygen. When the photosensitizer (PS) is activated by light, it triggers a photochemical reaction by which singlet oxygen ($^1O_2$) and other reactive oxygen species (ROS) are produced and selectively kill cancer cells [119,120].

Anti-tumor effects of PDT derive from three principal mechanisms: direct cytotoxicity on cancer cells, indirect effects consequence of damage to the tumor vasculature, and the activation of the immune response.aminolevulinic acid (ALA, Levulan® (Wilmington, DE, USA), Ameluz® (Leverkusen, Germany), and its methylated derivate (MAL, Metvix® (Alby sur Cheran, France)) are the main substances utilized in cutaneous cancer [119,121].While ALA is only advised for AK, MAL is approved in Europe for the treatment of AK, BD, and superficial and nodular (less than 2 mm of depth) BCC.ALA is a precursor of Protoporphyrin IX, a photoactive molecule, and other intermediate porphyrins in heme group biosynthesis (PpIX)When ALA is administered, cancer cells produce and accumulate the PS PpIX in a targeted manner.

Studies on PDT's application to lymphomas and other forms of skin cancer are also available [122] This can occasionally be accompanied by a severe inflammatory response, which is characterized by a rise in cytokines and a concentration of leukocytes in the areas where the tumor is being targeted, encouraging tumor death. On the other hand, MAL-PDT of BCC lowers regional epidermal Langerhans cells, according to Evangelou et al. [123].Therefore, a less robust antitumor response could possibly result from this inhibition of the skin immune response.

Table (2-1): properties of photosensitizer 5-Aminolevulinic acid [119].

Applications	5-Aminolevulinic acid (ALA) is a common precursor of tetrahydropyrrole compounds in organisms. It can be used in the preparation of Heme enzyme, porphyrin and vitamin B12 compounds in the field of microbial fermentation. ALA can be used as a light-activated pesticide with high selectivity and environmental friendliness in agriculture.	
Trade name	ALA 5-ALA	
Synonyms	5-aminolevulinic acid; 5-amino-4-oxo-pentanoicaci; Aminolevulinic acid	
Structural formula	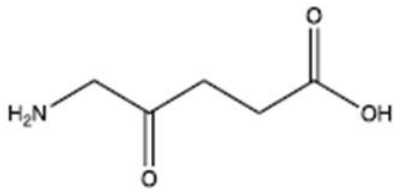	
Formula	C5H9NO3	
Molecular weight	131.13	
CAS No.	106-60-5	
Specifications	Purity :	≥98%
	Moisture :	≤1.0%
	Ash :	≤0.5%
	Heavy metal :	≤10ppm
	Residual Solvents :	≤5000ppm (ethanol)
Typical Properties	Appearance :	White crystalline powder
	Melting point :	≥149℃

2-6 Light Source

The diode laser is basically just a combination of a LED and a laser. It means that the original photons are generated in a same fashion than in LEDs and then these photons are used to generate more photons by stimulated emission. In a diode laser all this is done inside the same device [124] .One of the main requirements in a laser is to have and excess amount of excited electrons. This is called populated inversion and in diode lasers it is achieved by injecting a large amount of electrons to the junction with a relatively high current. The amount of current that is needed to achieve the sufficient amount of excited electrons is called

lasing threshold. This lasing enables the device to produce really high optical power and because the emitted light is coherent it also enables various ways to control the light beam. As shown in Figure (2-4):

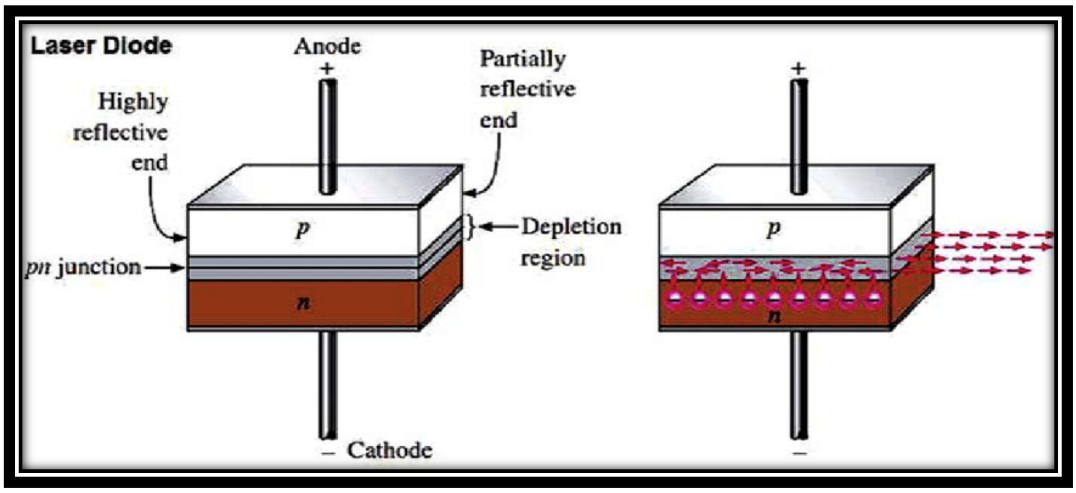

Figure (2-4): Structure of diode laser [124] .

Light that can activate the photosensitizer is one of the three components of PDT. The required wavelength depends on the electron absorption spectrum of the photosensitizer. Wavelengths between 600 and 800nm, referred to as the therapeutic window, are generally used in PDT [125], ROS are readily produced within this range, but longer wavelengths have low energy and are therefore incapable of producing singlet oxygen [126]. The efficacy of PDT depends primarily on the light penetration depth, which is influenced by light propagation through the tissues (i.e., reflection, scattering, transmission and absorption; [125,126].

Longer wavelengths penetrate tissues more deeply than shorter wavelengths. Other parameters influencing the efficacy of PDT include the total light dose, light delivery mode, and fluence rate [125,127] These factors should be considered along with the cost and operation method

when choosing a light source for PDT. Both lasers and conventional lamps have been used for PDT with similar efficacies [128-130].

Incoherent light sources including halogen, fluorescent, tungsten, and xenon lamps provide broad spectrumlight and are inexpensive, easy to operate, and stable [131]. These incoherent light sources have therefore been used in many PDT studies. However, lasers have the properties of monochromaticity and high power, which are advantageous for use in PDT [126].

Monochromaticity permits irradiation with a precise wavelength, and the high light fluence rate reduces therapeutic exposure time. The disadvantages of lasers are that they are generally expensive, large, and not portable. Diode lasers are relatively inexpensive, small, and portable; however, they operate at a single wavelength [131]. Light emitting diodes are alternative light sources that could be used in clinical PDT. Besides being inexpensive and portable, light-emitting diodes provide a relatively narrow emission spectrum (emission peak 631 nm) and high fluence rates [125].

Thorough knowledge of the physical nature of light and light perception provides the foundation for a comprehensive understanding of optical measurement techniques. Yet, from a practical point of view there is little necessity to fully understand formation and propagation of light as an electromagnetic wave as long as the reader accepts wavelength as the most important parameter describing the quality of light. The human eye perceives light with different wavelengths as different colors figure 2-5, as long as the variation of wavelength is limited to the range between 400 nm and 800 nm . In the optical range of the electromagnetic spectrum, wavelength is sometimes also given in Ångstrøm (Å= 10^{-10} m). Outside

this range, the human eye is insensitive to electromagnetic radiation and thus one have no perception of ultraviolet (UV, below 400 nm) and infrared (IR, above 800 nm) radiation.

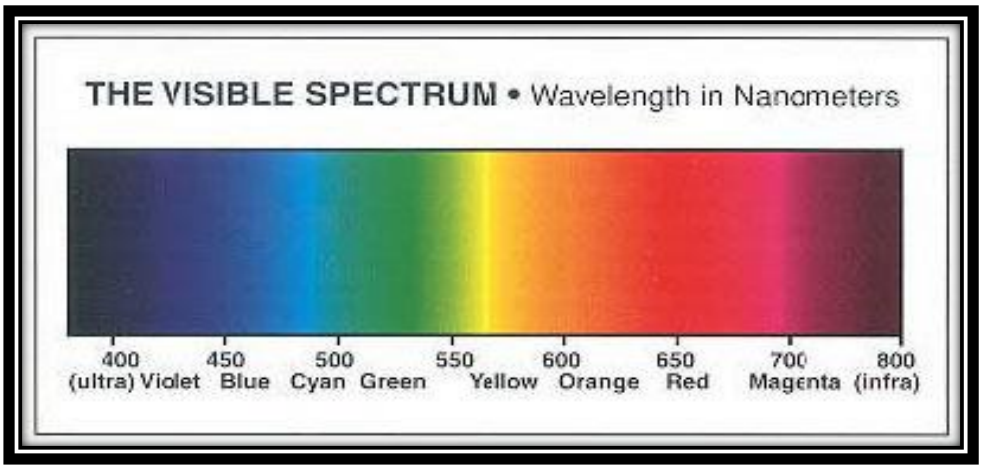

Figure (2-5): Monochromatic electromagnetic radiation of different wavelengths between 400 nm and 800 nm causes the impression of different colors. Outside this wavelength range, the human eye is insensitive [125].

2-7 Fluorescence

Fluorescence describes a phenomenon where light is emitted by an atom or molecule that has absorbed light or electromagnetic radiation from a source. In absorption, high energy light excites the system, promoting electrons within the molecule to transition from the ground state, to an excited state. Here, the electrons quickly relax to the lowest available energy state. Once this state is achieved and after a fluorescence lifetime, the electrons will relax back to ground state, releasing their stored energy as an emitted photon. Usually, the emitted light has lower energy than the absorbed radiation.

Methods regarding this subject are mostly used in the biochemical and biophysical field [132]. Fluorescence requires a fluorophore (molecule

with a rigid conjugated structure) In absorption, high energy light excites the system, promoting the electron within the molecule to transition from the ground state, to the excited state. The entire fluorescence process is cyclical. Unless the fluorophore is irreversibly destroyed in the excited state, the same fluorophore can be repeatedly excited and detected. So, a single fluorophore can create thousands of photons, due to the high sensitivity of detection techniques [133]. fluorescence plays a key role in oncology. Through flourescending-protein-markers that attach only to cancer cells, it will be possible to differentiate precisely between healthy and mutated cells. Thus, these cancer cells can be specifically targeted and attacked, whilst, the healthy cells remain unharmed. This will result in a very effective new form of chemotherapy for the benefit of the patients [134].

2-8 Laser penetration in tissues

The behavior of a light beam propagating inside a tissue mainly depends on λ and on the specific tissue type, being described in terms of absorption and scattering. We now want to merge these two effects to define a single model describing light penetration. Let us consider a collimated laser beam impinging on a tissue surface in the case of a pure absorbing medium. This hypothesis of absence of scattering may look like a brutal simplification for biological tissues, even if it will be possible to include the scattering effect by a proper modification of this simple model. This assumption allows us to start from the Beer-Lambert law ,

$$I(x) = I\,o\ exp\ (-\mu_a x) \text{ where } Io = I\ (x= 0) \qquad (2\text{-}1)$$

That describes the light intensity at various depths in the medium. If we introduce a new parameter called 'penetration depth' or 'extinction length' La (usually measured in mm or um) defined as [135]:

$$La = 1/\mu_a \quad (2\text{-}2)$$

Equation (1) can be written as:

$$I(x) = Io\ exp\ (-x/La) \quad (2\text{-}3)$$

The penetration depth *La* indicates the depth increase (in the tissue or medium) where the light intensity is reduced by a factor e (or at about 36%) with respect to any depth x. This is notably applicable for light penetration with respect to the intensity at the skin level, if external in-air irradiation is performed. It is important to note that the definition of La is independent both from the laser intensity *Io* and laser power *Po* , being it dependent only on λ via the wavelength dependence of μ_a . This is valid both for continuous and pulsed lasers (exception made for the presence of nonlinear processes) since the Beer-Lambert law does not depend on the laser pulse duration. In a practical application, in order to calculate La, we simply need the proper value of μa at the specific laser wavelength λ for the specific tissue type. It is worth noticing that *La* is often misinterpreted as the maximum penetration length of light in a given material or tissue, wrongly assuming that I = 0 for $x > La$.

This could be possibly considered as a rough 'rule of thumb' when comparing the effects of different laser sources, but nothing more than that. Up to now we have considered purely absorbing media, but for a comprehensive description of the light-tissue interaction, we need to merge absorption with scattering. If we now add scattering properties to the medium, both absorption and scattering will contribute to deplete the

beam of photons. We can calculate the amount of un scattered light intensity Ins (also called coherent component, meaning photons that have not experienced any scattering event) at any position x inside the medium as:

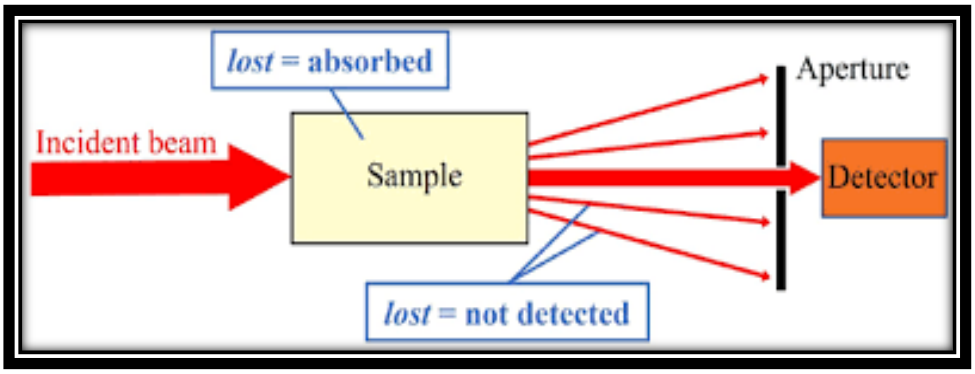

Figure (2-6): Example of a simple setup used to measure the unscattered light intensity, also called coherent or ballistic component, that arise from the propagation of a collimated light beam through an absorbing and weakly scattering media. The usage of an aperture allows for the detection of only the un scattered light [135].

$$I_{ns}(x)\ Io\ e^{-(\mu a+\mu s)x} = Io\ e^{-\mu t\, x} \qquad (2\text{-}4)$$

where $\mu_t = \mu_a + \mu_s$ is called the 'total attenuation coefficient'. A practical way to measure I_{ns} is to illuminate a slab of tissue with collimated light and use an aperture to shield the scattered light, thus measuring only the un scattered one. In such a setup, knowing the slab thickness and μa, it is possible to estimate the scattering coefficient μs , as shown in Figure 2-6. In many practical cases, light intensity measurements intrinsically select the forward component without the use of any aperture (e.g. due to the limited acceptance angle of the detector and /or the associated optical elements), in accordance with equation (2-4) and the setup shown in Figure (2-6).

2-9 Blue Light and Its Effect on the Skin

The wavelengths of visible light that fall between 400 and 500 nm are referred to as blue light. Due to the fact that blue light has the shortest wavelength and, hence, the most energy of all the colors in the visible light spectrum (Figure 2-5), it is sometimes referred to as high energy visible light. It is important to keep this distinction clear from the subsequent categorization that takes place within the region of 400 to 500 nm as "low energy" or "high energy." The light is said to have low energy when it is at the upper end of the blue light range, and it is said to have high energy when it is at the lower end of the blue light range; nonetheless, blue light as a whole has the most energy when compared to the rest of the visible light spectrum. Additionally, just as its name says, blue light is seen as having a blue color. Sunlight is the most important contributor of blue light. Additional sources include light-emitting diodes (LEDs), fluorescent lights, and digital displays like those found on smartphones, computers, laptops, and televisions. As a direct consequence of this, exposure to blue light is unavoidable [136].

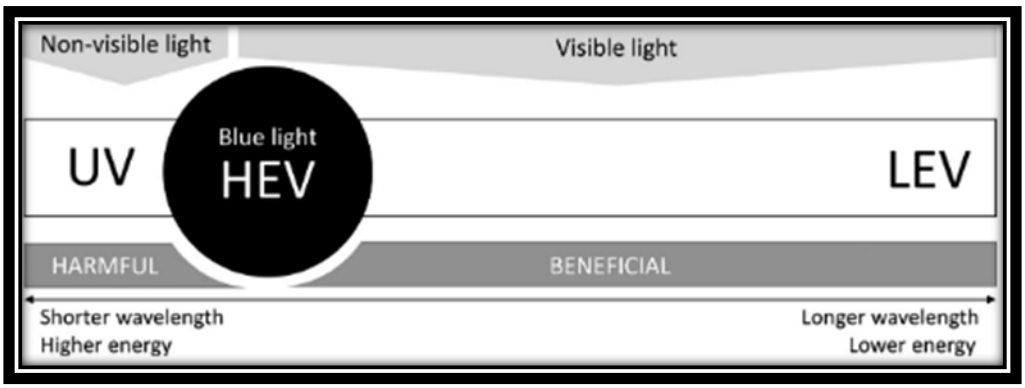

Figure (2-7) : Blue light, that is, high energy visible light. Abbreviations: HEV, high-energy visible; LEV, low-energy visible; UV, ultraviolet [136].

It is a relatively new scientific interest. However, it is a field of study that is just a few decades old. On the other hand, recent research has shown that exposure to blue light may have both negative and positive effects. Researchers have discovered that shorter wavelengths of blue light with greater energy create effects that are comparable to those of longer wavelengths of blue light with lower energy. In therapeutic practice, the wavelength and intensity of blue light might vary from patient to patient depending on the objective of the therapy being administered.

It should be emphasized that blue light therapies normally employ the light-emitting device for a short length of time (for example, 15-25 minutes) every session, and the treatments are often short-term, that is, they last for a few weeks at most.

Although blue light has become an essential part of the therapy of many dermatologic disorders, it is crucial to highlight that blue light treatments typically only last for a few weeks. The majority of trials that were only conducted for a short period of time shown that any potential adverse effects did not last for an extended period of time and often disappeared within a few weeks or months.

In the process of photodynamic treatment, a photosensitizing chemical is combined with light and oxygen to produce highly reactive singlet oxygen, which is then used to treat various skin problems, both those that cause cancer and those that do not cause cancer. In the treatment of inflammatory skin illnesses and proliferative diseases, blue light is often combined with aminolevulinic acid (ALA). When performed correctly, photodynamic treatment with blue light for photo-rejuvenation is regarded to be both effective and safe. It is possible to reduce the amount

of damage done to the healthy tissue that is around the affected area by increasing selectivity of absorption and limiting the length and depth of exposure to blue light [136].

2-10 Tumor Cell Killing

PDT can partially or completely kill tumor cells directly, and this removal is not the result of a single process [137]. PDT has the ability to lower the quantity of clonogenic tumor cells. After the light irradiation of tumors treated with photosensitizers was finished, it was claimed that the number of clonogenic cells might be reduced by up to about 72% [138] Additionally, the number of clonogenic cells continued to decline over time following PDT, suggesting that tumor cell death is a kinetic process [139]. On target tumor cells, PDT directly causes a combination of apoptosis and necrosis PDT has been shown by Agarwal et al. to cause DNA fragmentation and promote apoptosis [139]. Time and dose both had an impact on the DNA fragmentation. In addition, they noted damage to cytoplasmic structures and chromatin condensation towards the nucleus's outer edge.

2-11 Nanomedicine in Cancer

Nanomedicine is known as a new branch of medical science and holds five main sub-disciplines including: medical diagnosis, nanoimaging, chemotherapy analytical tools, nanodevices, and drug delivery systems. It can be said that the potential benefits of nanobiotechnologies raise great hopes in therapies for cancer diseases, antiviral and antifungal agents, diabetes, chronic lung diseases, and gene therapy Besides medicine therapy, nanomedicine can be applied in surgery such as photodynamic therapy [140]. Most scientists have been drawn to nanomedicine over the past 10 years in order to treat cancer, diagnose it, or perform imaging

procedures .includes a list of nanomedicine's applications, which are [141,142].

1. Nanoparticles in nanomedicine to target

2. Nano valves for drug delivery

3. Imaging

4. Diagnosis

5. DNA analysis

6. Gene therapy

7. Delivery system

8. Cleaning robots

9. Implant materials

10. Wound healing bandages

11. Body surveillance

12. Artificial tissue and organs

Polymers, dendrimers, liposomes, fullerene, silver and gold nanoparticles, metal-based nanoparticles, carbon nanotubes, graphene, micelles, quantum dots, silica, hydrogel, and other materials are examples of nano sized particles that can range in size from 1 to 100 nm [143].

The advantages of a nanoparticle-based drug delivery system over commercially available medications in clinical practice include protection from drug solubility and inactivation of drug or biodegradation [144], prolonged circulation without rapidly clearing from the body [145]

targeting the specific site increases the concentration of drug to kill the tumors [146], and the ability to load multiple drugs for synerg [147].

2-11-1 Hybrid Photo Catalyst of TiO_2/Ag

Silver, Ag nanoparticles are chemically very reactive and can form silver oxide (Ag_2O) when in direct contact with TiO_2.

TiO_2/Ag has been successfully used to enhance the photocatalytic degradation of organic compounds and the photokilling of bacteria. Decelerating the electron-hole recombination at the surface of the TiO_2 particles is made possible by the Ag core in the TiO_2/Ag hybrid system [148]. Because of this, the trapped electron in the conduction band and the trapped hole in the valence band are now free charge carriers in those bands.

The Ag core can, in fact, charge electrons under UV radiation and discharge them when needed in the dark [149].

The amount of Ag determines how the TiO_2/Ag hybrid system charges and discharges. Once the photo-induced excitation of TiO_2/Ag is performed with an electron acceptor present, the photo-generated electrons can then be scavenged by the molecules of the acceptor. Beginning with the creation of photo-excited electrons that quickly convert via the TiO_2 shell into the Ag nano core, the probable mechanism of TiO_2/Ag photocatalytic against cancer cells continues until the Fermi level charge equilibrium is established between shell and core systems [150].

The achievement of a good Fermi level allows for the quick transfer of electrons from excited TiO_2, triggering redox reactions at the interface between the TiO_2 shell and suspension. On the photo excited TiO_2/Ag

hybrid system, the reactive oxygen species, such as hydroxyl radicals and hydrogen peroxide, are produced. It is anticipated that the highly oxidizable hydroxyl and hydrogen peroxide species will be harmful to cell health [151]. The photoinduced electron transfer to the excited TiO_2's interfacial surface before transferring to the Ag core will continue until the Fermi level equilibrium is reached. Because dissolved oxygen is one of the best electron acceptors, some electrons can be transported to the TiO_2 surface and lower the dissolve O_2 readily.

The Ag core prevents electron-hole recombination by acting as a Schottky barrier for TiO_2 stimulated electrons [152]. Thus, photocatalytic cell killing is improved over TiO_2 alone and photoinduced solid-liquid interfacial charge-transfer activities are encouraged. It showed that the photocatalytic cytotoxicity of TiO_2/Ag only needed one-fourth the amount of time that single TiO_2 required for irradiation [153,154].

At the same volume, TiO_2/Ag has a killing effectiveness that is more than three times larger than TiO_2 alone. The photo-luminescence intensities of TiO_2 and TiO2/Ag hybrid for the HeLa cell killing studies showed that the TiO_2/Ag fluorescence intensity is significantly higher than TiO_2 alone.TiO_2/Ag hybrid has been created in advance using citrate reduction. In order to create the Ag metal core-TiO_2 shell structure, the citrate can cap the Ag nanoparticles and hydrolysis of titanium (IV) (triethanolamine) isopropoxide can condense quickly in boiling temperature on the Ag nanoparticles surface in solution [148].

2-11-2 Single Walled Carbon Nanotubes

Carbon nanotubes are nano sized cylindrical tubes that are rolled up by graphene sheets where both ends are opened, and carbon atoms are exclusively arranged like a benzene ring. The structural representation of

the CNTs are armchair, According to Mehra *et al*. [155], the CNTs have the following structural representations: zigzag, and chiral, with both sp2 planar and sp3 cubic allotropic forms. Single walled carbon nanotubes (SWCNTs), with a diameter of 1-3 nm and a length of several micrometers, are what CNTs are categorized as based on the graphene sheets.

Rolling double-layered graphene sheets creates a nanotube known as a double-walled carbon nanotube (DWCNTs).The term "multi walled carbon nanotube" (MWCNT) refers to a tube made of many sheets that rolled into one another. MWCNTs have an outer diameter of 1-3 nm and a length between 0.2 to several micrometers [156]. Many researchers are concentrating on the biological delivery of CNTs mixed with polymers, medicines, DNA, and PS to target cancer cells [157].

SWCNTs' distinctive size, shape, and physicochemical characteristics enhance their effectiveness as nanocarriers [157].When SWCNTs circulate in the body and directly enter cells, MWCNTs enter through the endocytosis route [158]. SWCNTs serve as a top nanocarrier for encapsulating various polymers, medications, and photo medicines [159]. SWCNTs are distinctive nano carriers in drug delivery systems because they make it easier for targeted moieties to be functionalized both covalently and noncovalently [160]. In the treatment of cancer, the carboxylated SWCNT exhibits high biocompatibility [161]. Carbon nanotubes (CNTs) have attracted great interest for biomedical applications, including the delivery of bioactive molecules such as drugs, the targeted cancer therapy, and biological imaging, because of their unique properties, including large surface area, relatively low density, high stability and other inherent mechanical, optical and electrical properties [162,163].

2-12 Combined Effects of Nanotubes and Photodynamic Therapy

Regarding overcoming the obstacles in clinical translation, cancer nanomedicine has both a good and negative response. The basics of nanoparticle interaction with biological molecules are not well reported in medication delivery systems [164]. PDT is widely utilized in treating a variety of cancer types with little or no invasive or non-invasive treatment, no cumulative damage, and no drug resistance. PDT application faces some difficulties in achieving completely side-effect-free treatment, including long-lasting photo activities of PS 31 molecule that may cause photosensitization on skin, the need for patients to remain in the dark for several weeks following treatment, and a lack of tumor selectivity and accumulation in normal tissues that results in toxic effects [165,166]. Nanomedicine may increase the bioavailability of drugs, prevent drug degradation, better target cells, regulate drug release at specific sites, and provide therapeutic efficacy with few side effects [167]. Effects of nano medicine and PDT in combination are mostly focused on reducing side effects of cancer treatments.

Chapter Three

Experimental Part

3-1 Introduction

This chapter describes the methodology and devices. It covers the methods for cell line culture, MTT assay and light exposure conditions parameters that are used in this project. Figure (3-1) presents a flow chart of the experimental part of the work in which the main sections are explained:

3-2 Culture Cell line

Cell culture refers to the removal of cells from an animal or plant and their subsequent growth in a favorable artificial environment. The cells may be removed from the tissue directly and dis-aggregated by enzymatic. Primary culture refers to the stage of the culture after the cells are isolated from the tissue and proliferated under the appropriate conditions until they occupy all of the available substrate (i.e., reach confluence). At this stage, the cells have to be sub-cultured by transferring them to a new vessel with fresh growth medium to provide more room for continued growth. After the first subculture, the primary culture becomes known as a cell line, cells with the highest growth capacity predominate, resulting in a degree of genotypic and phenotypic uniformity in the population [168].

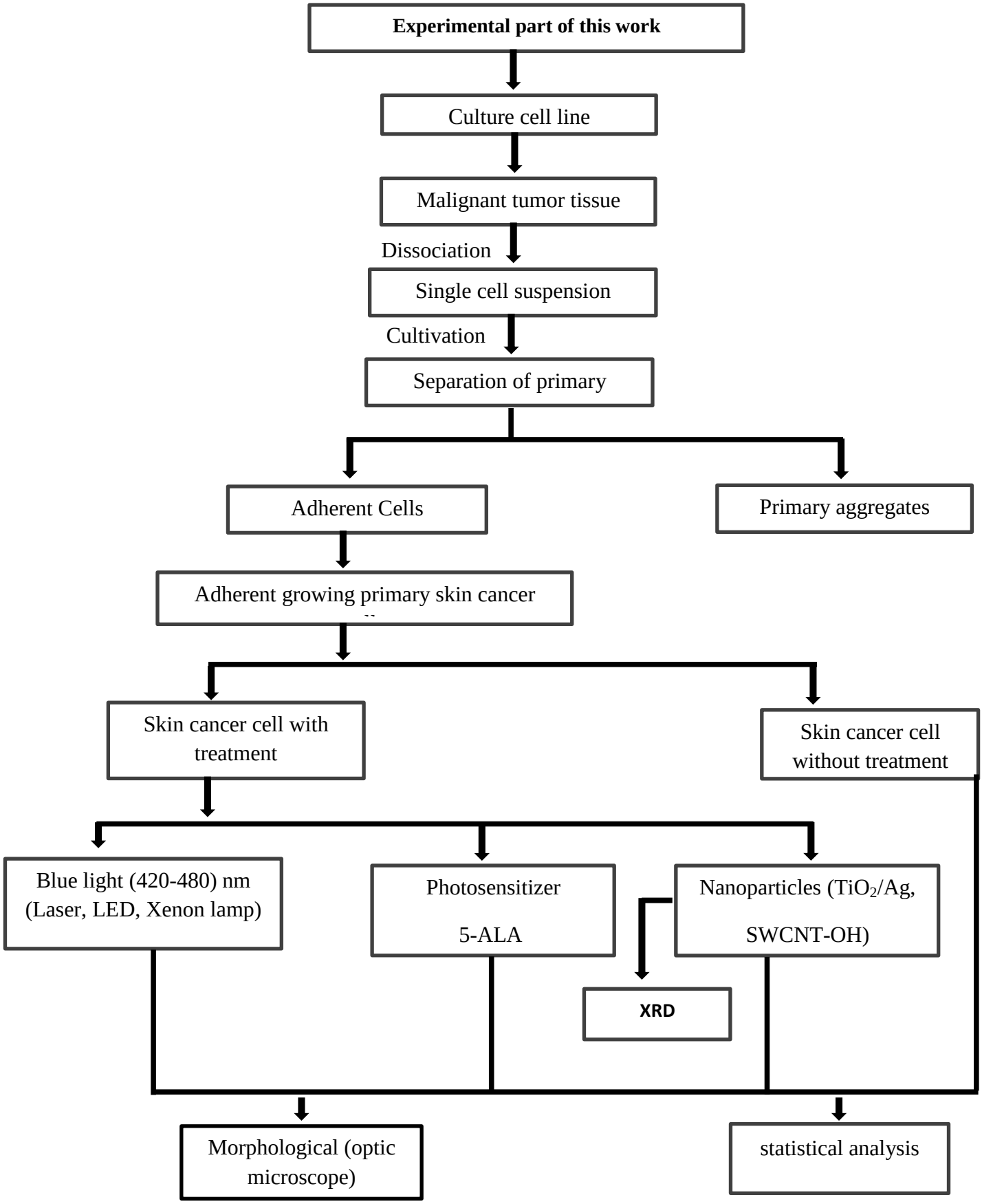

Figure (3-1): Block diagram of experimental work.

3-3 Chemical Material:

The chemical material used in this study are listed in (Table 3-1) with their suppliers.

Table (3-1): List of Chemicals Used in the Study.

Chemical material	Company	Country
Fetal bovine serum (FBS)	Gibco	UK
Dimethyl sulfoxide (DMSO)	Roth	Germany
Alcohol spray (ethanol 70%)	AMEYA FZE	UAE
Phosphate buffer saline tablet	Gibco	UK
MTT(3-(4,5-Dimethylthiazole-2-yl)-2,5-diphenyl-2H-tetrazolium bromide) dye powder	Roth	Germany
Roswell Park Memorial Institute-1640 (RPMI-1640) powder medium	Gibco	UK
Gentamycin (80 mg vial)	The Arab pharm.	Jordan
Sodium bicarbonate powder	Ludeco	Belgium
Trypsin-Ethylenediaminetetraacetic acid (EDTA) powder	US biological	USA
Cisplatin	JSL	India

3-4 Instruments and Tools:

The instruments and tools used in the study are listed in (Table 3-2) with their origins:

Table (3-2): List of Instruments and Tools Used in the Study.

instrument or tool	Company	Country
Cell culture flask (25ml)	SPL	Korea
Automatic micropipettes (different sizes)	Human	Germany
Autoclave	Jeiotech	Korea
Cell culture plate (96- wells)	SPL	Korea
Digital camera	Sony	Japan
Distiller	ROWA	Germany
Double distillation water stills	GFL	Germany
Electric oven	Memmert	Germany
ELISA Reader	Human	Germany
Incubator	Memmert	Germany
Sterile freezing vial (1.5 ml)	Biofil	Australia
Flow cytometer (BriCyte E6)	Mindray	China
Inverted microscope	T.C Meiji techno	Japan
Laminar air flow cabinet	Labtech	Korea
Liquid nitrogen container GT38	Air Liquide	France
Magnetic stirrer	Labinco	Netherland
Microcentrifuge	Memmert	Germany
Millipore filter (0.45, 0.22μm)	Biofil	Australia
PH Meter	WTW	Germany

3-5 Methods-Preparation of Reagents and Solutions

This section shows Preparation of Reagents and Solutions was used in the work.

3-5-1 Phosphate Buffer Saline (PBS)

The PBS was prepared according to Gibco manufacturer manual by dissolving one tablet of PBS in 500 ml deionized distilled water (DDW) with stirring constantly on a magnetic stirrer at room temperature, the pH will be 7.45 and requires no adjustment. Sterilization was done by autoclaving and kept sterile in a closed bottle until use.

3-5-2 Gentamycin Stock Solution:

The working concentration of gentamycin in the medium is 50 μg/ml. Gentamycin vial of 40 mg/ ml solution was considered as stock solution and stored at 4 C˚ for uses.

3-5-3 Trypsin Solution:

According to US Biological directions, A weight of 10.1 gm of trypsin powder was dissolved in 900ml of DDW and constantly mixed by stirring at room temperature. The pH of the solution was adjusted to 7.2, and the volume completed to one liter. The solution was sterilized by filtration using 0.45 and 0.22 μm millipore filters subsequently. The content was stored at (- 20C˚).

3-5-4 MTT Solution:

A weight of 0.5 g of MTT powder was dissolved in 100 ml PBS to obtain a concentration of 5 mg/ml. Then the MTT solution was sterilized by filtration through a 0.2 μm milli pore filter into a sterile and light

protected container and stored at 4°C for frequent use or at (-20)°C for long term storage [169].

3-6 Preparation of Tissue Culture Medium

Tissue culture medium was prepared in the following ways:

3-6-1 Preparation of Serum-Free Medium

Liquid RPMI-1640 medium was prepared from powdered RPMI-1640 medium according to the Gibco product manual as the following: From the RPMI-1640 powdered medium, 10.43 g was dissolved in approximately 900 ml of DDW in a volumetric flask. The other components include: 2 g sodium bicarbonate powder or according to need and 1.25 ml from gentamycin stock solution had been added with continuous stirring. The volume was completed by DDW to one liter and the pH of the medium adjusted to 7.4. Sterilization was done by 0.4 and 0.2 μm Millipore filters subsequently. After the end of the procedure, 5 ml of the medium was incubated at 37 ºC in a sterile flask for 4 days with daily examination for signs of bacterial and fungal contamination. It was considered sterile only in case of no signs of contamination during the four days of incubation. Then the medium was stored at 4ºC until use.

3-6-2 Preparation of Serum-Medium:

Serum-medium was prepared as described in (3-6-1) with the addition of 10% FBS.

3-6-3 Preparation of Skin Cancer

Skin cancer A431 cell line in frozen vials were obtained from **the American Type Culture Collection (ATCC)**.

3-7 Primary Culture Methods

1- obtain the samples of cancer, and place pieces into tissue culture media RPMI-1640 in sterile plastic containers, Universal container, and other sterile containers. Maintain a cool temperature for the material (by placing it on ice), and move as quickly to the tissue culture suite. Within the confines of a sterile environment, wash the tissue in a medium PBS balanced salt solution.

2- Trypsinization was be utilized to segregate more adherent cell types from fast attaching/detaching cells.

3- The cell lines were cultured according to the Gibco manual with 10% fetal bovine serum (FBS) and 1% penicillin/streptomycin antibiotics and incubated at 37 ˚C.

4- The cultures were checked on a frequent basis in order to determine which cell types adhered and grew.

5- When a monolayer of cells has formed, The medium was aspirated and thrown away. The cells were then carefully pipetted up and down to separate clusters of cells into individual cells. The cells were then cultivated with a culture plate.

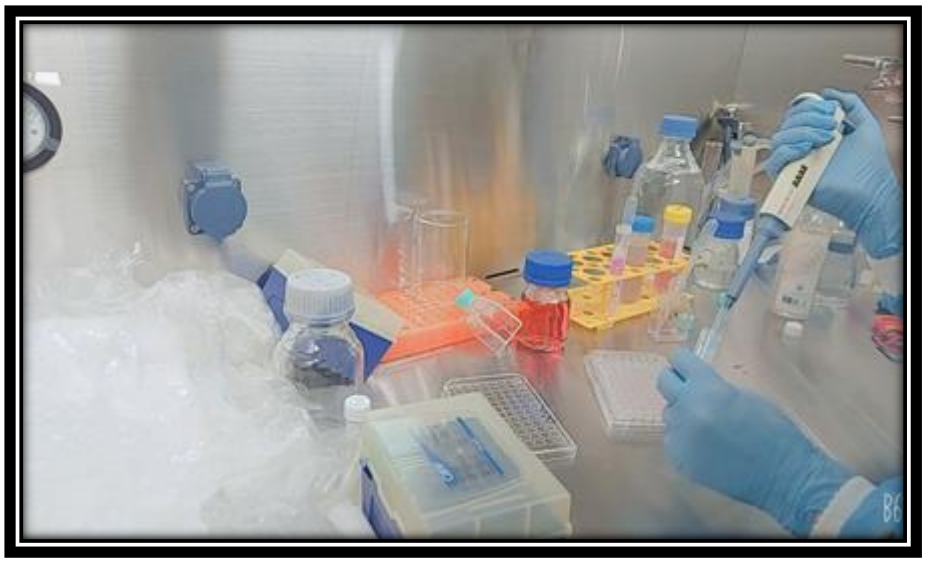

Figure (3-2): Preparation the 96-well plates for MTT assay test.

3-8 Thawing of Skin Cell Line

The frozen cell line vial was removed from the liquid nitrogen container with caution and directly placed into a beaker containing pre-warmed (37°C) sterile DDW. The vial was removed from the water before the ice floccule dissolved completely, and then it was wiped with 70% ethanol. Without delay, the cell suspension content of the vial was pipetted under laminar flow into a 15-ml sterile plastic centrifuge tube containing 10 ml of pre-warmed serum-free medium. Centrifugation was done at 1000 rpm for 5 minutes, and the supernatant was aspirated and decanted. The cell pellet was re-suspended into 5 ml of warm (37 °C) serum medium. replaced the next day. A solution of a nanoparticles with distilled water , an appropriate amount of a specific substance in a specific volume of nanoparticles at a concentration (1000) µg of nano powder is dissolved in a volume of 1cm^3) of solvent (water), according to the following relationship[170]:

$$\frac{C \times V \times M.W}{1000} \qquad (3\text{-}1)$$

*w*m = Nano powder weight

C: the concentration to be prepared in mol

V: the volume of the solvent cm^3 to be added to the substance.

M.W: The molecular weight of the dye used is gm/mol.

To dilute the prepared (400, 200, 100, 50, 25, 12.5) µg/ml from TiO_2/Ag, (200, 100, 50, 25, 12.5, 6.25) µg/ml from SWCNT-OH, and (1000, 500, 250, 125, 62.5, 31, 25)µg/ml from 5ALA photosensitizer, this is done using the following relationship, which is called the dilution relationship:

$$\mathbf{C_1V_1 = C_2V_2} \qquad (3\text{-}2)$$

Where :

C_1: First concentration.

C_2: second concentration.

V_1: the necessary volume of the first concentration.

V_2: The volume needed to be added to the first concentration to obtain C_2

3-9 Material Preparation

The material used in the study

1- Photosensitizer Preparation

5-ALA photosensitizer the chemical formula (C5H9NO3.HCl) was purchased from "SIGMA-ALDRICH" suitable for cell culture. molecular weight 167.59. it was dissolved in distilled water to obtained stock solution (2000 µg/ml) and was stored in dark. For each experiment a new aliquot was thawed immediately 3 hours prior to use. The working drug

solutions of varying concentrations were prepared by diluting the stock solution (31.35 – 1000 µg/ml) was prepared by dissolving a 50 mg of the 5-ALA in 25 ml of distilled water to obtain the stock solution that was finally sterilized by 0.22 µm Millipore filter [171,172].

2- Single Walled Carbon Nanotube-OH

Nanoparticles was obtain from "ottokemi" OH Functionalized Single Walled Carbon Nanotubes are made by CVD (Chemical vapor deposition) and purified and functionalized using concentrated acid chemistry. Carbon Nanotubes (CNTs) have proven to offer a unique properties of stiffness and strength largely due to their high aspect ratio and all carbon structure. The thermal and electrical conductivity found in CNTs is much higher than that of other conductive or fibrous additive materials. Surfactants are used to stabilize dispersions in DI Water or other aqueous solvent mixtures. The carbon atoms in CNTs are arranged in a planar honeycomb lattice structure in which each atom is connected via a strong chemical bond to the three neighboring atoms. These strong bonds are the reason that the basal plane elastic modulus of graphite is one of the largest of any known material. Having such strong bonds at the atomic level as well as a high aspect ratio, Carbon Nanotubes are expected to be the ultimate high-strength fibers. Outer Diameter: 1-2nm, Inside Diameter: 0.8-1.6nm, Content of –OH 3.76 - 4.16 wt% and Purity: >90 wt%. The solution was prepared by drag a 200 µl of the SWCNT (1000 µg/ml) in 1800 µl of culture media to obtain 2000 µl at concentration 200 µg/ml. done using the dilution relationship. then drag by micropipette 200 µl and placed into the plate.

3- Nanoparticles of TiO_2 Decorated Ag

Silver Titanium Oxide / Ag-TiO2 Nanoparticles 20wt% dispersion was obtain from "SIGMA-ALDRICH" fully dispersed in Water (Doped with 100 ppm 15 nm Ag light brown color). The solution was prepared by dissolving a 800 µl of the TiO2/Ag (1000 µg/ml) in 1200 µl of culture media to obtain 2000 µl at concentration 400 µg/ml done us`ing the dilution relationship. After that drag by micropipette 200 µl and placed into the plate. Figure(3-5) shows the preparation of used material in this study.

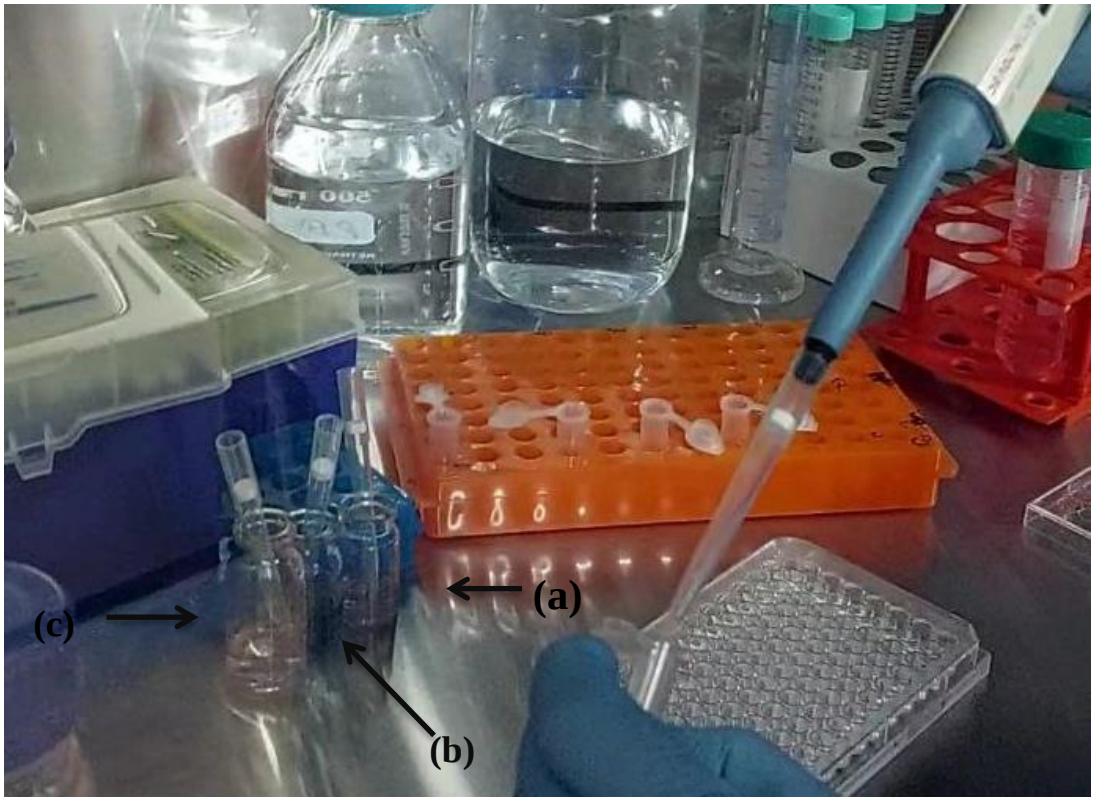

Figure (3-3) : The Prepared materials of (a) Culture medium+Tio_2/Ag (b) Culture medium+ SWCN-OH (c) Culture medium+ 5-ALA.

3-10 Light Devices and Protocols

Cells were seeded on sterile 96-well plates (well area: 0.2826 cm^2) in 200 µl of medium with cover during irradiation The emission tip was

hold perpendicular above the culture media and the irradiation was carefully timed and carried out in a dark room. The emitted light completely covered the irradiated field of each culture plate, as assessed using an optical power meter. The control group was not exposed to laser. cells were kept at 37C. This work was done at the rowafid alelom center for cell culture techniques in Babylon. Three different light source protocols were employed which are:

a. Light Emitting Diode (LED)

The blue-light lasers were obtained from the Dental clinic of Hilla. emitting at around 420-480 nm with output light wave intensity 1600-1800 mw/cm LED, irradiance 400 mW/cm^2, An optical power meter was used to measure irradiance (Laboratory optics and laser in college of science department of Physics).

Figure (3-4): Setup of Photodynamic Therapy (PDT) by blue LED in this work.

b. Xenon Lamp

The Xenon lamp used in these experiments is based on commercially available LED, emitting at around 420-480 nm. 35 W optical emission power for Xenon (12 V).

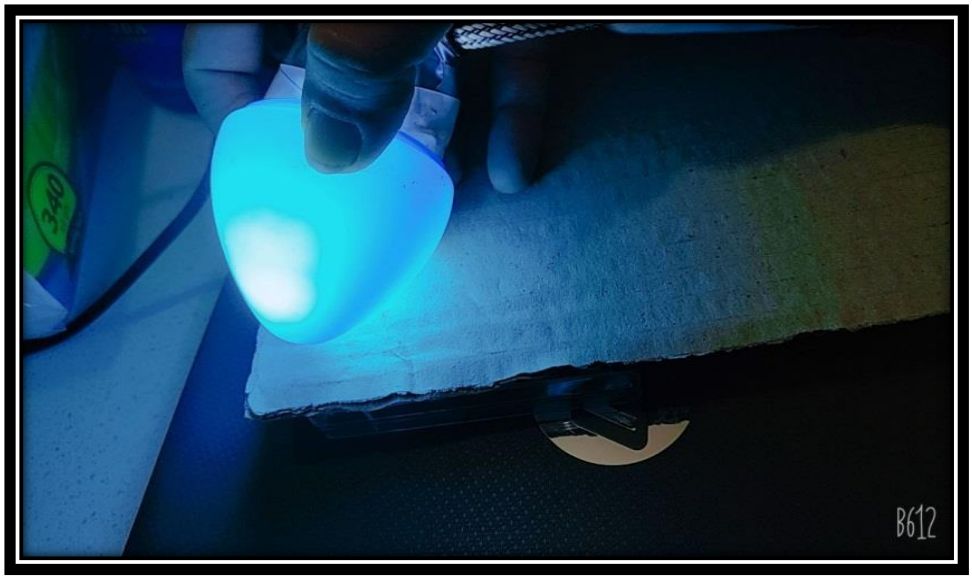

Figure (3-5): Setup of Photodynamic Therapy (PDT) by Xenon in this work.

c. Blue Laser

Diode lasers, which emitted 473 nm was used as light sources. The exposure conditions used were as following: blue laser λ=473 nm, power= 100 mW, mode laser (CW), Threshold Current = 20 mA, Applied voltage = 220 v, Height of laser =10 cm. This work done in laser physics laboratory in College of Science for women, University of Babylon.

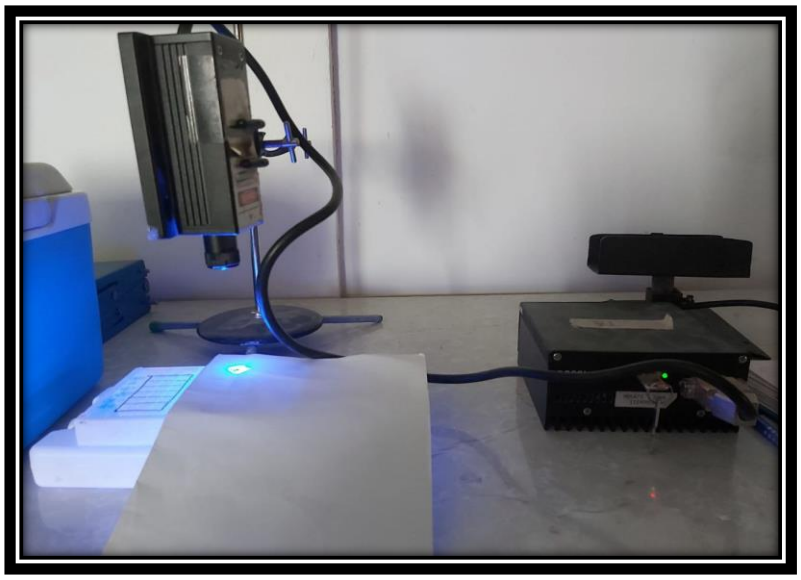

Figure (3-6): Setup of Photodynamic Therapy (PDT) by blue Laser in this work.

3-11 Laser Irradiation

After 24 hours of cell seeding, the irradiation was carried out in the 96-well plate. The laser's tip was 10 centimeters away from the plate's bottom, which corresponded to the size of a single well on a 96-well plate, and the cells were uniformly exposed to radiation .The exposure time in seconds was multiplied by the laser power density (W/cm^2) to determine the energy-density (fluence) (J/cm^2) for all treatment groups. The exposed surface area used for the study was the same size as each culture well's surface area on a 96-well plate, which is (0.2826 cm^2).

Surface area (cm^2) = π x r^2.When the power is divided by the area on which is it distributed, then we got the power density (irradiance):

The power-density (irradiance) (W/cm^2) =Power/Area (3-3)

The energy-density (fluence) (J/cm^2) =

Time (s) x [Power (W)/ Area (cm^2)] [13] (3-4)

3-12 Cytotoxicity Assays (MTT Assay)

Cell growth was determined by measuring absorbance of -3(4,5-dimethylthiazol-2-yl)-2,5-diphenyltetrazolium bromide (MTT; Sigma–Aldrich) in living cells as described previously [170].

At the end of the exposure period, the medium was removed from the wells and then the cells were washed with PBS. A blank control was carried to assess unspecific formazan conversion. The MTT solution (10 µl: 5 mg/ml in PBS) was add to each of the 96 wall plates. The plates were further incubated for 3-4 hours at 37 ℃ until intracellular purple formazan crystals were visible under the inverted microscope. The supernatant was removed and 100 µl DMSO was added in each well to dissolve the resultant formazan crystals. The plate was incubated at room temperature for 30 minutes until the cells have lysed and purple crystals have dissolved. Absorbance was measured by a microplate reader at 570 nm.

The absorbance reading of the blank must be subtracted from all samples. Absorbance readings from test samples must then be divided by those of the control and multiplied by 100 to give percentage cell viability or proliferation. Absorbance values greater than the control indicate cell proliferation, while lower values suggest cell death or inhibition of proliferation. Percent of cell viability or percent of inhibition was calculated by the following formula [173]:

The percentage of inhibition was calculated according to the following equation :

Inhibition % = (optical density of control wells –
optical density of test wells) / optical density of control wells (X 100) **(3-5)**

The percentage of viability was calculated according to the following equation:

Viability % = 100- (optical density of control wells- optical density of test well) / optical density of control wells (X 100)
(3-6)

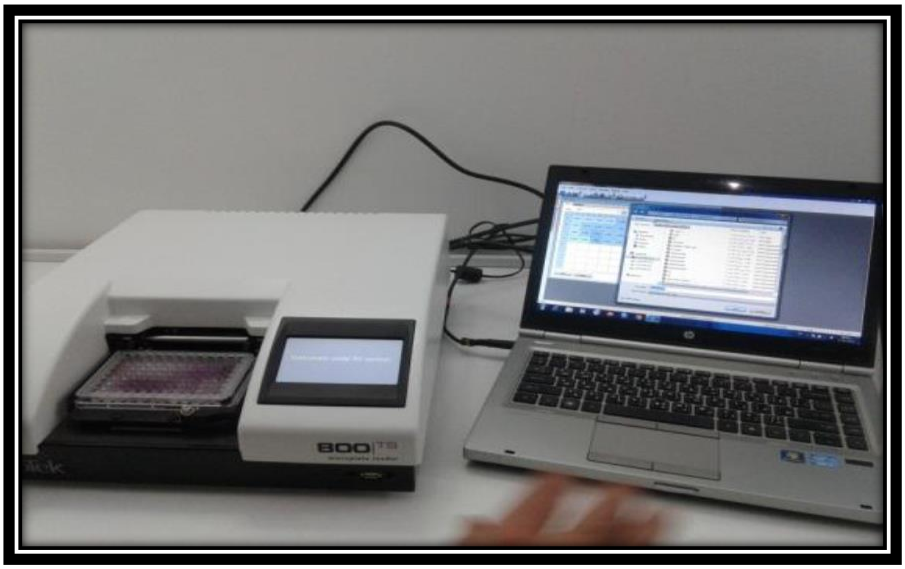

Figure (3-7): The micro plate reader instrument.

3-13 X-ray Diffraction (XRD)

X-ray diffraction (XRD) is a powerful technique for determining the crystal structure and lattice parameters. The basic principles of X-ray diffraction are found in textbooks e.g. by Fox [174]. A basic instrument for such study is the Bragg spectrometer [175]. The relationship describing the angle at which a beam of X-rays of a particular wavelength diffracts from a crystalline surface was discovered by

William H. Bragg and W. Lawrence Bragg and is known as Bragg's law [176].

$$\mathbf{2d_{(hkl)}\sin\theta = m\lambda} \quad \textbf{(3-7)}$$

Where, (λ) is wavelength of the X-ray, (θ) is Bragg diffraction angle of the XRD peak in degree (scattering angle), (m) is integer representing the order of the diffraction peak, and ($d_{(hkl)}$) is inter-plane distance of (i.e atoms or ions or molecules). The crystallite size of the deposits is estimated from the full width at half maximum (FWHM) of the most intense diffraction line by Debye Scherrer's formula as follows [177].

$$\mathbf{D_S = \frac{0.94\,\lambda}{\beta\cos\theta}} \quad \textbf{(3-8)}$$

Where, D_S is crystallite size, and β is (FWHM) in radians. The X- ray diffraction data can also be used to determine the dimension of the unit cell. The lattice constants (a) and (c) of the wurtzite structure for thin film can be calculated using following relations [178].

$$\mathbf{a = \frac{2}{\sqrt{3}}\, d_{(hkl)}} \quad \textbf{(3-9)}$$

$$\mathbf{C = 2d_{(hkl)}} \quad \textbf{(3-10)}$$

The X-ray diffraction measures structures of crystalline compounds and surface chemistry. The XRD patterns were determined using a diffractometer equipped with a rotating target X-ray tube and a wide-angle goniometer. The X-ray source were Kα radiated from a copper target with a graphite mono chromator. The X ray tube was operated at a potential of 30 kV and a current of 20 mA. The range (2 θ) of scans was performed from 10 to 80. The XRD pattern were analyzed for SWCNTs-OH and TiO_2/Ag. Samples were examined at the faculty of engineering, university of Kufa, and the XRD system is shown in the Figure (3-8).

Figure (3-8) : Image of the XRD.

3-14 Statistical Analysis

Sigma Plot version 13 and Microsoft Office Excel 2010 were used to collect and analyses all the data. The significance of differences between the data means was evaluated using the ANOVA test, where a p-value between 0.001 and 0.05 was deemed statistically significant.

Chapter Four

Results and Discussion

4- Introduction

The skin cancer cell line A431 was transferred to 96-well culture plates containing 150 µL of medium per well and planted one day before treatment at a density of 5×10^4 cells per well. PDT was irradiated with continuous-wave radiation (CW). In this study, three different sources of light at wavelengths (420-480). nanoparticles, and photosensitizers were used to treat skin cancer at period of times. and then performed assays and were validated by applying the percentage viability of cells equation (3-6)

4-1 Effect of Laser Beam Irradiation at 473 nm on the A431 Cell Line

Effect of a blue laser (λ= 473 nm, Optical Output Power = 100 mW) on the A431 cell line after incubation for 24 hours. The results showed that there was no significant stimulatory effect on the viability percent of the cells at the lower exposure time. In the viability percent at all exposure times (150, 160, 170, 180, 190, and 200 seconds) for 24 hours of incubation, no effect was clearly seen after incubation for 24 hours in comparison with the control group, as shown in Table (4-1) and Figure (4-1).

Table (4-1):Parameters of Photodynamic Therapy PDT for blue laser on cell line.

Time (Sec)	optical density of test well	Average optical density of control wells	Viability of cells %	Average Viability cells %
150	0.272 0.285 0.273	0.2865	94.938 99.476 95.287	96.567
160	0.27 0.285 0.28	0.2865	94.240 99.476 97.731	97.149
170	0.24 0.322 0.282	0.2865	83.769 112.390 98.429	98.196
180	0.258 0.271 0.28	0.2865	90.052 94.589 97.731	94.124
190	0.254 0.277 0.243	0.2865	88.656 96.684 84.816	90.052
200	0.249 0.22 0.23	0.2865	86.910 76.788 80.279	81.326

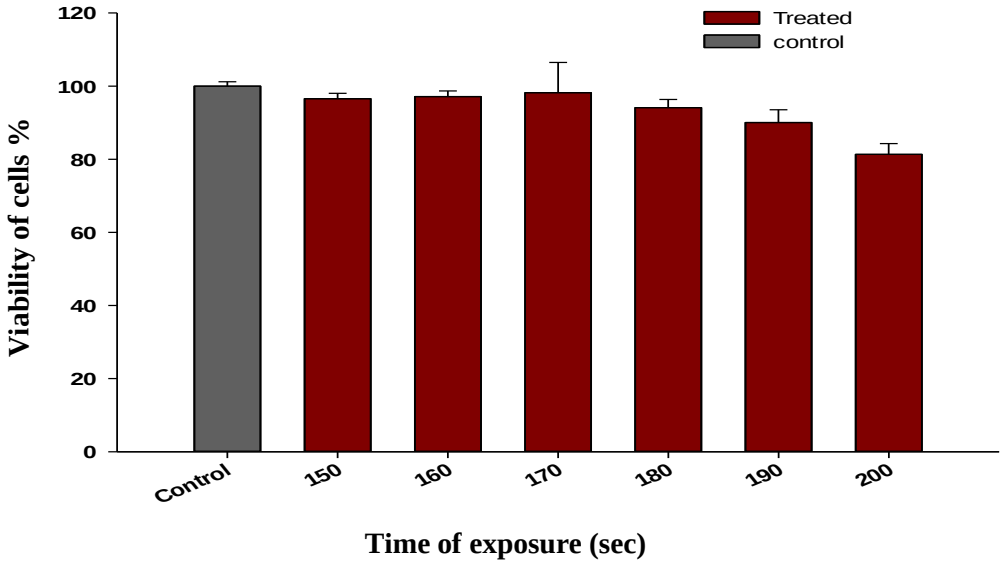

Figure (4-1): Effect of different irradiation times of the laser (473 nm–100 mW) on the A431 cell line after incubation for 24 hours.

4-2 Effect of Light Emitting Diode on the A431 Cell Line

The LED result showed that there was a significant cytotoxic effect. The growth rate of the A431 cells decreased gradually at different irradiation times, and the effect of cell death got bigger with increased exposure time; the viability of cells was reduced to 45.526 at 240 seconds, as shown in Table 4-2.

Table (4-2): Parameters of Photodynamic Therapy PDT for Blue LED on cancer cell.

Time (sec)	optical density of test well)	Average optical density of control wells	Viability of cells %	Average Viability of cells %
190	0.217 0.181 0.19	0.38	57.105 47.631 50	51.578
200	0.184 0.185 0.192	0.38	48.421 48.684 50.526	49.210
210	0.208 0.193 0.186	0.38	54.736 50.789 48.947	51.491
220	0.218 0.196 0.168	0.38	57.368 51.578 44.210	51.052
230	0.18 0.204 0.186	0.38	47.368 53.684 48.947	50
240	0.17 0.172 0.177	0.38	44.736 45.263 46.578	45.526

After exposing the cells for 190, 200, 210, 220, 230 and 240 seconds, it was observed that irradiation with 400 mW/cm^2 killed nearly half of the cells (Figure 4-2);

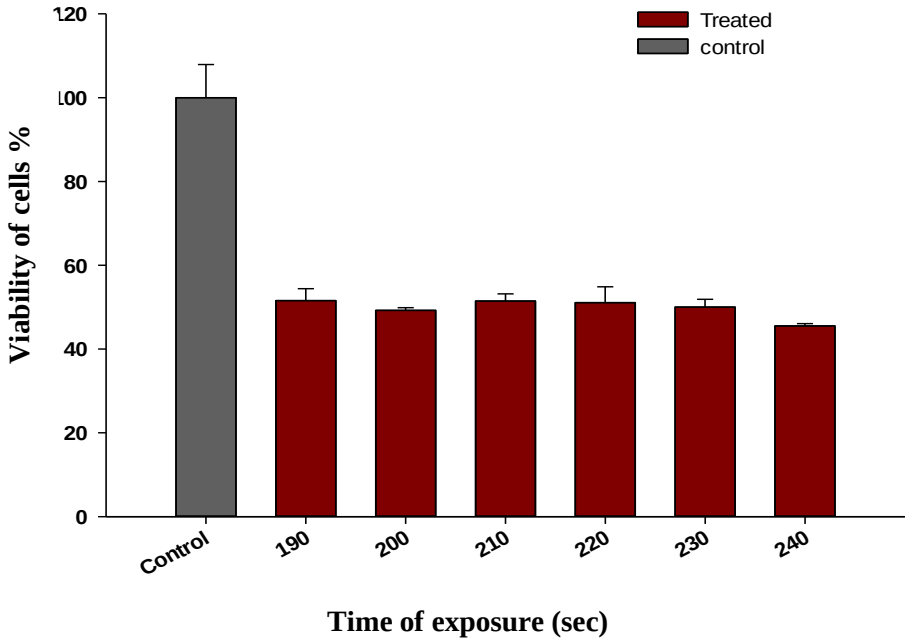

Figure (4-2): Effect of different irradiation times of LED blue light (420-480 nm) on A431 cell line after incubation for 24 hours.

Table 4-2 shows that cell viability decreased from 51.57% at 190 seconds to 45.526% at 240 seconds. The LED blue light with a wavelength range of 420–480 nm and a power density of 400 mW/cm^2 caused a considerable amount of PDT cytotoxicity on the cells, and the effect of death cells became more pronounced with longer exposure times. After being exposed to blue light for 240 seconds, approximately half of the cells in the sample died as a result. Therefore, blue light at 420–480 nm was used to treat SCC cells in order to study cell reactions to PBM at various irradiances and doses. This reduction was dependent on dosage and wavelength. The viability of cells is obviously different when compared to a blue laser at 200 seconds because of the low radiation dose. When compared to the previously reported study [179-182].

The morphology of the treated cells was examined using a CKX41 inverted light microscope (Molecular Devices in the United

States),connected to a camera with get IT software . After 24 hours of treatment, the morphology of each plate, including both live and dead cells, was photographed. As shown in Figure (4-3).

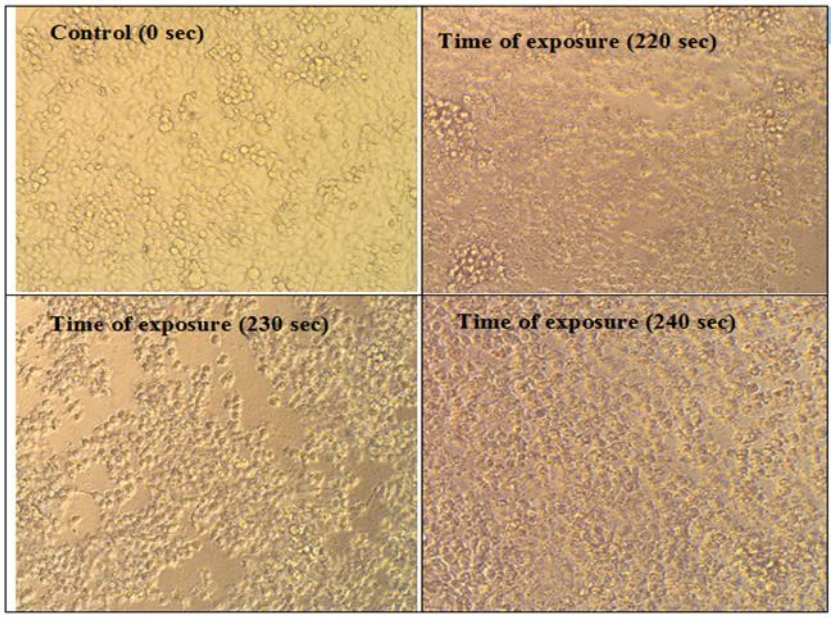

Figure (4-3): Observations of A431 cell morphological changes after exposure by blue LED, the cells were observed by optic microscope directly.

4-3-1 Effect of TiO_2/Ag Nanoparticles on the A431 Cell Line

The MTT test was used to see if human skin cancer cells would still live after being exposed to TiO_2/Ag nanoparticle concentrations that were doubled over , ranging from 12.5, 25, 50, 100, 200 and 400 µg/ml. The blue light results showed a big decrease in cell viability ($p \leq 0.001$) after 24 hours of incubation; the nanoparticle results showed a big decrease in cell viability ($p \leq 0.001$) for all concentrations. It was observed that the viability of cells was very low, and this indicates the destruction of cancer cells due to the small size of the nanomaterial that can penetrate into the cell and spread into the cytoplasm of the cell. The best concentration was 400 µg/ml, which resulted in the greatest number of cancer cells destroyed.

Nanoparticles' considerable suppression of cell viability was clearly detected in a dose-dependent manner. The cytotoxicity of TiO_2/Ag NPs against cancer cells was dependent on size, as shown in Tables 4–3.

Table (4-3) : Parameters of concentration TiO_2 decorated Ag on A431 cell line.

Concentration µg/ml	Optical density of test well)	Average optical density of control wells	Viability of cells %	Average Viability cells %
12.5	0.541 0.545 0.553	0.587	92.137 92.818 94.181	93.0457
25	0.513 0.556 0.608	0.587	87.368 94.692 103.548	95.20295
50	0.54 0.579 0.517	0.587	91.967 98.609 88.049	92.87539
100	0.56 0.548 0.546	0.587	95.373 93.329 92.988	93.89725
200	0.385 0.398 0.352	0.587	65.569 67.783 59.948	64.43372
400	0.201 0.319 0.328	0.587	34.232 54.328 55.861	48.14079

Figure (4–4) show the cell viability of TiO_2/Ag NPs with a minimal serial doubling increase. The cell survival rate diminishes as the concentration of nanoparticles rises. The viability of cells nearly dropped marginally as the concentration of TiO_2/Ag nanoparticles was raised.

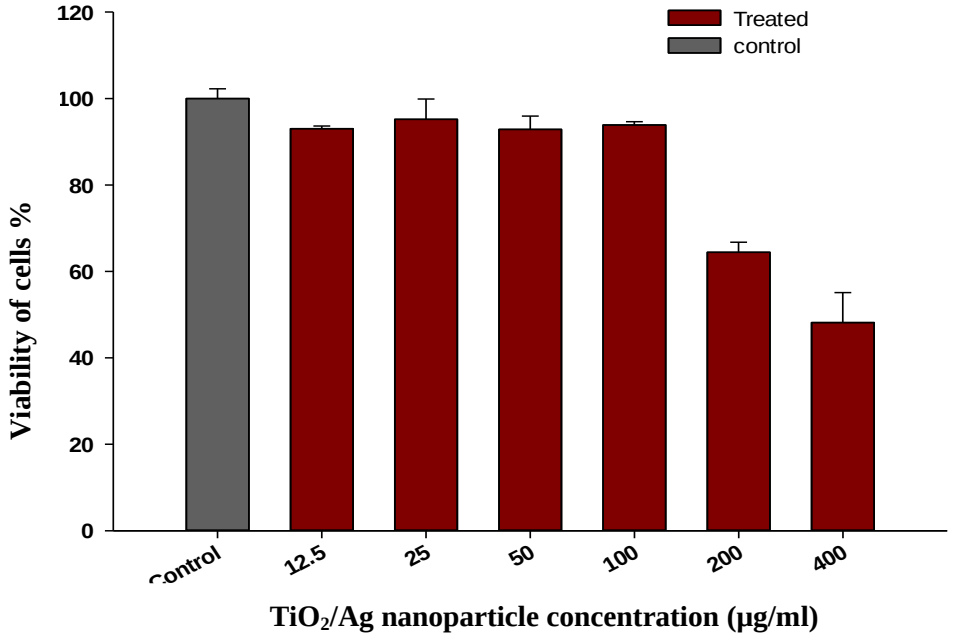

Figure (4-4): Effect of different concentrations of TiO_2/Ag on the A431 cell line after incubation for 24 hours.

4-3-2 Effect of TiO_2/Ag Nanoparticles in Combination with Blue Light Emitting Diode (400 mW/cm^2) on the A431 Cell Line

The cytotoxicity of TiO_2/Ag NPs against cancer cells was size-dependent. There was a big decrease in cell viability with the best concentration when exposed to irradiation for 220 s, 230 s, and 240 s after 24 hours of incubation compared to the control group, As shown in table 4-4

Table (4-4): Parameters of Tio_2/Ag in combination with blue LED on A431 cell line.

Time (Sec)	optical density of test well)	Average optical density of control wells	Viability of cells %	Average Viability of cells %
220	0.348 0.256 0.174	1.062	32.742 24.086 16.371	24.400
230	0.209 0.164 0.19	1.062	19.664 15.430 17.876	17.657
240	0.198 0.218 0.194	1.062	18.629 20.511 18.253	19.131

PDT treatment of the A431 cells noted major cell death of almost 19.13% of the viability of cells when combined irradiation with 400 µg/ml of TiO_2/Ag, which has been considered the optimal concentration in current work. In the results of photodynamic treatment of a human skin cancer cell line with the optimum parameter, there was obvious cytotoxicity in A431 cells at a concentration of 400 µg/ml ($P > 0.05$) (Figures 4–5). The viability of cells decreased by approximately 19.13% with increasing exposure time by applying equations (3-6) to skin cancer without and with nanoparticles with photodynamic therapy, which indicated the Ag-TiO_2 NPs exhibited good biocompatibility. There was a decrease in the number of surviving cancer cells due to the presence of TiO_2 and Ag nanoparticles. The number of surviving malignant cells was decreasing with increased exposure time. As shown in Figure (4-5), the evidence at hand points to multiple processes that may be involved in cell death as the mechanism underlying the anticancer characteristics.

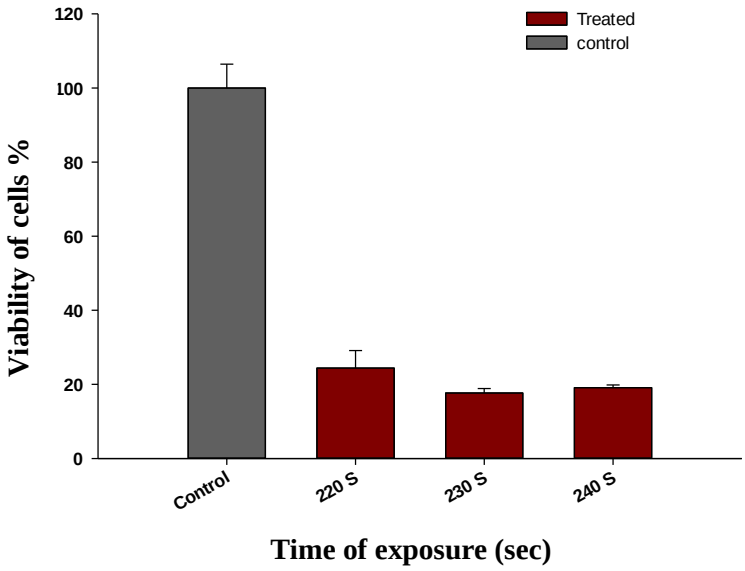

Figure (4-5) Effect of TiO_2/Ag (400 µg/ml) in combination with blue LED on the A431 cell line after incubation for 24 hours.

According to a theory put forth by De Matteis et al. [183], silver nanoparticles are taken up by cells by endocytosis. The released cytosolic silver ions may then produce large amounts of intracellular ROS, which may eventually lead to DNA damage and mitochondria-related apoptosis [183]. According to the Gurunathan et al. report, the MDA-MB-231 breast cancer cell line was susceptible to the cytotoxicity of silver nanoparticles by a conventional p53-dependent apoptotic mechanism [184]. Autophagy, however, has also recently been put forward as a potential mechanism. According to Lin et al.'s research, administering an autophagy inhibitor to patients increases the anticancer effect of nanoparticles [185]. It is well known that the plasma and mitochondrial membranes may be harmed by oxidative stress brought on by a high quantity of ROS [183]. This ROS production, specifically for silver NPs, has repeatedly been noted as a key mechanism underlying their cytotoxic activity [183, 186].

The morphology of the treated cells was examined using a CKX41 inverted light microscope (Molecular Devices in the United States), connected to a camera with get IT software . After 24 hours of treatment, the morphology of each plate, including both live and dead cells, was photographed. As shown in Figure (4-6).

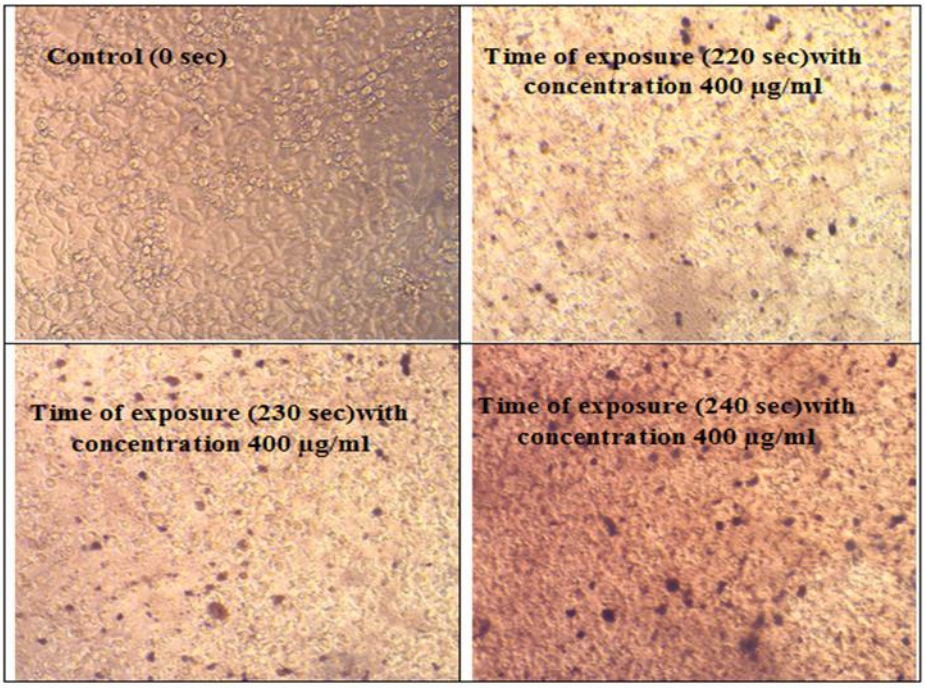

Figure (4-6) Observations of A431 cell morphological changes after exposure blue LED with TiO_2/Ag nanoparticles (400 µg/ml), the cells were observed by optic microscope directly.

4-4-1 Effect of SWCNT-OH Nanoparticles on the A431 Cell Line

Table (4–5) displays the findings of the viability of the cell assay. The results showed that the non-treated 0 µg/ml demonstrated a decrease in the percentage of viability of cell behavior for SWCNTS-OH at concentrations of 200 µg/ml (48.140%).

Table(4-5): parameter of concentration SWCNT-OH on A431 cell line.

Concentration µg/ml	optical density of test well)	Average optical density of control wells	Viability of cells %	Average Viability cells %
6.2	0.477 0.498 0.454	0.587	81.237 84.814 77.320	93.0457
12.5	0.462 0.538 0.493	0.587	78.682 91.626 83.962	95.20295
25	0.5 0.492 0.384	0.587	85.154 83.792 65.398	92.87539
50	0.451 0.478 0.511	0.587	76.809 81.407 87.028	93.89725
100	0.409 0.427 0.481	0.587	69.656 72.722 81.918	64.43372
200	0.404 0.289 0.362	0.587	68.804 49.219 61.652	48.14079

The cytotoxicity behavior of SWCNTs-OH was analyzed using MTT assay kit. The A431 cell line were prepared with SWCNTs-OH, After the successful PDT treatment, the measured absorbance value of untreated cells was kept as a control. The assay results are shown in the Figure (4-7).

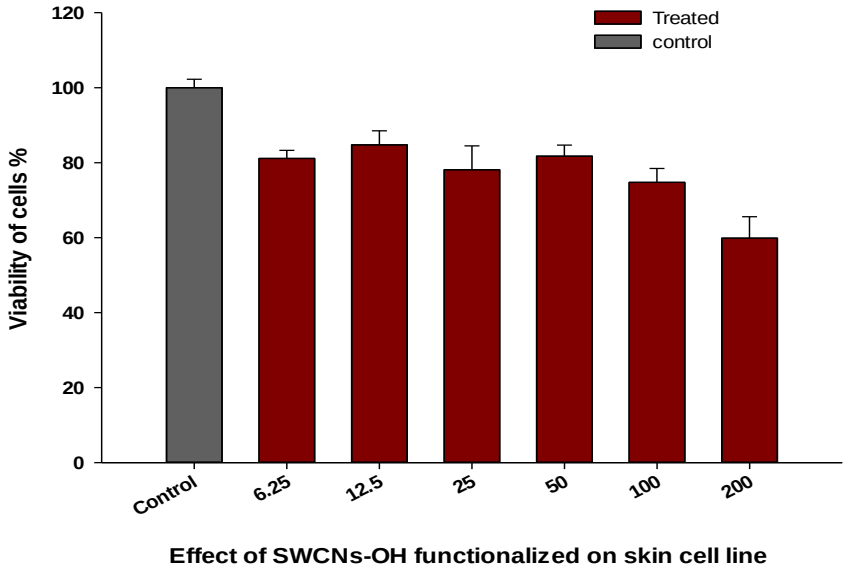

Figure (4-7): Effect of different concentrations of SWCNT-OH on A431 cell line after incubation for 24 hours.

4-4-2 Effect of SWCNT-OH Nanoparticles in Combination with Blue Light Emitting Diode (400 mW/cm^2) on the A431 Cell Line

Figure (4-8) , The viability of cells decreased with increasing time of exposure. The percentage viability of the cells treated with SWCNTs-OH at 220 seconds exhibited a viability of 30.421%, whereas the percentage viability of the cells at 230 and 240 seconds was 29.857% and 24.870%, respectively, as shown in Table 4-6. The exposure of blue LEDs at 400 mW/cm^2 on the plate significantly reduced the percentage of cell viability under 240-second irradiation in combination with SWCNTs-OH compared to cells alone.

The irradiated samples showed prominent apoptotic effects on the A431 cell line compared to the control. It indicates the number of viable cell counts was gradually decreased in both with and without photodynamic therapy. The assay results are shown in Figure (4-8).

Table(4-6): parameter of SWCNT-OH in combination with blue LED on A431 cell line.

Time (sec)	optical density of test well)	Average optical density of control wells	Viability of cells %	Average Viability of cells %
220	0.297 0.368 0.305	1.062	27.944 34.624 28.696	30.421
230	0.355 0.307 0.29	1.062	33.401 28.885 27.285	29.857
240	0.339 0.165 0.289	1.062	31.895 15.524 27.191	24.870

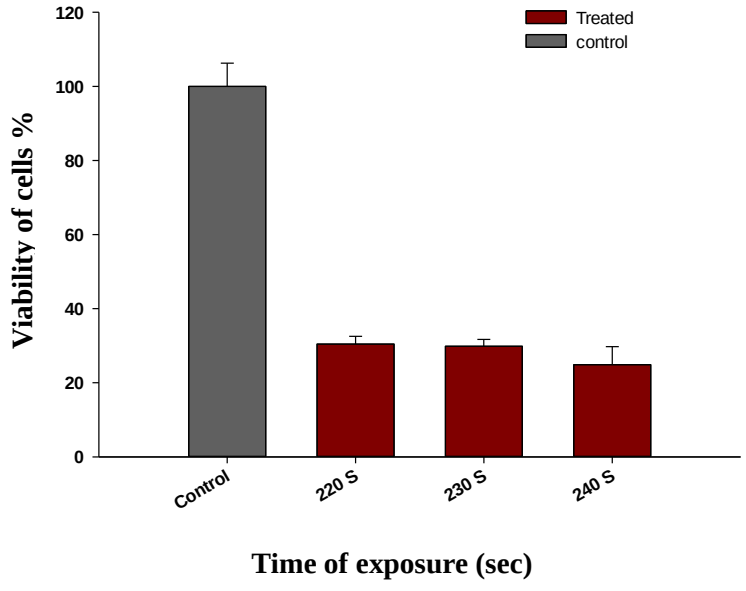

Figure (4-8): Effect of SWCNT-OH in combination with blue LED on the A431 cell line after incubation for 24 hours.

The results of the biological evaluations of the exposure in the initial test by optic microscope on culture cell line before the MTT assay when conducted on human skin cancer (A431) are depicted in figure 4-9,The inverted light microscope was used to capture the morphological observation of treated and untreated cells for a period of twenty-four hours. The qualitative and preliminary confirmation of cellular viability and cell death were examined from the cellular morphology utilizing acquired microscopic pictures. This was done in order to get a better understanding of both concepts. the SWCNTs-OH, nanoparticles treated cells morphology revealed that severe morphological changes and pronounced increased cell death was found after 24 hours, and the photographs of this phenomenon are displayed in the Figure (4-9).

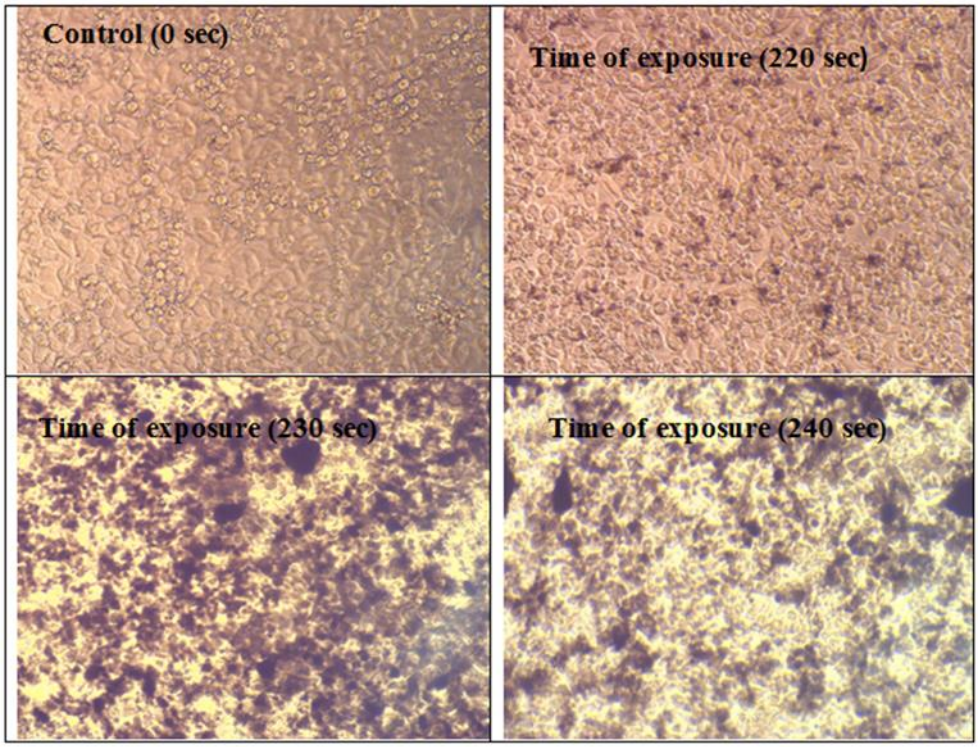

Figure (4-9) Observations of A431 cell morphological changes after exposure blue LED with SWCNT-OH (200 µg/ml), the cells were observed by optic microscope directly.

4-5-1 Effect Photosensitizer 5-ALA on the A431 Cell Line

The A431 cell line was utilized in the present research in order to investigate the practicability of using 5-aminolevulinic acid hydrochloride (ALA-PDT) in the treatment of skin cancer. The results showed that there was no significant stimulatory effect ($p > 0.001$) on the viability percent of the cells, but 250 µg/ml was the most effective concentration (Table 4-7). In comparison to the control group.

Table (4-7): parameters of concentration photosensitizer 5-ALA on the A431 cell line.

Concentration µg/ml	optical density of test well)	Average optical density of control wells	Viability of cells %	Average Viability cells %
31.25	0.886 0.918 0.842	0.845	104.769 108.553 99.566	104.296
62.5	0.797 0.78 0.72	0.845	94.245 92.234 85.139	90.540
125	0.952 0.792 0.738	0.845	112.573 93.653 87.268	97.832
250	0.813 0.697 0.799	0.845	96.137 82.420 94.481	91.013
500	0.922 0.798 0.696	0.845	109.026 94.363 82.301	95.230
1000	0.675 0.691 0.804	0.845	79.818 81.710 95.072	85.534

Photosensitizer 5-ALA was given at a dose of 250 µg/ml, but as can be seen in Figure (4–10), even this amount had no discernible effects on the viability of A431 cells. Yet after 250 µg/mL 5-ALA administration, a substantial decline in cell viability was seen when the cells were exposed to light depending on the beam's intensity .

When compared to the previously reported study [187], many of these researchers found that 5-ALA (PpIX) has positive effects.

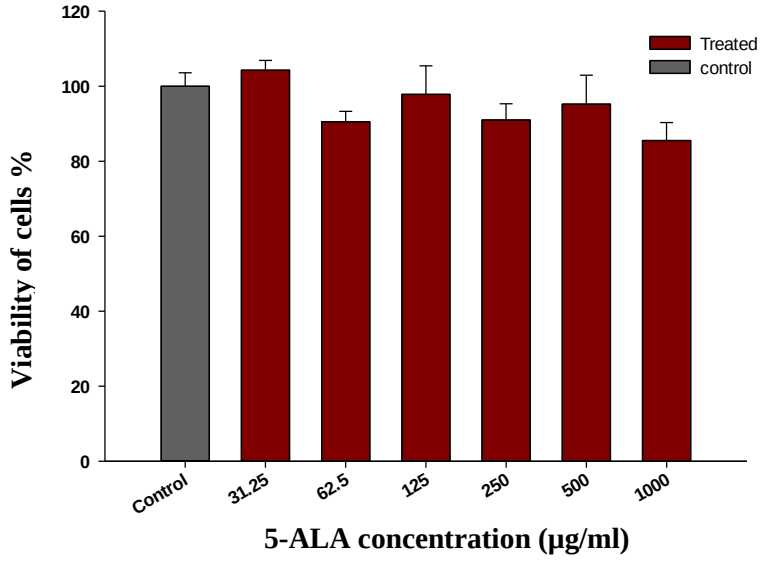

Figure (4-10): Effect of concentration photosensitizer 5-ALA on the A431 cell line after incubation for 24 hours.

4-5-2 Effect Photosensitizer 5-ALA in Combination with Blue LED on the A431 Cell Line

It is apparent in Table 4-8 that PDT-treated A431 cells with photosensitizer exhibit significant cell death, close to 73% in Table 4-8, after 240 seconds of radiation exposure at a photosensitizer 5-ALA concentration of 250 µg/ml, which was considered the ideal concentration in the current study. The

optimum parameter for the photodynamic treatment of the human skin cancer cell line (A431) was 400 mW/cm^2 with an output power of a PDT blue LED.

Table (4-8): Parameters of photosensitizer 5-ALA in combination with blue LED on A431 cell line.

Time (sec)	optical density of test well)	Average optical density of control wells	Viability of cells %	Average Viability of cells %
220	0.658 0.913 0.729	1.062	61.909 85.902 68.590	72.134
230	0.697 0.882 0.786	1.062	65.579 82.985 73.953	74.172
240	0.867 0.802 0.685	1.062	81.574 75.458 64.450	73.827

Figure (4–11) showed the effect of photosensitizer 5-ALA in combination with blue LED on the A431 cell line after incubation for 24 hours. Cell viability was reduced by 73% when compared to the control group. This agreement with the literature survey [187] Several researchers investigated whether 5-ALA (PpIX) has good therapeutic outcomes due to its high absorption, both in vitro and in vivo [188,189].

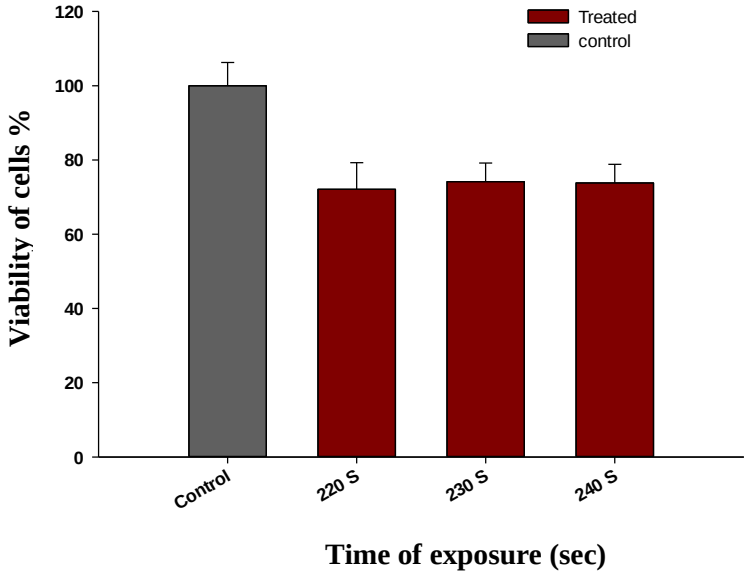

Figure (4-11): Effect of photosensitizer 5ALA in combination with blue LED on the A431 cell line after incubation for 24 hours.

The findings imply that 5-ALA is a secure photosensitizer that can be used to create a useful PDT treatment for skin cancer. in contrast to the study that had been presented prior to this one [187]. During the phase of the experiment by M. Atif et al. [187], 5-ALA-exposed RD cells were subjected to a total light exposure of 80 J/cm^2 from a red light produced by a diode laser at 635 nm. The effects of various 5-ALA incubation durations and concentrations, variable radiation doses, and diverse combinations of photosensitizer and light doses were investigated for their potential to have an impact on the viability of RD cells. When analyzed on

their own, the concentration of the sensitizer and the amount of light that was administered were shown to have no discernible effect on the survival of the cells. The maximum amount of cellular absorption was achieved after an in vitro incubation time of 47 hours. In the phototoxic experiment, it was discovered that a medicine concentration of 250 µg/ml and a light exposure of 80 J/cm^2 caused ALA-PDT to kill 76% of the cells. Optimal dosing of photodynamic therapy (PDT) following photosensitization with 5-ALA was investigated by Zeiyad Alkarakooly et al. [188], and the researchers also found that 5-ALA did not cause any significant changes in the cell viability of MCF-7 cells, even at the maximum dose that was used in the study, which was 2.0 mM. Cell viability was significantly reduced, however, after the cells were treated with 2.0 mM 5-ALA and then irradiated with laser light. This resulted in the cells being significantly less viable. These alterations were determined by the intensity of the laser beam that was used.

The morphology of the treated cells was examined using a CKX41 inverted light microscope (Molecular Devices in the United States), connected to a camera with get IT software . After 24 hours of treatment, the morphology of each plate, including both live and dead cells, was photographed. As shown in Figure (4-12).

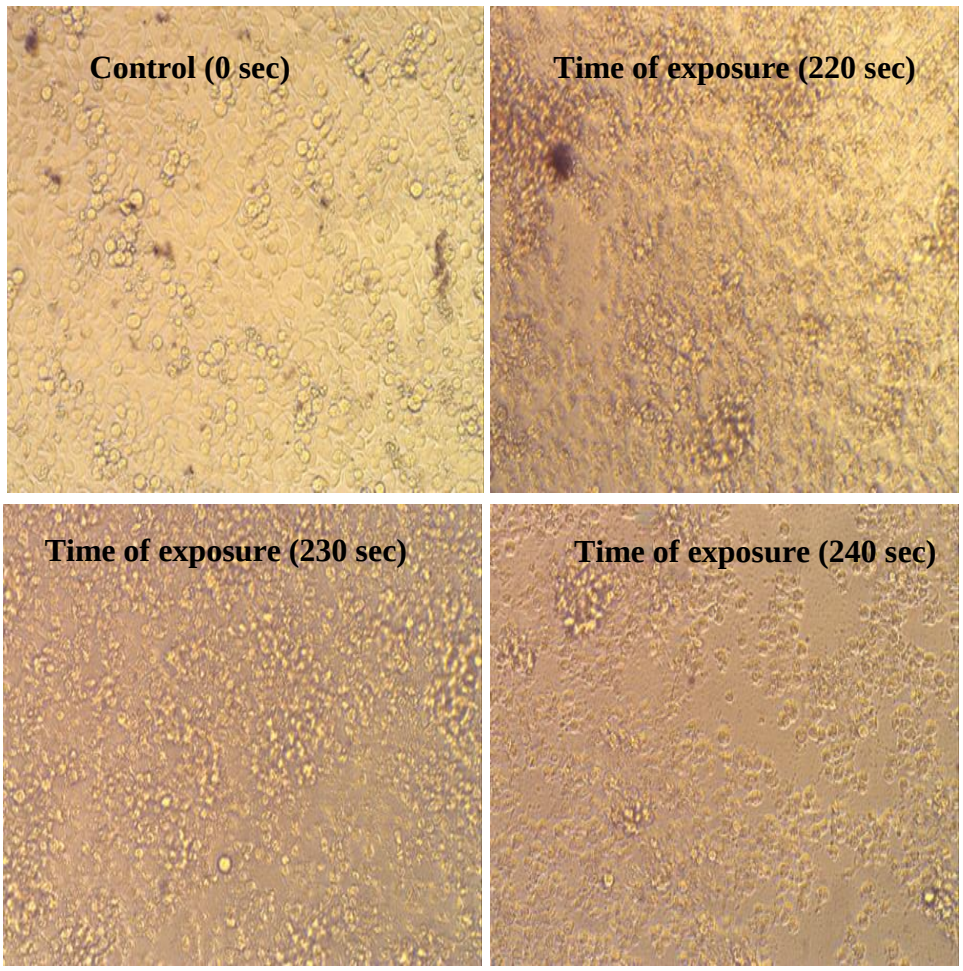

Figure (4-12): Observations of A431 cell morphological changes after exposure in a blue LED with 5-ALA(250 µg/ml), the cells were observed by optic microscope direct.

4-6 Effect of Xenon Lamp on the A431 Cell Line

The skin cells were subjected to irradiation at wavelengths ranging 420-480 nm. power of 40 W at 15,30 and 45 min. When we exposed the cells to direct light for different periods of time, through the measurements, we found the response of the cells to the power density of the source used, and therefore the change was made depending on the cell's response, and the best response was also searched for. the Xenon lamp had an effect of 82% in time 45 minutes, as shown in Table (4-9) and Figure (4-13). In times 15 and 30 minutes, It was observed that there was enhancement in

cells rather than death, which is due to the high direction and non-monochromatic nature of the lamp.

Table (4-9) : Parameters of Photodynamic Therapy PDT for Xenon lamp on cancer cell.

Time	optical density of test well)	Average optical density of control wells	Viability of cells %	Average Viability of cells %
15 min	0.794 0.791 0.803	0.579	137.132 136.614 138.687	137.478
30 min	0.72 0.68 0.709	0.579	124.352 117.443 122.452	121.416
45 min	0.47 0.496 0.47	0.579	81.174 85.664 81.174	82.671

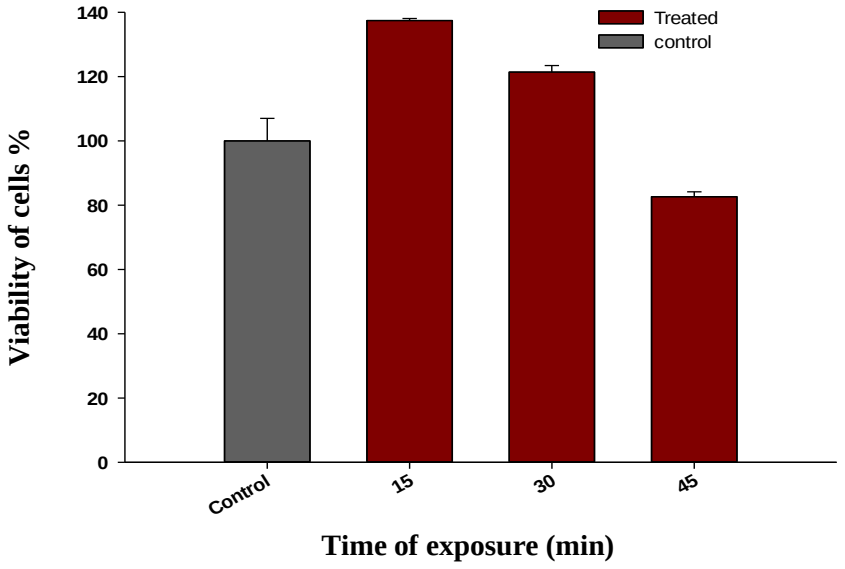

Figure (4-13): Effect of different irradiation times of Xenon lamp(420-480 nm) on A431 cell line after incubation for 24 hours.

The morphology of the treated cells was examined using a CKX41 inverted light microscope (Molecular Devices in the United States), connected to a camera with get IT software . After 24 hours of treatment,

the morphology of each plate, including both live and dead cells, was photographed. As shown in Figure (4-14).

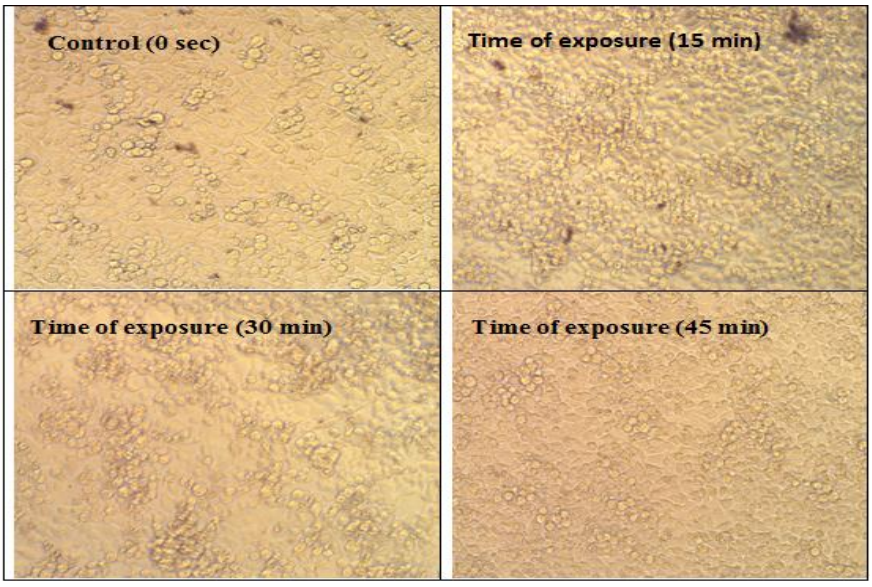

Figure (4-14): Observations of A431 cell morphological changes after exposure by Xenon lamp, the cells were observed by optic microscope direct.

4-7 Effect of TiO_2/Ag Nanoparticles (400 µg/ml) in Combination with Xenon Lamp (40 W) on the A431 Cell Line

Figure 4-15 shows that the combination results showed that there was a significant decrease in cell viability percent ($p \leq 0.001$) at exposure times (15, 30, and 45 min) for 24 hours of incubation and that PDT by Xenon lamp-treated A431 cells showed major cell death, almost 42.79% in comparison to the control group, as shown in Table 4-10, at 400 µg/ml of TiO_2/Ag, which has been considered the optimal concentration in this study.

Table (4-10): Parameters of TiO_2/Ag in combination with Xenon lamp on A431 cell line.

Time	optical density of test well)	Average optical density of control wells	Viability of cells %	Average Viability of cells %
15 min	0.221 0.258 0.226	0.562	39.300 45.880 40.189	41.790
30 min	0.257 0.206 0.202	0.562	45.702 36.633 35.921	39.419
45 min	0.234 0.218 0.27	0.562	41.612 38.767 48.014	42.797

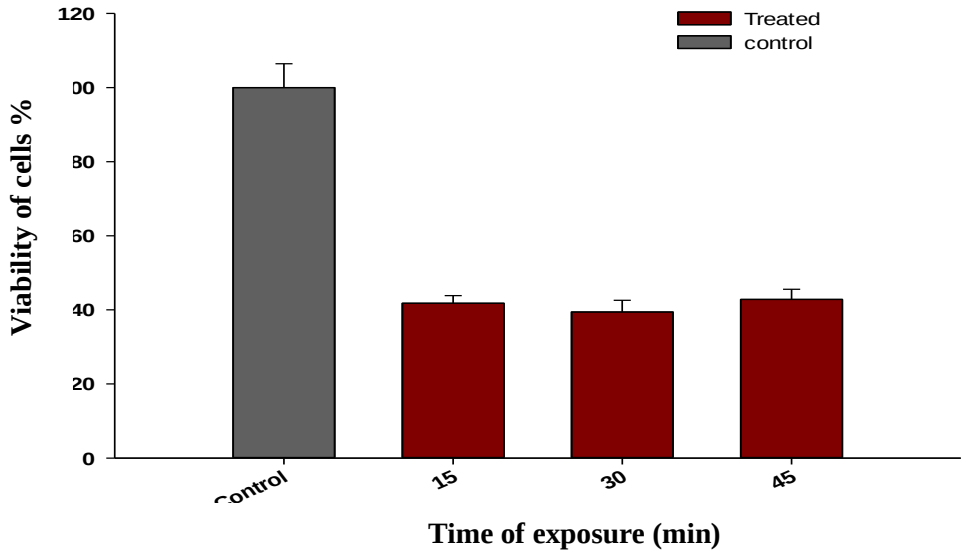

Figure (4-15): Effect of Tio_2/Ag in combination with Xenon lamp on A431 cell line after incubation for 24 hours.

Skin cancer with a lower survival rate than cells cultured in control medium (0 µg/ml). At optimal concentrations of NPs 400 µg/ml in Figure (4-16) there were obvious changes in cell survival, and as the exposure

time increased, there was a modest change in cell survival, but as the time reached 45 min, cell survival dropped dramatically. Cells grown for 24 hours in media containing NPs exhibit a modest decrease in viability. There is a consistent change in cell viability with irradiation and NPs, and this change is distinct from that of cancer cells only. When the concentration of TiO_2/Ag NPs on cancer cells grows, there will be cell shrinkage and death; the highest mortality was found when the cell could still display roughly 42% of viability at a concentration of (400 µg/ml) after exposure of time 45 min by xenon lamp.

This is due to the fact that TiO_2/Ag NPs are so minute that they are able to infiltrate cancer cells and bring about the death and shrinkage of those cells.

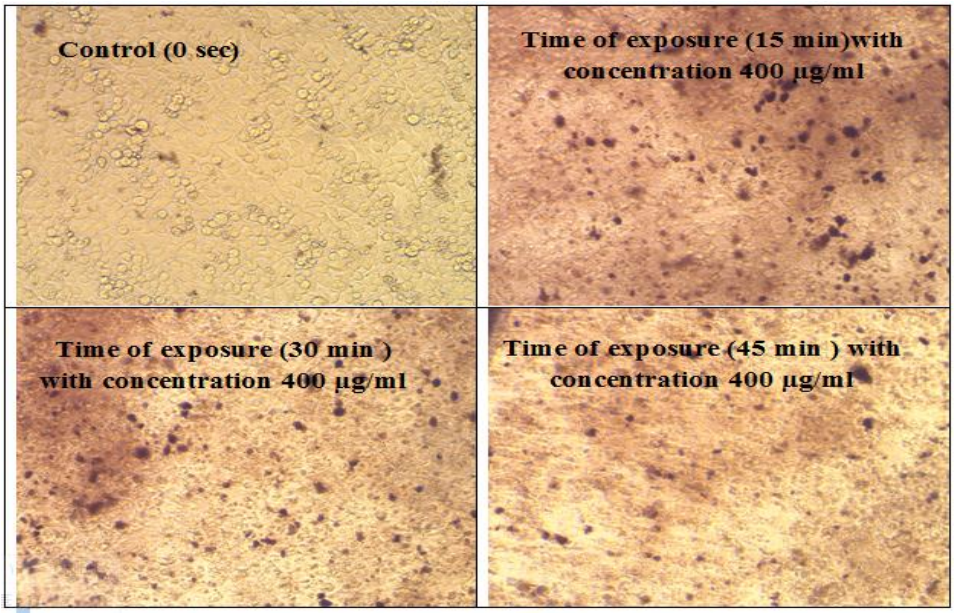

Figure (4-16): Observations of A431 cell morphological changes after exposure xenon lamp with TiO_2/Ag nanoparticles (400 µg/ml), the cells were observed by optic microscope directly.

4-8 Effect of SWCNT-OH Nanoparticles in Combination with Xenon Lamp (40 W) on the A431 Cell Line

Table (4–11) shows that the percentage viability of the cell with SWCNTs-OH treated cells was 82.691% after 15 minutes of xenon lamp exposure and decreased to 80.260% and 74.985 after 30 and 45 minutes, respectively. Table (4–11) shows that the percentage viability of the cell with SWCNTs-OH-treated cells was 82.691% after 15 minutes of xenon lamp exposure and decreased to 80.260% and 74.985 after 30 and 45 minutes, respectively. It was discovered that nanoparticles significantly suppressed the viability of cells when compared to control groups.

Table (4-11): parameters of SWCNT-OH in combination with xenon lamp on A431 cell line.

Time	optical density of test well)	Average optical density of control wells	Viability of cells %	Average Viability of cells %
15 min	0.462 0.481 0.452	0.562	82.157 85.536 80.379	82.691
30 min	0.458 0.408 0.488	0.562	81.446 72.554 86.781	80.260
45 min	0.396 0.443 0.426	0.562	70.420 78.778 75.755	74.985

Figure (4-17) shows that the combination results showed that there was a significant decrease in cell viability percent ($p \leq 0.001$) at exposure times (15, 30, and 45 min) for 24 hours of incubation and that PDT by Xenon lamp-treated A431 cells showed cell death.

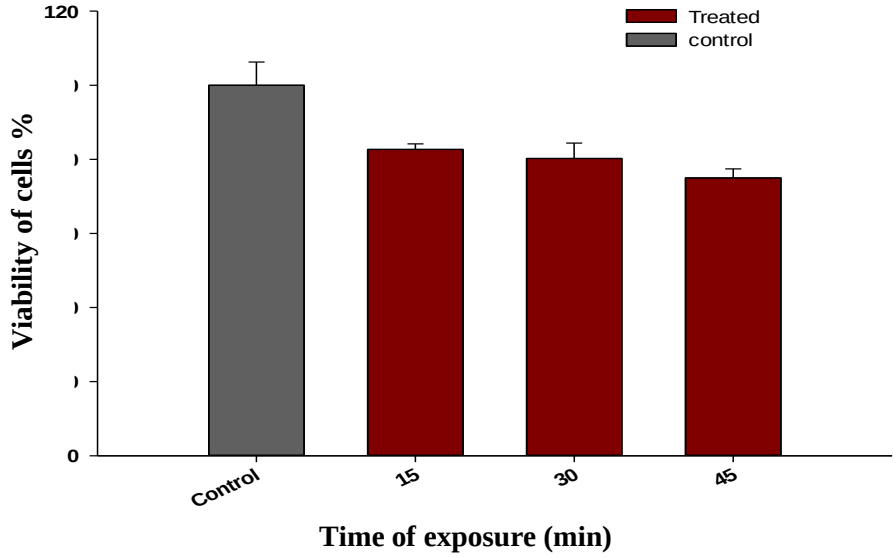

Figure(4-17): Effect of SWCNT-OH in combination with xenon on A431 cell line after incubation for 24 hours.

Figure (4-18) shows that morphology at optimal concentrations of NPs (200 µg/ml) there were obvious changes in cell survival, and as the exposure time increased, there was a modest change in cell survival, but as the time reached 45 min, cell survival dropped dramatically. Cells grown for 24 hours in media containing NPs exhibit a modest decrease in viability. There is aggregate and consistent change in cell viability with irradiation and NPs, and this change is distinct from that of cancer cells only (control).

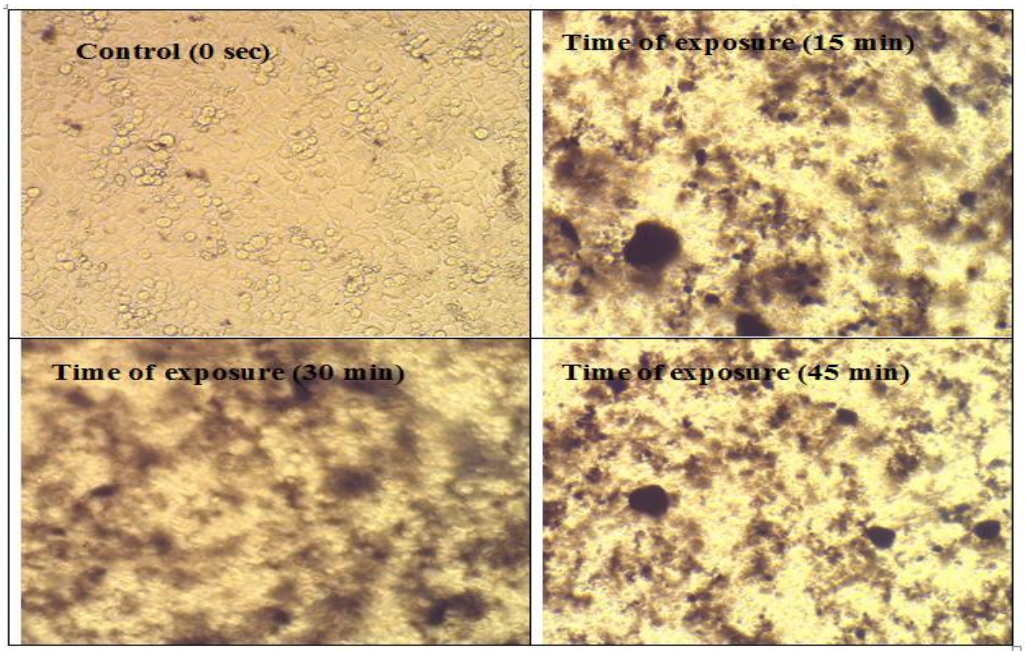

Figure (4-18): Observations of A431 cell morphological changes after exposure Xenon lamp with SWCNT-OH (200 µg/ml), the cells were observed by optic microscope directly.

4-9 Effect of Photosensitizer 5-ALA in Combination with Xenon Lamp (40 W) on the A431 Cell Line

In the results of photodynamic treatment of a human skin cancer cell line with the optimum parameter of 250 µg/ml, there was cytotoxicity in A431 cells at the concentration of 250 µg/ml ($P > 0.05$) Table (4-12); the viability of cell rate was all approximately 83% with increasing time of exposure.

Table (4-12): Parameters of photosensitizer 5-ALA in combination with Xenon lamp on A431 cell line.

Time	optical density of test well)	Average optical density of control wells	Viability of cells %	Average Viability of cells %
15 min	0.697 0.721 0.834	0.829	84.077 86.972 100.603	90.550
30 min	0.788 0.63 0.712	0.829	95.054 75.995 85.886	85.645
45 min	0.764 0.619 0.688	0.829	92.159 74.668 82.991	83.273

The number of surviving malignant cells is decreasing with increased exposure time. as shown in figure (4-19).

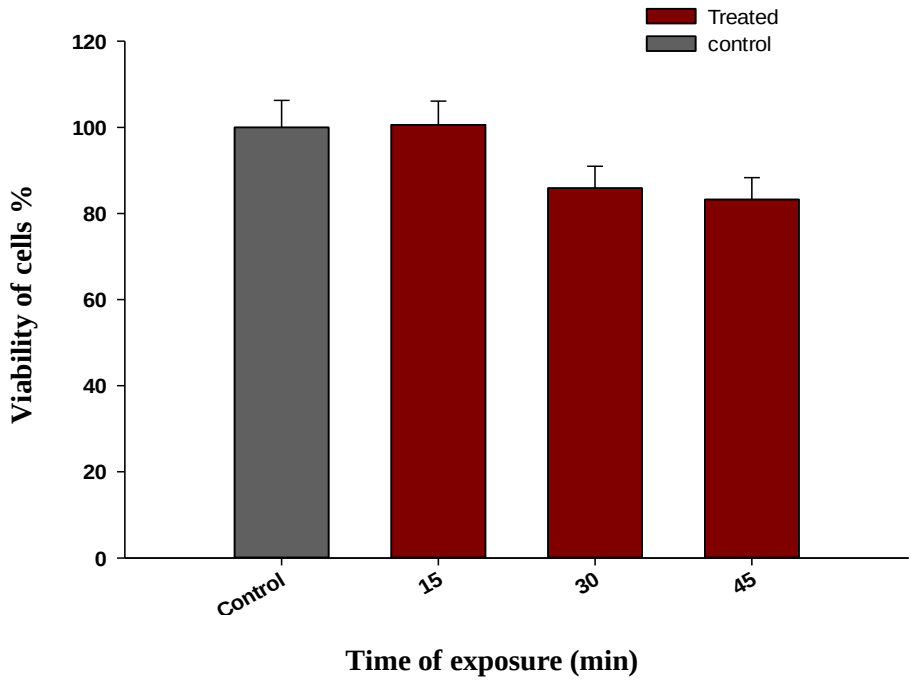

Figure (4-19): Effect of photosensitizer 5-ALA in combination with xenon on A431 cell line after incubation for 24 hours.

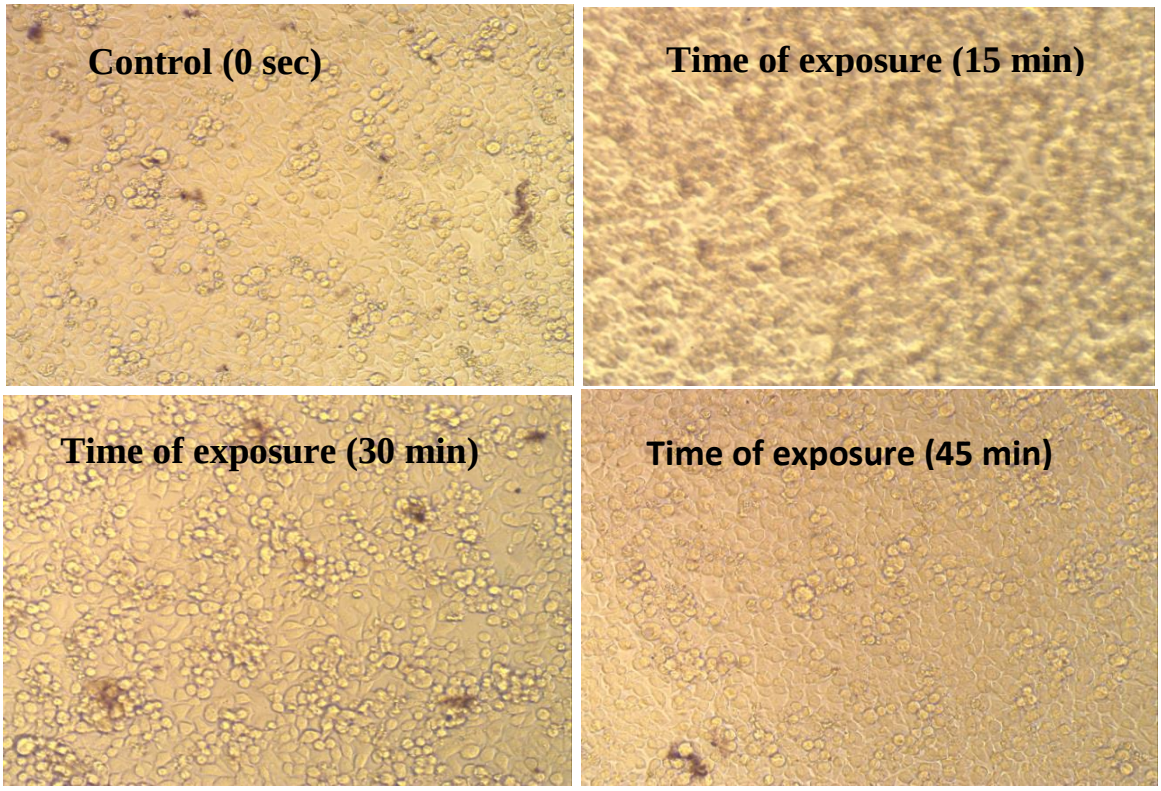

Figure (4-20): Observations of A431 cell morphological changes after exposure in a Xenon lamp with 5-ALA (250 µg/ml) were observed by optic microscope direct.

The morphology of the treated cells was examined using a CKX41 inverted light microscope (Molecular Devices in the United States), connected to a camera with IT software. After PDT for 24 hours, the morphology of each plate, including both live and dead cells, was photographed. The results of the biological evaluations of the exposure in the initial test by optic microscope on a culture cell line before the MTT assay when conducted on human skin cancer (A431) are depicted in figure 4–20 and cells revealed alterations in their morphology after adding 5-ALA.

4-10 XRD Analysis of TiO_2/Ag Nanoparticle Characterization

Under specific conditions, the X-ray diffraction (XRD) technique was used to determine the type of crystal structure, the major crystalline stages, and the orientation of the films that were generated as well as to identify some structural elements including the crystal size. Figure(4-21) shows the XRD pattern of the TiO_2/Ag produced films. XRD pattern showed peaks at $2\theta = 25.4°$ corresponding to planes (101) this agreement with [189]. Furthermore, weak peaks corresponding to metal silver can be found at "2 θ = 44.3◦ (2 0 0), 64.4◦ (2 2 0) and 77.4◦ (3 3 0)". It showed that Ag had attached itself to the TiO_2 supports successfully. Unluckily, this is because there are few metals present and the TiO_2 supports have high diffraction peaks .The strength of the primary signal in PEG following Ag photo reduction on the surface of TiO_2 declines, showing that the anchoring procedure did not alter TiO_2 distinctive crystal surface structure [189]. The samples had rather tiny crystallite sizes for TiO_2/Ag, ranging from 5 to 25 nm.

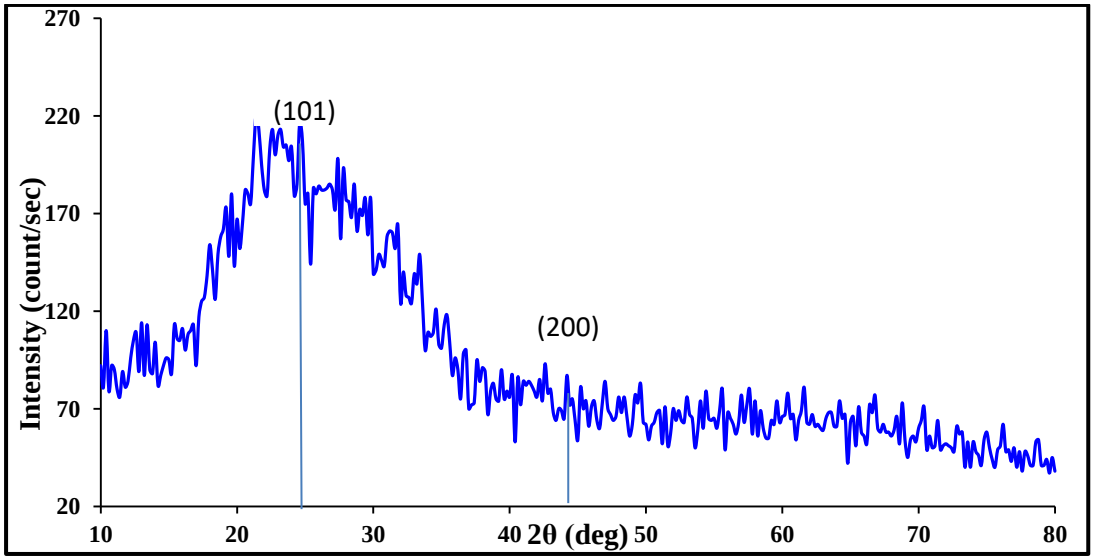

Figure (4-21): The XRD analysis of sample of TiO_2/Ag nanoparticle.

4-11 XRD Analysis of Single Walled Carbon Nanotube-OH Characterization

X-ray diffraction examinations were utilized in order to conduct analysis on the crystallinity as well as the structural properties of the Nano sized particles. The XRD data that were obtained were evaluated using the numbers provided by the Joint Committee on Power Diffraction Standards (JCPDS). In order to conduct an XRD study, TiO2/Ag and SWCNTs were both placed on a wafer made of crystal glass. According to JCPDS # 751621 reflecting graphite, the XRD patterns of the SWCNTs are shown in Figure 4-21. These patterns indicate that the characteristic peak at 24.2° and 25.6° was generated by reflections from hexagonal carbon atom layers and nanotube stacking layers that correspond to (002) planes. In single-walled carbon nanotubes (SWCNTs), the existence of SP2-bonded carbon groupings is indicated by the plane 002 [190].

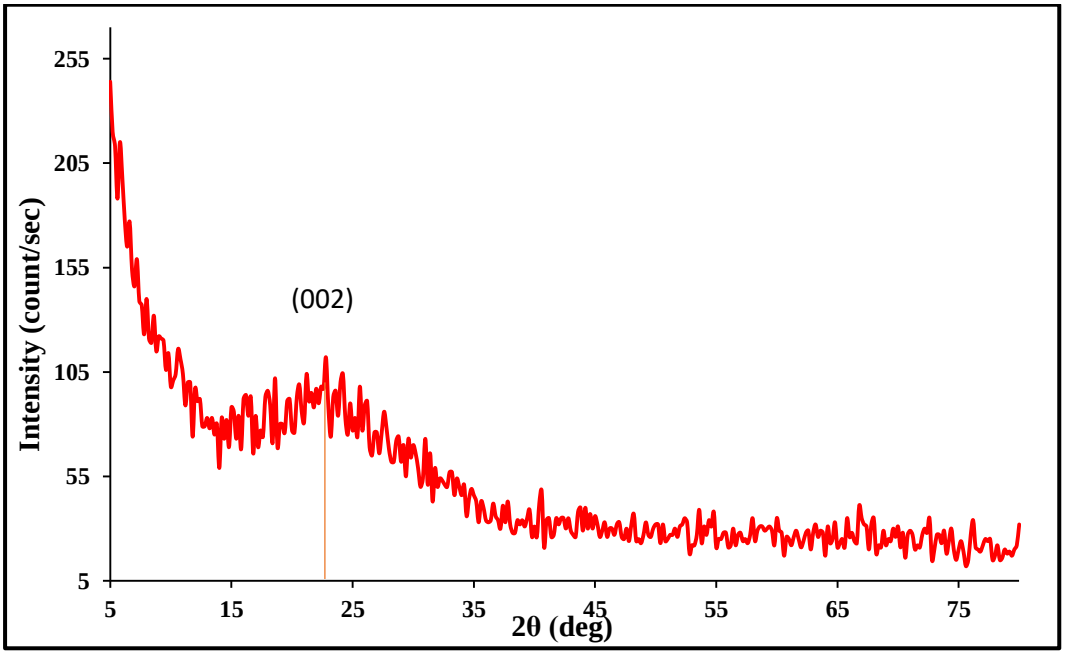

Figure (4-22): The XRD analysis of sample of SWCNTS-OH.

There was a slight shift at 25.8 degrees for the nanobiocomposite that was synthesised, and the strength of the peak was less distinctive when viewed in the plane.

4-12 Conclusion

From the overall results and measurements, it can be concluded that:
1- It was observed that by using a LED with a wavelength of 420–480 nm, a large number of cancer cells have been killed using the wavelength (420–480 nm) a specific cell (Squamous cell carcinoma).
2- The results of the PDT treatment method with high radiation doses at various exposure times show that the intensity of 400 mW/cm^2 of irradiation has killed 50% of the cancer cells at 240 seconds.
3- By observing the effect of skin cancer cells after adding several concentrations of the nanomaterial (12.5, 25, 50, 100, 200, 400)μg/ml of TiO_2/Ag and (6.23, 12.5, 25, 50, 100, 200) μg/ml of SWCNT-OH, it was observed that the higher the concentration, the less viable the cell.

4- X-ray diffraction examinations were utilized in order to conduct analysis on the crystallinity as well as the structural properties of the nanosized particles. shows the XRD pattern of the TiO_2/Ag-produced films. The XRD pattern showed peaks at $2\theta = 25.4°$ corresponding to planes (101) and the characteristic peaks at 24.2° and 25.6° were generated by reflections from hexagonal carbon atom layers and nanotube stacking layers (SWCNT-OH) that correspond to planes (002). The samples had rather tiny crystallite sizes for NPs, ranging from 5 to 25 nm.

5- The results of the biological evaluations of the exposure in the initial test by optic microscope on culture cell line before the MTT assay when conducted on human skin cancer (A431) .The inverted light microscope was used to capture the morphological observation of treated and

untreated cells for a period of twenty-four hours. The qualitative and preliminary confirmation of cellular viability and cell death were examined from the cellular morphology utilising acquired microscopic pictures. the nanoparticles treated cells morphology revealed that severe morphological changes and pronounced increased cell death was found after 24 hours.

6- It was found that PDT-treated A431 cells showed that the highest percentage of inhibition close to 73% after 240 seconds of radiation exposure with a photosensitizer 5-ALA concentration of 250 µg/ml, which was considered the ideal concentration in this study. Our findings imply that 5-ALA is a secure photosensitizer that can be used to create a useful PDT treatment for skin cancer. In light of these findings.
7- The results of adding TiO_2/Ag NP have demonstrated that the size, shape, and concentration of the nanoparticles, as well as the type and energy of the irradiation, play an important role in the treatment enhancement. The best results were obtained with a 240-second exposure time in light with a TiO_2/Ag concentration of 400 µg/ml. The combination of the nanoparticle with light had a synergistic effect by reducing the cell numbers more than that noticed during using the nanoparticle or photodynamic therapy separately.

4-13 Future Recommendations

1- Involve different lasers sources with different wavelengths.

2- Try using other cancer cells such as melanoma cancer cells and colon cancer.
3- Apply the photodynamic therapy PDT to the squamous cell carcinoma human cancer cells.

Reference

Reference

[1] Lopez-Lazaro M., **What is the main cause of cancer**, Europe PMC,1(1), 1- 2, (2016).

[2] Martin TA., Ye L., Sanders A.J., **Cancer Invasion and Metastasis: Molecular and Cellular Perspective**, Madame curie Bioscience, 1-56,(2013).

[3] Bray F., Ferlay J., Soerjomataram I., Siegel R.L., Torre L.A., Jemal A. ,**Global cancer statistics, GLOBOCAN estimates of incidence and mortality worldwide for 36 cancers in 185 countries**, CA: Cancer J. clin, 68, 394-424,(2018).

[4] Sundaram P., **The Use of Biopolymer Functionalized Single Walled Carbon Nanotubes for Effective Targeted Photodynamic Therapy of Colon Cancer Stem Cells**, University of Johannesburg (South Africa), (2020).

[5] Page M., **Tumor targeting in cancer therapy**, first edition, Springer Science Business Media, New York, (2002).

[6] Gallagher R. P., Lee T. K., Bajdik C. D., and Borugian M. , **Ultraviolet radiation,** Chronic diseases and injuries in Canada, 29,(2010).

[7] Suschek C., Schroeder P., Aust O., Sies H., Mahotka C. and Horstjann M. , **The presence of nitrite during UVA irradiation protects from apoptosis**,. Faseb J 17, 2342–4, (2003).

[8] Kappes U., Luo D., Potter M., Schulmeister K. and Runger T.**, Short- and long-wave UV light (UVB and UVA) induce similar mutations in human skin cells**, J Invest Dermatol 126, 667– 75,(2008).

[11] Bray F., Simmons B., Wolfson A. and Nouri K. **, Acute and chronic cutaneous reactions to ionizing radiation therapy**, Dermatol Ther (Heidelb) , 6, 185‑206, (2016).

[12] Ando N. , Kato H., Igaki H., Shinoda M. , Ozawa S., Shimizu H,Nakamura T., Yabusaki H., Aoyama N, Kurita A., **A random‑ized trial comparing postoperative adjuvant chemotherapy with cisplatin and 5‑fluorouracil versus preoperative chemotherapy for localized advanced squamous cell carcinoma of the thoracicesophagus**, (JCOG9907). Ann Surg Oncol 19, 68‑74, (2012).

[13] Shi T., Jiang R., Yu J., Yang H., Tu D, Dai Z, Shen Y, Zhang Y,Cheng X and Jia H, **Addition of intraperitoneal cisplatin and etoposide to first‑line chemotherapy for advanced ovarian cancer:A randomized**, phase 2 trial. Br J Cancer 119, 12‑18, (2018).

[14] Tempfer CB., Giger‑Pabst U., Seebacher V., Petersen M., Dogan A and Rezniczek GA, **A phase I, single‑arm, open‑label, dose escalation study of intraperitoneal cisplatin and doxorubicin inpatients with recurrent ovarian cancer and peritonealcarcinoma**, tosis. Gynecol Oncol 150, 23‑30, (2018).

[15] Gupta S., Maheshwari A. , Parab P., Mahantshetty U. , Hawaldar R. ,Sastri Chopra S, Kerkar R., Engineer R. , Tongaonkar H. and Ghosh J., Neoadjuvant, **chemotherapy followed by radical surgery versus concomitant chemotherapy and radiotherapy in patients**

with stage IB2, IIA, or IIB squamous cervical cancer, A randomized controlled trial. J Clin Oncol 36, 1548‑1555, (2018).

[16] Kitagawa R, Katsumata N, Shibata T, Kamura T, Kasamatsu T,Nakanishi T, Nishimura S, Ushijima K, Takano M, Satoh T and Yoshikawa H, **Paclitaxel Plus carboplatin versus pacli‑taxel plus cisplatin in metastatic or recurrent cervical cancer:The open‑label randomized**, phase III trial JCOG0505. J Clin Oncol 33, 2129‑2135, (2015).

[17] Rosen V. M., Guerra I , McCormack M., Nogueira-Rodrigues, A., Sasse A., Munk, V. C., and Shang, A. **Systematic review and network meta-analysis of bevacizumab plus first-line topotecan-paclitaxel or cisplatin-paclitaxel versus non–bevacizumab-containing therapies in persistent, recurrent, or m etastatic cervical cancer**, International Journal of Gynecological Cancer, 27(6), 1237, (2017).

[18] Small W. Jr. , Bacon MA. , Bajaj A., Chuang LT., Fisher BJ,Harkenrider MM., Jhingran A., Kitchener HC. , Mileshkin LR.,Viswanathan AN. and Gaffney DK., **Cervical cancer: A global health crisis** , Cancer 123, 2404‑2412, (2017).

[19] Noronha V., Joshi A., Patiln V. M., Agarwal J., Ghosh-Laskar S., Budrukkar A., and Prabhash K. , **Once-a-week versus once-every-3-weeks cisplatin chemoradiation for locally advanced head and neck cancer: a phase III randomized noninferiority trial**, Journal of Clinical Oncology, 36(11), 1064-1072, (2018).

[20] Strojan P., Vermorken JB. , Beitler JJ. , Saba NF., Haigentz M. Jr, Bossi P., Worden FP. , Langendijk JA., Eisbruch A. and Mendenhall

WM., **Cumulative cisplatin dose in concur‐ren chemoradio therapy for head and neck cancer**, A systematicreview . Head Neck 38 (Suppl 1), E2151‐E2158, (2016).

[21] Szturz P., Wouters K., Kiyota N., Tahara M., Prabhash K., Noronha V. ,Castro A. , Licitra L. , Adelstein D. and Vermorken JB. , **Weekly low‐dose versus three‐weekly high‐dose cisplatin for concurrent chemoradiation in locoregionally advanced non‐nasopharyngeal head and neck cancer: A systematic review and meta‐analysis of aggregate data**, Oncologist 22, 1056‐1066, (2017).

[22] Terenziani M., De Pasquale MD, Bisogno G, Biasoni D, BoldriniR, Collini P, Conte M, Dall'Igna P, Inserra A and Melchionda F, **Malignant testicular germ cell tumors in children and adoles ‐cents**, **The AIEOP (Associazione Italiana Ematologia Oncologia Pediatrica) protocol**, Urologic Oncology: Seminars and Original Investigations,36 (11) Elsevier, (2018).

[23] Gridelli C., Morabito A., Cavanna L., Luciani A., Maione P., Bonanno L. and Perrone F. , **Cisplatin-based first-line treatment of elderly patients with advanced non–small-cell lung cancer: joint analysis of MILES-3 and MILES-4 phase III trials**, Journal of Clinical Oncology, 36(25), 2585-2592,(2018).

[24] Rossi A. and Massimo D., **Platinum-based chemotherapy in advanced non-small-cell lung cancer: optimal number of treatment cycles**, Expert review of anticancer therapy 16(6), 653-660,(2016).

[25] Hamblin M. R. , **Photobiomodulation, Photomedicine, and Laser Surgery: A New Leap Forward Into the Light for the 21 st Century,** Photomedicine and Laser Surgery, 36(8), 395-396, (2018).

[26] Niu T., Tian Y., Wang G., Guo G., Tong, Y., and Shi Y. ,**Inhibition of ROS-NF-κB-dependent autophagy enhances Hypocrellin A united LED red light-induced apoptosis in squamous carcinoma A431 cells**, Cellular Signalling, 69, 109550, (2020).

[27] Patel A. D., Rotenberg S., Messer R. L., Wataha J. C., Ogbureke K. U., McCloud V. V., and Lewis J. B. , **Blue light activates phase 2 response proteins and slows growth of A431 epidermoid carcinoma xenografts**, Anticancer research, 34(11), 6305-6313, (2014).

[28] Meulemans J., Delaere P., Vander Poorten V. , **Photodynamic therapy in head and neck cancer: indications, outcomes, and future prospects,** Current opinion in otolaryngology & head and neck surgery. 27(2), 136-41,(2019).

[29] Compagnin C., Mognato M., Celotti L., Canti G., Palumbo G., and Reddi E., **Cell proliferation and cell cycle alterations in oesophageal p53-mutated cancer cells treated with cisplatin in combination with photodynamic therapy**, Cell Proliferation, 43(3), 262-274, (2010).

[30] Kerr C., Adhikary G., Grun D., George N., and Eckert R. L. , **Combination cisplatin and sulforaphane treatment reduces proliferation, invasion, and tumor formation in epidermal squamous cell carcinoma** , Molecular Carcinogenesis, 57(1), 3-11, (2018).

[31] Hwang H., Biswas R., Chung P. S., and Ahn J. C. , **Modulation of EGFR and ROS induced cytochrome c release by combination of photodynamic therapy and carboplatin in human cultured head and neck cancer cells and tumor xenograft in nude mice**, Journal of Photochemistry and Photobiology B: Biology, 128, 70-77, (2013).

[32] Powsner R. and Powsner E**., Essential Nuclear Medicine Physics** ",

second edition, Blackwell Publishing , (2006).

[33] Hanahan D., Weinberg R., **The Hallmarks of Cancer Cell**, 100, 57-70, (2000).

[34] Counter C.M., Avilion A.A., Lefeuvre C.E., Stewar N.G. and Bacchetti S. ,**Telomere shortening associated with chromosome instability is arrested in immortal cells which express telomerase activity**, EMBO J. 11, 1921-1929, (1992).

[35] Helms V. ,**Fluorescence Resonance Energy Transfer**, Principles of Computational Cell Biology. Weinheim: P. P 202, (2008).

[36] Braslavsky, S. E., **Glossary of Terms Used in Photochemistry** , Pure Appl. Chem., 79 (3), 293–465, (2007).

[37] Dalmas O., Do Cao M.-A., Lugo M. R., Sharom F. J., Di Pietro A., and Jault J.-M., **Time-Resolved Fluorescence Resonance Energy Transfer Shows that the Bacterial Multidrug ABC Half-Transporter BmrA Functions as a Homodimer**, Biochemistry,44 (11), 4312–4321, (2005).

[38] Schaufele F., Demarco I., Day. RN , **FRET Imaging in the Wide-Field Microscope**, FRET Microscopy and Spectroscopy, 72–94, (2005).

[39] Lee S., Lee J., Hohng S. , **Single-molecule three-color FRET with both negligible spectral overlap and long observation time**, Plos One, 5(8), (2010).

[40] King C., Barbiellini, B., Moser D., and Renugopalakrishnan V. , **Exactly soluble model of resonant energy transfer between molecules**, Physical Review B, 85(12), 125106, (2012).

[41] Förster T., **Delocalized Excitation and Excitation Transfer** , Modern Quantum Chemistry, Academic Press. 93–137, (1965).

[42] Show P. L., Chai W. S., and Ling T. C. (Eds.). ,**Microalgae for Environmental Biotechnology: Smart Manufacturing and Industry 4.0 Applications** , CRC Press.(2020).

[43] Alagarasi A. ,**Chapter-introduction to nanomaterials**, Indian Institute of Technology Madras, 1-24,(2013).

[44] Bidram, E., Esmaeili, Y., Ranji-Burachaloo H., Al-Zaubai, N. Zarrabi A., Stewart A., Dunstan D.E. , **A concise review on cancer treatment methods and delivery systems**, J Drug Deliv Sci Technol, 54, 101350 ,(2019).

[45] Ventimiglia E., Seisen T., Abdollah F.; Briganti A., Fonteyne V., James N., Roach M., Thalmann G.N., Touijer K., Chen R.C., Cheng L. A **Systematic, Review of the Role of Definitive Local Treatment in Patients with Clinically Lymph Node-positive Prostate Cancer**, Eur. Urol. oncol, 2, 294-301,(2019).

[46] Brown J. E., Brown S. B. and Vernon D. I. **Photodynamic therapy: new light on cancer treatment**, Coloration Technology, 115:249-253,(1999).

[47] Dolmans D. E. J. G. J., Fukumura D. and Jain R. K. , **Photodynamic therapy for cancer**, Nat Rev Cancer, 3, 380-387,(2003).

[48] Grzybowski A., Sak, J., Pawlikowski J., **A brief report on the history of phototherapy**, Clin. Dermatol, 34, 532–537,(2016).

[49] Needham J., Gwei-Djen L. **Science and Civilisation in China. Spagyrical Discovery and Invention**, Physiological Alchemy, 5(5),1-5,(1983).

[50] Sundaram P., Abrahamse H., **Phototherapy Combined with Carbon Nanomaterials (1D and 2D) and their Applications in Cancer Therapy**, Materials 13: 4830,(2020)b.

[51] Asgari M., Gazor R., Abdollahifar M., Fadaei Fathabady, F.,Zare, F., Norouzian, M. Amini, A.; Khosravipour A. Kiani P., Atashgah R.B. Rezaei F., Ghoreishi S.K., Chien S., Hamblin M.R., Bayat, M. , **Combined therapy of adipose-derived stem cells and photobiomodulation on accelerated bone healing of a critical size defect in an osteoporotic rat model**, Biochem. Biophys. Res. Commun, 530(1), 173-180,(2020).

[52] Eun Ji, H., Dae Gun, C., Min Suk S., **Targeted and effective photodynamic therapy for cancer using functionalized nanomaterials** , Acta Pharma Sin. B., 6:297–307,(2016).

[53] Junqi C., Chengyun N., Zhengnan Z., Peng Y., Ye Z., Guoxin T., Chuanbin., M. **Nanomaterials as photothermal therapeutic agents**, Prog. Mater. Sci. 99,1-26,(2019).

[54] Allison R.R., Downie G.H., Cuenca, R.; Xin-Hua Hu., Childs, C.J., Sibata C.H., **Photosensitizers in clinical PDT**, Photodiagnosis Photodyn.Ther,1, 27-42,(2004).

[55] Agostinis P., Berg K., Cengel K.A., Foster T.H., Girotti, A.W., Gollnick S.O., Hahn S.M., Hamblin M.R., Juzeniene A., Kessel D., Korbelik M., Moan J., Mroz P., Nowis D. Piette, J. Wilson, B.C., Golab, J. , **Photodynamic therapy of cancer: an update**, CA: Cancer J. Clin, 61,250–281,(2011).

[56] Kou J., Dou D., Yang, L., **Porphyrin photosensitizers in photodynamic therapy and its applications**, Oncotarget, 8, 81591–81603, (2017).

[57] Abrahamse H., Hamblin M.R., **New photosensitizers for photodynamic therapy**, Biochemical J, 473,137-364,(2016).

[58] Marmur E. S., Schmults C. D., and Goldberg D. J. , **A review of laser and photodynamic therapy for the treatment of nonmelanoma skin cancer**, Dermatologic Surgery, 30, 264-271,(2004).

[59] Hleb E. Y., Yakush N. A., Hafner J. H., Drezek R. A., McNew J. A., and Lapotko D. O., **Plasmon nanoparticle-generated photothermal bubbles as universal biomedical agents**, une,13(15), (2016).

[60] Hu X., and Liu S., **Recent advances towards the fabrication and biomedical applications of responsive polymeric assemblies and nanoparticle hybrid superstructures**, Dalton Transactions, 44(9), 3904-3922, (2015).

[61] AL-Hashimi M. M., **Trends in skin cancer Incidence in Iraq during the period 2000-2019**.

[62] Brown S. B., Brown E. A. and Walker I., **The present and future role of photodynamic therapy in capncer treatment**, The Lancet Oncology, 5, 497-508, (2004).

[63] Lopez R. F. V., Lange N., Guy R., and Bentley M. V. L. B. , **Photodynamic therapy of skin cancer: controlled drug delivery of 5-ALA and its esters**, Advanced drug delivery reviews, 56(1), 77-94, (2004).

[64] Kimura M., Kashikura K., Yokoi S., Koiwa, Y., Tokuoka, Y., and Kawashima, N. ,**Photodynamic therapy for cancer cells using a flash wave light xenon lamp**, Optical review, 12: 207-210,(2005).

[65] Liebmann J., Born M. and Kolb-Bachofen V., **Blue-light irradiation regulates proliferation and differentiation in human skin cells**, Journal of Investigative Dermatology. 130(1), 259-69, (2010).

[66] Atif M., Fakhar-e-Alam M., Firdous S., Zaidi SS, Suleman R., Ikram M., **Study of the efficacy of 5-ALA mediated photodynamic therapy on human rhabdomyosarcoma cell line (RD)**, Laser Physics Letters. 7(10), 757,(2010).

[67] Salman M. and Naseem I, **Riboflavin as adjuvant with cisplatin: Study in mouse skin cancer model**, Front Biosci (Elite Ed) 7, 242-254, (2015).

[68] Jukapli N. M., and Bagheri S., **Recent developments on titania nanoparticle as photocatalytic cancer cells treatment**, Journal of Photochemistry and Photobiology B: Biology, 163, 421-430,(2016).

[69] Abdel-Fattah W. I., and Ali, G. W., **On the anti-cancer activities of silver nanoparticles**, J Appl Biotechnol Bioeng, 5(1), 43-46,(2018).

[70] Mignon C., Uzunbajakava N. E., Castellano-Pellicena, I., Botchkareva N. V. and Tobin D. J., **Differential response of human dermal fibroblast subpopulations to visible and near-infrared light: Potential of photobiomodulation for addressing cutaneous conditions. Lasers in surgery and medicine**, 50(8), 859-882, (2018).

[71] Nie C., Du, P., Zhao H., Xie H., Li, Y., Yao, L., ... and Sun, Z. ,**Ag/ TiO_2 nanoprisms with highly efficient near-infrared photothermal conversion for melanoma therapy**, Chemistry–An Asian Journal, 15(1), 148-155,(2020).

[72] Ghaleb R., Hadi Z. and Mohammed N., **Synergistic Effect of Photobiomodulation and Viscum album Extract on Colorectal Cancer HCT-116 Cell Line**, International Journal of Pharmaceutical Research. India. 0975-2366,2058-2064, (2020).

[73] Magni G., Banchelli M., Cherchi F., Coppi E., Fraccalvieri M., Rossi M. and Rossi F. , **Experimental study on blue light interaction with human keloid-derived fibroblasts**, Biomedicines, 8(12), 573, (2020).

[74] Chen Z., Li W., Hu X. and Liu M. , **Irradiance plays a significant role in photobiomodulation of B16F10 melanoma cells by increasing reactive oxygen species and inhibiting mitochondrial function**. Biomedical optics express, 11(1), 27-39, (2020).

[75] Tartaglione M F., **Apoptotic mechanism activated by blue light and cisplatinum in cutaneous squamous cell carcinoma cells**, International journal of molecular medicine 47(4) ,1-1, (2021).

[76] Lee Y. J., Yi Y. C., Lin Y. C., Chen C. C., Hung J. H., Lin J. Y., and Ng, I. S. ,**Purification and biofabrication of 5-aminolevulinic acid for photodynamic therapy against pathogens and cancer cells**, Bioresources and Bioprocessing, 9(1), 1-10,(2022).

[77] Alghuthaymi, M. A., Patil, S., Rajkuberan, C., Krishnan, M., Krishnan, U., and Abd-Elsalam, K. A. , **Polianthes tuberosa-Mediated Silver Nanoparticles from Flower Extract and Assessment of Their Antibacterial and Anticancer Potential: An In Vitro Approach**, Plants, 12(6), 1261,(2023).

[78] Zhao, B., He, Y.Y. , **Recent advances in the prevention and treatment of skin cancer using photodynamic therapy**, Expert Rev. Anticancer Ther. 10, 1797–1809, (2010).

[79] Katalinic A., Kunze U., Schafer T., **Epidemiology of cutaneous melanoma and non-melanoma skin cancer in Schleswig-Holstein, Germany: Incidence, clinical subtypes, tumour stages and localization (epidemiology of skin cancer)**. Br. J. Dermatol. 149: 1200–1206,(2003).

[80] Eisemann N., Waldmann A., Geller A.C., Weinstock M.A., Volkmer B., Greinert, R., Breitbart, E.W., Katalinic, A., **Non-melanoma skin cancer incidence and impact of skin cancer screening on incidence**, J. Investig. Dermatol , 134, 43–50,(2014).

[81] Kim Y., He Y.Y., **Ultraviolet radiation-induced non-melanoma skin cancer: Regulation of DNA damage repair and inflammation**. Genes Dis. 1, 188–198,(2014).

[82] Blanpain C., Fuchs E**., Plasticity of epithelial stem cells in tissue regeneration**, Science.344(6189), 1242281, (2014).

[83] Ericso, M.B., Wennberg A.M., Larkö O., **Review of photodynamic therapy in actinic keratosis and basal cell carcinoma**, Ther. Clin. Risk Manag. 4, 1–9, (2008).

[84] Berking C., Hauschild A., Kölbl O., Mast G., Gutzmer R., **Basal cell carcinoma-treatments for the commonest skin cancer**, Dtsch. Arztebl. Int. , 111, 389–395, (2014).

[85] Sidoroff A., Thaler P., **Taking treatment decisions in non-melanoma skin cancer—The place for topical photodynamic therapy (PDT),** Photodiagnosis and Photodynamic Therapy. 7(1), 24-32, (2010).

[86] Dlugosz A., Merlino, G., Yuspa, S.H., **Progress in cutaneous cancer research**, J. Investig. Dermatol. Symp. Proc.7, 17–26,(2002).

[87] Martorell-Calatayud, A., Sanmartín, O., Cruz J., Guillén C. **Cutaneous squamous cell carcinoma: Defining the high-risk variant**, Actas Dermosifiliogr, 104, 367–379,(2013).

[88] Hofbauer G.F., Bouwes J.N., Euvrard, S., **Organ transplantation and skin cancer: Basic problems and new perspective,** Exp. Dermatol. 19, 473–482, (2010).

[89] Lucena SR., Salazar N., Gracia-Cazaña T., Zamarrón A., González S., Juarranz Á., Gilaberte Y., **Combined treatments with photodynamic therapy for non-melanoma skin cancer**, International journal of molecular sciences. 16(10), 25912-33,(2015).

[90] Cockerell C.J. , **Histopathology of incipient intraepidermal squamous cell carcinoma ("actinic keratosis")**. J. Am. Acad. Dermatol. 42, 11–17,(2000).

[91] Fernández-Figueras, M.T., Carrato, C., Sáenz, X., Puig, L., Musulen, E., Ferrándiz, C., Ariza, A., **Actinic keratosis with**

atypical basal cells (AK I) is the most common lesion associated with invasive squamous cell carcinoma of the skin, J. Eur. Acad. Dermatol. Venereol. 29, 991-997, (2015).

[92] Patel R.V. , Frankel A., **Goldenberg, G. An update on nonmelanoma skin cancer**, J. Clin. Aesthet. Dermatol. 4, 20–27,(2011).

[93] Madan, V., Lear, J.T., **Szeimies, R.-M. Non-melanoma skin cancer**, Lancet , 375, 673–685 ,(2010).

[94] Harms P.W., Harms K.L., Moore, P.S., DeCaprio, J.A., Nghiem P., Wong M.K.K., Brownell I.,**The biology and treatment of Merkel cell carcinoma: Current understanding and research priorities**, Nat. Rev. Clin. Oncol. 15, 763–776, (2018).

[95] Narayanan D.L., Saladi R.N.,Fox J.L., **Ultraviolet radiation and skin cancer**, Int. J. Derm. 49, 978–986, (2010).

[96] Kaskel P., Lange U., Sander, S., Huber M.A., Utikal J., Leiter U., Krähn G., Meurer M., Kron M., **Ultraviolet exposure and risk of melanoma and basal cell carcinoma in Ulm and Dresden, Germany**, J. Eur. Acad Derm. Venereol. 29, 134–142, (2014).

[97] Chang N.-B., Feng, R., Gao, Z., Gao, W. , **Skin cancer incidence is highly associated with ultraviolet-B radiation history**, Int. J. Hyg. Environ. Health, 213, 359–368, (2010).

[98] Benjamin C.L., Melnikova, V.O., **Ananthaswamy, H.N. P53 protein and pathogenesis of melanoma and nonmelanoma skin cancer,** Adv. Exp. Med. Biol. 624, 265–282,(2008).

[99] Gibson K. F., and Kernohant W. G**., Lasers in Medicine-A Review**, J. Med Eng. Technology 17 (2): 51–57,(1993).

[100] Brancaleon L., and Moseley, H., **Laser and Non-laser Light Sources for Photodynamic Therapy**, Lasers Med. Sci. 17 (3): 173–186,(2002).

[101] Pariser D., Loss, R., Jarratt, M., Abramovits, W., Spencer, J., Geronemus, R., **Topical Methyl-Aminolevulinate Photodynamic Therapy Using Red Light-Emitting Diode Light for Treatment of Multiple Actinic Keratoses: A Randomized, Double-Blind, Placebo-Controlled Study**, J. Am. Acad. Dermatol. 59 (4), 569–576,(2008).

[102] Hempstead J., Jones DP., Ziouche A, Cramer GM, Rizvi I, Arnason S, Hasan T, Celli JP.,**Low-cost photodynamic therapy devices for global health settings: Characterization of battery-powered LED performance and smartphone imaging in 3D tumor models**, Scientific reports. 5(1), 10093,(2015).

[103] Cantisani C., Paolino, G., Bottoni, U., and Calvieri, S., **Daylight Photodynamic Therapy for the Treatment of Actinic Keratosis in Different Seasons**, J. Drugs Dermatol. 14 (11),1349–1353,(2015).

[104] Lacour JP., Ulrich C., Gilaberte Y., Von Felbert V, Basset-Seguin N, Dreno B, Girard C, Redondo P, Serra-Guillen C, Synnerstad I, Tarstedt M., **Daylight photodynamic therapy with methyl aminolevulinate cream is effective and nearly painless in treating actinic keratoses: a randomised, investigator-blinded, controlled, phase III study throughout Europe**, Journal of the European Academy of Dermatology and Venereology. 29(12), 2342-8, (2015).

[105] Assikar S., Labruni A., Kerob D., Couraud, A., and Bédane, C. , **Daylight Photodynamic Therapy with Methyl Aminolevulinate Cream Is as Effective as Conventional Photodynamic Therapy with Blue Light in the Treatment of Actinic Keratosis: a Controlled Randomized Intra-individual Study,** J. Eur. Acad. Dermatol. Venereol. 34 (8), 1730–1735,(2020).

[106] Stolik S., Delgado J. A., Perez, A., and Anasagasti, L. , **Measurement of the Penetration Depths of Red and Near Infrared Light in Human "Ex Viv" Tissues**, J. Photochem. Photobiol. B 57 (2-3), 90–93, (2000).

[107] Gunaydin G., Gedik ME, Ayan S., **Photodynamic therapy—current limitations and novel approaches,** Frontiers in Chemistry. 9, 691697,(2021).

[108] Mourant JR., Canpolat M., Brocker C., Esponda-Ramos O, Johnson TM, Matanock A, Stetter K, Freyer JP., **Light scattering from cells: the contribution of the nucleus and the effects of proliferative status**, Journal of biomedical optics. 5(2), 131-7,(2000).

[109] Frangioni J., **In Vivo near-infrared Fluorescence Imaging**. Curr. Opin. Chem. Biol. 7 (5), 626–634,(2003).

[110] Van Straten D., Mashayekhi V., de Bruijn H., Oliveira S., and Robinson, D. **Oncologic Photodynamic Therapy: Basic Principles, Current Clinical Status and Future Directions**, Cancers 9 (2), 19,(2017)

[111] Agostinis P., Berg K., Cengel KA., Foster TH., Girotti AW, Gollnick SO, Hahn SM, Hamblin MR, Juzeniene A, Kessel D,

Korbelik M., **Photodynamic therapy of cancer: an update. CA**, a cancer journal for clinicians. 61(4), 250-81,(2011).

[112] Dolmans D.E., Fukumura D., Jain, R.K., **Photodynamic therapy for cancer**, Nat. Rev. Cancer 3, 380–387,(2003).

[113] Bacellar IOL., Tsubone TM, Pavani C, Baptista MS. **Photodynamic efficiency: from molecular photochemistry to cell death**, Int J Mol Sci ,16, 20523-59,(2015).

[114] Almeida R.D., Manadas B.J., Carvalho A.P., Duarte C.B., **Intracellular signaling mechanisms in photodynamic therapy**, Biochim. Biophys. Acta 1704, 59–86, (2004).

[115] Berlanda J., Kiesslich T., Engelhardt V., Krammer B., Plaetzer, K., **Comparative in vitro study on the characteristics of different photosensitizers employed in PDT**, J. Photochem. Photobiol. B 100, 173–180,(2010).

[116]PalumboG., **Photodynamic therapy and cancer: a brief sightseeing tour**, Expert Opin. Drug Deliv. 4, 131–148,(2007).

[117] Juarranz A., Jaen P., Sanz-Rodriguez F., Cuevas J., Gonzalez, S., **Photodynamic therapy of cancer. Basic principles and application,** Clin. Transl. Oncol. 10, 148–154,(2008).

[118] O'Connor A.E., Gallagher W.M., Byrne A.T., **Porphyrin and nonporphyrin photosensitizers in oncology: preclinical and clinical advances in photodynamic therapy Photochem**, Photobiol. 85, 1053–1074,(2009).

[119] Choudhary S., Nouri K., Elsaie, M.L., **Photodynamic therapy in dermatology: A review**, Lasers Med. Sci. 24, 971–980, (2009).

[120] Mfouo-Tynga, I., Abrahamse H., **Cell death pathways and phthalocyanine as an efficient agent for photodynamic cancer therapy**, Int. J. Mol. Sci. 16, 10228–10241, (2015).

[121] Blume J.E., Oseroff A.R., **Aminolevulinic acid photodynamic therapy for skin cancers**, Dermatol. Clin. 25: 5–14, (2007).

[122] Morton C., Szeimies R.M., Sidoroff A., Wennberg A.M., Basset-Seguin N., Calzavara-Pinton, P., Gilaberte, Y., Hofbauer, G., Hunger, R., Karrer S., **European Dermatology Forum Guidelines on topical photodynamic therapy**, Eur. J. Dermatol. 25, 296–311, (2015).

[123] Evangelou, G., Farrar M.D., Cotterell L., Andrew S., Tosca A.D., Watson R.E., Rhodes L.E., **Topical photodynamic therapy significantly reduces epidermal Langerhans cells during clinical treatment of basal cell carcinoma**, Br. J. Dermatol. 166, 1112–1115,(2012).

[124] Han J., Zhang, J., Shan X., Zhang Y., Peng H., Qin L., and Wang L. , **Beam homogenization structure for a laser illuminator design based on diode laser beam combining technology**, Chinese Optics Letters, 21(3), 031405,(2023).

[125] Garg AD., Krysko DV., Vandenabeele P., Agostinis P. , **Hypericin-based photodynamic therapy induces surface exposure of damage-associated molecular patterns like HSP70 and calreticulin**, Cancer Immunology, Immunotherapy. 61, 215-21, (2012).

[126] Nowis D., Makowski M., Stoklosa T., Legat M., Issat T., Golab J., **Direct tumor damage mechanisms of photodynamic therapy**, Acta Biochim. Pol. 52, 339–352, (2005).

[127] Henderson B.W., Busch T.M., Snyder J.W., **Fluence rate as a modulator of PDT mechanisms**, Lasers Surg. Med. 38, 489–493,(2006).

[128] Brancaleon L., Moseley H., **Laser and non-laser light sources for photodynamic therapy**, Lasers Med. Sci. 17, 173–186,(2002).

[129] Calin M.A., Diaconeasa A., Savastru D., Tautan M., **Photosensitizers and light sources for photodynamic therapy of the Bowen's disease**, Arch. Dermatol. Res. 303, 145–151,(2011).

[130] Morton C.A., McKenna K.E., Rhodes L.E., **Guidelines for topical photodynamic therapy: update**, Br. J. Dermatol. 159: 1245–1266,(2008).

[131]Triesscheijn M., Baas P., Schellens, J.H., Stewart F.A., **Photodynamic therapy in oncology**, Oncologist 11, 1034–1044,(2006).

[132] Richeng L., Wei Z, Liang C. , Yanming Z. , MengXuan X., Xiaoping O. and Feng H., **X-ray radiation excited ultralong (>20,000 seconds) intrinsic phosphorescence in aluminum nitride single-crystal scintillators**, Nature Communications, 11(1), (2022).

[133] Hellen C. Ishikawa-Ankerhold, Richard Ankerhold, and Gregor P. C. Drummen, **Advanced Fluorescence Microscopy Techniques—FRAP, FLIP, FLAP, FRET and FLIM**, National library of medicine , 17(4), 4047–4132, (2012).

[134] Siyuan Q. , Jingwen J., Yi L. , Edouard C. , Canhua .g, Jian Z., and Weifeng H., **Emerging role of tumor cell plasticity in modifying therapeutic response**, Signal Transduction and Targeted Therapy,5 (1), (2020).

[135] Insero G., Fusi F., and Romano G. , **The safe use of lasers in biomedicine: Principles of laser-matter interaction**, Journal of Public Health Research, 12(3), 22799036231187077, (2023).

[136] Wilson B.C., Patterson M.S., **The physics, biophysics and technology of photodynamic therapy**, Phys. Med. Biol. 53, R61–R109,(2008).

[137] Coats JG., Maktabi B., Abou-Dahech MS,. Baki G., **Blue Light Protection, Part I—Effects of blue light on the skin**, Journal of cosmetic dermatology. 20(3), 714-7,(2021).

[138] Henderson B. W., Owczarczak B., Sweeney J., and Gessner T., **Effects of Photodynamic Treatment of Platelets or Endothelial Cells In Vitro on Platelet Aggregation**, Photochem. Photobiol. 56 (4), 513–521,(1992).

[139] Chan W. S., Brasseur N., LaMadeleine C., and van Lier J. E. **Evidence for Different Mechanisms of EMT-6 Tumor Necrosis by Photodynamic Therapy with Disulfonated Aluminum Phthalocyanine or Photofrin: Tumor Cell Survival and Blood Flow**. Anticancer Res. 16 (4A), 1887–1892,(1996).

[140] Hleb E. Y., Yakush N. A., Hafner, J. H., Drezek R. A., McNew J. A., and Lapotko D. O., **Plasmon nanoparticle-generated photothermal bubbles as universal biomedical agents**, une,13, 15,(2016).

[141] Fadeel B., Alexiou C., **Brave new world revisited: Focus on nanomedicine. Biochem. Biophys**, Res. Commun, 533: 36-49,(2020).

[142] Alexiou C., Fadeel B., **Brave new world - focus on nanomedicine, Biochem. Biophys** , Am. J. Res. Commun, 468 (3), 409-410,(2015).

[143] Hassan S. S., Kamel A. H., Hashem H. M., and Bary E. A., **Drug delivery systems between metal, liposome, and polymer-based nanomedicine: a review**, European Chemical Bulletin, 9(3), 91-102,(2020).

[144] Bernabeu E., Cagel M., Lagomarsino E., Moretton M., and Chiappetta D. A**., Paclitaxel: What has been done and the challenges remain ahead,** International journal of pharmaceutics, *526*(1-2), 474-495, (2017).

[145] Gabizon A., Catane R., Uziely B., Kaufman B., SafraT., Cohen, R., and Barenholz Y., **Prolonged circulation time and enhanced accumulation in malignant exudates of doxorubicin encapsulated in polyethylene-glycol coated liposomes**, Cancer research, 54(4), 987-992.

[146] Gabizon A, Shmeeda H, Barenholz Y., **Pharmacokinetics of pegylated liposomal Doxorubicin: review of animal and human studies**, Clinical pharmacokinetics. 42, 419-36,(2003).

[147] Lyon P. C., Gray, M. D., Mannaris C., Folkes L. K., Stratford M., Campo L., and Coussios, C. C. , **Safety and feasibility of ultrasound-triggered targeted drug delivery of doxorubicin from thermosensitive liposomes in liver tumours (TARDOX): a single-**

centre, open-label, phase 1 trial , The Lancet Oncology, 19(8), 1027-1039, (2018).

[148] Abdulla-Al-Mamun M., Yang H., and Kusumoto Y., **Enhancement of Photocatalytic Cancer Cell-Killing Activity by Using Ag@ TiO2 Core-Shell Composite Nanoclusters**, une, 13,15,(2016).

[149] Daghrir R., Drogui P., and Robert D., **Modified TiO2 for environmental photocatalytic applications: a review**, Industrial and Engineering Chemistry Research, 52(10), 3581-3599, (2013).

[150] Abdulla-Al-Mamun M., Kusumoto Y., and Islam M. S., **Enhanced photocatalytic cytotoxic activity of Ag@ Fe-doped TiO2 nanocomposites against human epithelial carcinoma cells**, Journal of Materials Chemistry, 22(12), 5460-5469, (2012).

[151] Hou Y., Li X., Zhao Q., Chen, G., and Raston C. L., **Role of hydroxyl radicals and mechanism of Escherichia coli inactivation on Ag/AgBr/TiO2 nanotube array electrode under visible light irradiation**, Environmental science and technology, 46(7), 4042-4050, (2012).

[152] Khanna A., and Shetty V. K., **Solar light induced photocatalytic degradation of reactive blue 220 (RB-220) dye with highly efficient Ag@ TiO 2 core–shell nanoparticles: a comparison with UV photocatalysis**, Solar Energy, 99, 67-76,(2014).

[153] Chang S. Y., Huang W. J., Lu B. R., Fang G. C., Chen Y., Chen H. L., and Hsu C. F., **An Environmentally Friendly Method for Testing Photocatalytic Inactivation of Cyanobacterial Propagation on a Hybrid Ag-TiO_2 Photocatalyst under Solar**

Illumination. International journal of environmental research and public health, 12(12), 15819-15833,(2015).

[154] Hosseinnia A., Pazouki M., and Banifatemi M., **Photocatalytic Decomposition of Epichlorohydrin by TiO_2/Ag Coated Sintered Glass Filters**, Iranian Journal of Chemical Engineering, 11(1),(2014).

[155] Singh B., Baburao C., Pispati V., Pathipati, H., Muthy, N., Prassana, S., Rathode B.G., **Carbon nanotubes: A novel drug delivery system**, Int. J. Res. Pharm. Chem. 2, 523–532,(2012).

[156] Lei W., Jinjin S., Ruiyuan L., Yan L., Jing Z., Xiaoyuan, Y., Jun G., Chaofeng Z., Zhenzhong Z., **Photodynamic effect of functionalized singlewalled carbon nanotubes: A potential sensitizer for photodynamic therapy,** Nanoscale 6, 4642–4652, (2014).

[157] Sajid M.I., Jamshaid U. Jamshaid, T. Zafar, N., Fessi, H., Elaissari, A., **Carbon nanotubes from synthesis to in vivo biomedical applications**, Int. J. Pharm. 501, 278–299, (2016).

[158] Mu, Q., Broughton, D.L.,Yan B., **Endosomal leakage and nuclear translocation of multiwalled carbon nanotubes: Developing a model for cell uptake**, Nano Lett. 9, 4370–4375, (2009).

[159] Marangon I., Ménard-Moyon C., Silva A.K.A., BianconA., Luciani N. Gazeau., F., **Synergic mechanisms of photothermal and photodynamic therapies mediated by photosensitizer/carbon nanotube complexes**, Carbon 97, 110–123,(2016).

[160] Tuncel D., **Non-covalent interactions between carbon nanotubes and conjugated polymers**, Nanoscale 3, 3545–3554, (2011).

[161] Tan J.M., Arulselvan P., Fakurazi S., Ithnin H., Hussein M.Z., **A Review on Characterizations and Biocompatibility of functionalized carbon nanotubes in drug delivery design**, J. Nanomater. 917024, (2014).

[162] Bates K., and Kostarelos K. , **Carbon nanotubes as vectors for gene therapy: past achievements, present challenges and future goals**, Advanced drug delivery reviews, 65(15), 2023-2033, (2013).

[163] Wong B. S., Yoong S. L., Jagusiak A., Panczyk T., Ho H. K., Ang W. H., and Pastorin G., **Carbon nanotubes for delivery of small molecule drugs. Advanced drug delivery reviews**, 65(15), 1964-2015, (2013).

[164] Editors, **The two directions of cancer nanomedicine**, Nat. Nanotechnol, 14, 12, 1083, (2019).

[165] Dolmans D.E., Fukumura D., Jain R.K**., Photodynamic therapy for cancer**, Nat. Rev. Cancer. 3, 380-387, (2003).

[166] Li X., Lee, S., Yoon J., **Supramolecular photosensitizers rejuvenate photodynamic therapy**, Chem. Soc. Rev, 47, 1174–1188, (2018).

[167] Singh B., Mitragotri S., **Harnessing cells to deliver nanoparticle drugs to treat cancer**, Biotechnol. Adv, 42, 107339, (2020).

[168] Rigby C. C., and Franks L. M., **A Human tissue culture cell line from a transitional cell tumour of the urinary bladder: growth, chromosome pattern and ultrastructure**, British Journal of Cancer, 24,(4), 746–754, (1970).

[169] Johan V., Gertjan J L., Jacqueline Cloos, **Cell sensitivity assays: the MTT assay**, 731,(2011).

[170] Kimoto S., Dick W. D., Hunt B., Szymanski W. W., McMurry P. H., Roberts D. L., and Pui D. Y. H**., Characterization of nanosized silica size standards**, Aerosol Science and Technology, 51(8), 936–945, (2017).

[171] Shameem SA., Ganai BA., Rather MS., Khan KZ., **Chemical composition and antioxidant activity of Viscum album L. growing on Juglans regia host tree in Kashmir, India**, International Journal of Research in Science and Engineering, 6(01), 921-7, (2017).

[172] Kim Y. S., Lumbera W. M. L., and Hwang S. G. , **Viscum album var hot water extract mediates anti-cancer effects through G1 phase cell cycle arrest in SK-Hep1 human hepatocarcinoma cells**, Asian Pacific Journal of Cancer Prevention, 16(15), 6417-6421, (2015).

[173] Celebi c., **Taghizadehghalehjoughi Baser**, Biofilm Analysis. 29, 3 (May-June), 241, (2023).

[174] Fox M., **Quantum optics, an introduction**, OUP Oxford,15, (2006).

[175] Guinier A., **X-ray Diffraction in Crystals**, Imperfect Crystals, and Amorphous Bodies, Freeman, San Francisco, (1963).

[176] Als-Nielsen J. and McMorrow D., **Elements of Modern X-ray Physics**, John Wiley and Sons, Ltd., Chichester,(2001).

[177] Barrett C. S. and Massalski T.B., **Structure of Metals**, Mc Graw-Hill, New York, (1966).

[178] Singh A., Kumar D., Khanna P. K., Joshi B. C., and Kumar M. , **Effect of post annealing temperature on structural and optical properties of ZnCdO thin films deposited by sol–gel method**, Applied Surface Science, 258(5), 1881-1887, (2011).

[179] Oh PS., Na KS, Hwang H., Jeong HS., Lim S., Sohn MH., Jeong HJ., **Effect of blue light emitting diodes on melanoma cells: involvement of apoptotic signaling**, Journal of Photochemistry and Photobiology B: Biology. 142, 197-203, (2015).

[180] Garza ZC., Born M., Hilbers PA., Van Riel NA., Liebmann J. , **Visible blue light therapy: molecular mechanisms and therapeutic opportunities**, Current medicinal chemistry, 25(40), 5564-77, (2018).

[181] Liebmann J., Born M., Kolb-Bachofen V., **Blue-light irradiation regulates proliferation and differentiation in human skin cells**, Journal of Investigative Dermatology. 130(1), 259-69, (2010).

[182] Zhang W., Zhao Y., Dong J., **Impact of blue light irradiation on the viability of four types of human cells**, In 2022 19th China International Forum on Solid State Lighting and 2022 8th International Forum on Wide Band gap Semiconductors (SSLCHINA: IFWS) ,259-262,(2023).

[183] De Matteis V., Malvindi M.A., Galeone, A., Brunetti, V., De Luca, E., Kote, S., Kshirsagar P., Sabella S., Bardi G., Pompa P.P., **Negligible particle-specific toxicity mechanism of silver**

nanoparticles: The role of Ag+ ion release in the cytosol, Nanomed. Nanotechnol. Biol. Med.11, 731–739,(2015).

[184] Gurunathan, S., Park, J.H., Han, J.W., Kim, J.H., **Comparative assessment of the apoptotic potential of silver nanoparticles synthesized by Bacillus tequilensis and Calocybe indica in MDA-MB-231 human breast cancer cells: Targeting p53 for anticancer therapy**, Int. J. Nanomed. 10, 4203–4222, (2015).

[185] Lin J., Huang Z., Wu H., Zhou W., Jin P., Wei, P., Zhang, Y., Zheng, F., Zhang, J., Xu, J., **Inhibition of autophagy enhances the anticancer activity of silver nanoparticles**, Autophagy 2014, 10, (2006–2020).

[186] Gopinath P., Gogoi S.K., Chattopadhyay A., Ghosh S.S. **Implications of silver nanoparticle induced cell apoptosis for in vitro gene therapy**, Nanotechnology 19, 075104,(2008).

[187] Atif M., Fakhar-e-Alam M., Firdous S., Zaidi SS., Suleman R., Ikram M., **Study of the efficacy of 5-ALA mediated photodynamic therapy on human rhabdomyosarcoma cell line (RD)**, Laser Physics Letters, 7(10), 757, (2010).

[188] Alkarakooly Z., Al-Anbaky QA., Kannan K., Ali N., **Metabolic reprogramming by Dichloroacetic acid potentiates photodynamic therapy of human breast adenocarcinoma MCF-7 cells**, PLoS One, 13(10), e0206182, (2018).

[189] Díaz-Uribe C., Viloria J., Cervantes L., Vallejo W., Navarro K., Romero E., and Quiñones C., **Photocatalytic activity of Ag-TiO2 composites deposited by photoreduction under UV irradiation**, International Journal of Photoenergy, (2018).

[190] Burton KA., Ashack KA. and Khachemoune A., **Cutaneous squamous cell carcinoma: A review of high‐risk and metastatic disease**, Am J Clin Dermatol 17, 491‐508, (2016).

الخلاصة

في هذا العمل، تم زرع الخلايا على لوحات معقمة مكونة من 96 بئرًا في 200 ميكرولتر من الوسط مع غطاء أثناء التشعيع. زراعة الخلايا هي عملية إزالة الخلايا من الأنسجة الحية وزراعتها في بيئة معملية حتى تصبح جاهزة للاختبار باستخدام العلاج الديناميكي الضوئي والجسيمات النانوية. تم تشعيع صفائح خلايا الجلد (خط الخلية A431) المزروعة في وسط استزراع مكمل بـ 10٪ من مصل الأبقار الجنيني (FBS) بالضوء الأزرق بواسطة الصمام الثنائي الباعث للضوء والليزر ومصباح زينون بأطوال موجية 420 - 480 نانومتر وتم معالجتها بثنائي اوكسيد التيتانيوم المطعمة بالفضه (TiO_2/Ag) وأنابيب الكربون النانوية أحادية الجدار(SWCNT-OH) بعد إضافة عدة تراكيز من المادة النانوية (400، 200، 100، 50، 25 و12.5) ميكروغرام/مل و(200، 100، 50، 25، 12.5 و6.25) ميكروغرام/مل، على التوالي. تم استخدام فحوصات حيود الأشعة السينية لإجراء تحليل على البلورة وكذلك الخصائص الهيكلية للجزيئات النانوية. يُظهر نمط XRD للأفلام المنتجة بـ TiO_2 / Ag. أظهر نمط XRD قممًا عند θ = 25.42 درجة تتوافق مع المستويات (101) وتم إنشاء القمم المميزة عند 24.2 درجة و25.6 درجة بواسطة انعكاسات من طبقات ذرة الكربون السداسية وطبقات تكديس الأنابيب النانوية (SWCNT-OH) التي تتوافق مع المستويات (002). كانت العينات ذات أحجام بلورية صغيرة إلى حد ما بالنسبة للـ NPs، تتراوح من 5 إلى 25 نانومتر. تم أخذ جرعات الإشعاع المختلفة ووقت التعرض في الاعتبار. حقق الصمام الثنائي الباعث للضوء الأزرق (LED) بأطوال موجية 420-480 نانومتر وإشعاع 400 ملي وات/سم2 نتائج فعالة. أدى تعرض خلايا سرطان الجلد إلى مصابيح LED الزرقاء إلى انخفاض سريع وكبير في قابليتها للحياة، يليه موت ما يقرب من نصف الخلايا. العلاج الأحدث والأكثر أمانًا هو العلاج بتقنية LED. يؤدي علاج الخلايا المشعة بالـ LED إلى زيادة في موت الخلايا. قد يفتح التعرض للضوء الأزرق إمكانيات جديدة لعلاج سرطانات الجلد السطحية لدى البشر. حمض أمينوليفولينيك (ALA-5) هو محسس ضوئي آمن يمكن استخدامه لعلاج الضوئي مفيد لسرطان الجلد. أن خط الخلايا المعالج بـ PDT أظهر أعلى نسبة من صلاحية الخلايا، ما يقرب من 73٪، بعد 240 ثانية من التعرض للإشعاع مع تركيز محسس ضوئي ALA-5 قدره 250 ميكروغرام / مل ، والذي يعتبر التركيز المثالي في هذه الدراسة. أظهرت نتائج الصمام الثنائي الباعث للضوء الأزرق انخفاضًا كبيرًا عند 240 ثانية بعد 24 ساعة من وقت الحضانة في نسبة الصلاحية ؛ أظهرت نتائج الجسيمات النانوية (TiO_2/Ag) وأنابيب الكربون النانوية أحادية الجدار (SWCNT-OH) انخفاضًا كبيرًا

في نسبة بقاء الخلايا لجميع التركيزات؛ وكان التركيز الأكثر فعالية هو 400 ميكروغرام/مل؛ واظهرت نتائج الدمج انخفاضا معنويا في نسبة حيوية الخلية ($p<0.001$) مقارنة مع control. أنتجت جزيئات ثنائي اوكسيد التيتانيوم النانوية المطعمه بالفضه بتركيز 400 ميكروجرام/مل أفضل النتائج (19.131%) مقارنة بمجموعة التحكم (100%) عند دمجها مع فترة تعرض للضوء قدرها 240 ثانية. ولوحظ أن حيوية الخلايا منخفضة للغاية، وهذا يدل على تدمير الخلايا السرطانية بسبب صغر حجم المادة النانوية التي يمكنها اختراق الخلية والانتشار إلى سيتوبلازم الخلية. تم استخدام اختبار مقايسة ميثيل ثيازوليل تترزوليوم (MTT) لتحديد مدى صلاحية الخلايا في جميع التجارب، وتم قياس شدة اللون بواسطة قارئ اللوحة.

جمهورية العراق
وزارة التعليم العالي والبحث العلمي
جامعة بابل
كلية العلوم
قسم الفيزياء

معالجة خلايا الجلد السرطانية بأستخدام الطيف الضوء المرئي مع بعض الجسيمات النانوية

أطروحة مقدمة الى قسم الفيزياء في كلية العلوم - جامعة بابل
وهي جزء من متطلبات نيل درجة الدكتوراه في فلسفة علوم الفيزياء

من قبل:

دعاء جعفر ضياء جابر فياض

بكالوريوس علوم فيزياء , جامعة الكوفة 2015

ماجستير علوم فيزياء , جامعة الكوفة 2018

بأشراف

أ.م.د. سميرة عدنان مهدي

2023 م **1445هـ**